APPLICATIONS OF THE DIRECT CORRELATION FUNCTION SOLUTION THEORY TO THE THERMODYNAMICS OF FLUIDS AND FLUID MIXTURES

By

SYED WASEEM BRELVI

A DISSERTATION PRESENTED TO THE GRADUATE COUNCIL OF THE UNIVERSITY OF FLORIDA IN PARTIAL FULFILLMENT OF THE REQUIREMENTS FOR THE DEGREE OF DOCTOR OF PHILOSOPHY

UNIVERSITY OF FLORIDA
1973

TO FARAH

ACKNOWLEDGMENTS

The author sincerely thanks the many persons who gave him assistance during the course of this work.

Tracy Lambert, Jack Kalway and Myron Jones of the Chemical Engineering Shop and Ed Logsdon of the Engineering Glass Shop willingly and cheerfully provided assistance on request.

Lewis Moore's contribution to the early stages of experimental design and construction was considerable. Continuing discussions with Dr. M. S. Ananth enabled the author to unravel some complexities of perturbation theory. Anthony DeGance's suggestions on computations of thermodynamic properties were very timely.

Dr. Keith Gubbins elucidated some aspects of the molecular basis of the compressibility correlation. Valuable advice on the intricacies of experimental work and the loan of several pieces of experimental apparatus from Dr. T. M. Reed are deeply appreciated.

The author is thankful to Dr. O'Connell for his guidance through this work. His unlimited patience, easy accessibility and unfailing optimism were tremendous assets, especially during periods of low productivity. His encouragement, nay, insistence towards perfection resulted in some of the positive achievements of this study. Working with Dr. O'Connell has been an experience that will not be soon forgotten.

Finally, the author expresses his thanks to his wife for her support and devotion through these testing years. Her participation in this effort made it all possible and worthwhile.

TABLE OF CONTENTS

TABLE OF CONTENTS (Continued)

TABLE OF CONTENTS (Continued)

LIST OF TABLES

LIST OF TABLES (Continued)

LIST OF FIGURES

LIST OF FIGURES (Continued)

NOMENCLATURE

A	=	coefficient of Tait equation, equation (4.11)
A_{ij}	=	partial derivative at constant temperature and volume of chemical potential of species i w.r.t. concentration of species j, equation (2.9)
B	=	coefficient of Tait equation, equation (4.11)
B_{ij}	=	element of matrix in expression relating chemical potential derivatives to integrals of molecular distribution functions, equation (2.11)
C_{ij}	=	volume integral of pair direct correlation function of species i and j, equation (2.25)
C_{ijk}	=	volume integral of triplet direct correlation function of species i, j, k, equation (5.13)
F	=	matrix in expression relating derivatives of chemical potentials to integrals of direct correlation function, equation (2.31)
G_{ij}	=	volume integral using radial distribution function of species i and j, equation (2.12)
H_{im}	=	Henry's constant (reference fugacity) of component i in solvent m, atm, equation (1.7)
I	=	identity matrix, equation (2.22)
N_i	=	number of molecules of species i, equation (2.2)
P	=	pressure (atm), equation (1.4)
R	=	gas constant (cc atm/gm mole °K), equation (1.4)
T	=	absolute temperature (°K), equation (1.4)
V	=	total volume of system (cc), equation (2.5)

X_j = mole fraction of component j at zero composition of component 1, equation (2.39)

a = diameter of rigid core in hard sphere intermolecular potential (cm), equation (3.6)

$c(r)$ = pair direct correlation function between molecules distance r apart, equation (2.24)

$c_{ij}(\underline{r}_{12})$ = pair direct correlation function between molecules of species i and j, distance r_{12} apart, equation (2.25)

c_i = molecular concentration of species i (molecules/cc), equation (2.5)

d = reduced hard sphere distance, equation (3.6)

d_{ij} = partial derivative at constant temperature and pressure of chemical potential of species i w.r.t. concentration of species j

f_2 = coefficient in Margules expression for solute activity coefficient, equation (2.34)

f_3 = coefficient in Margules expression for solute activity coefficient, equation (2.34)

$f_i^{(j)}$ = fugacity of component i in phase j (atm), equation (1.3)

$g(r)$ = radial distribution function between molecules distance r apart, equation (2.24)

$g_{ij}^{(2)}(r_{12})$ = radial distribution function between molecules of species i and j separated by a distance r_{12}, equation (2.4)

k = Boltzmann's constant (erg/°K), equation (2.9)

r = radial distance (cm), equation (2.6)

v = molar volume (cc/gm mole), equation (1.4)

x = mole fraction in liquid phase, equation (1.4)

y = mole fraction vapor phase, equation (1.4)

Greek Letters

γ = liquid phase activity coefficient, symmetric convention, equation (1.4)

γ^* = liquid phase activity coefficient, unsymmetric convention, equation (1.6)

δ_{ij} = Kronecker delta

ε/k = energy parameter in intermolecular potential (°K), equation (3.6)

κ = isothermal compressibility (atm^{-1}), equation (1.14)

$\mu_i^{(j)}$ = chemical potential of species i in phase j (cals/mole), equation (1.1)

ρ = molar density (gm moles/cc), equation (1.14)

σ = size parameter in intermolecular potential (Å), equation (3.6)

$\phi(r)$ = spherically symmetric intermolecular potential at separation r (ergs), equation (3.1)

Superscripts

^{o} = standard state

^{o} = infinite dilution of component 1 in 2

^{o} = pure 2 in 2-3 mixture

* = pure 3 in 2-3 mixture

* = characteristic

L	=	liquid phase
v	=	vapor
-	=	partial molar property
sat	=	saturation
+	=	infinite dilution of component 1 in 2
hs	=	hard sphere
rf	=	real fluid
r	=	reduced
E	=	excess

Subscripts

i	=	component i
j	=	component j
m	=	mixture

Abstract of Dissertation Presented to the
Graduate Council of the University of Florida in Partial
Fulfillment of the Requirements for the Degree of Doctor of Philosophy

APPLICATIONS OF THE DIRECT CORRELATION FUNCTION SOLUTION THEORY TO THE THERMODYNAMICS OF FLUIDS AND FLUID MIXTURES

By

Syed Waseem Brelvi

March, 1973

Chairman: Dr. J. P. O'Connell
Major Department: Chemical Engineering

The formulation of a rigorous statistical mechanical solution theory relates thermodynamic properties in a fluid mixture to volume integrals of molecular distribution functions. These distribution functions are complex functions of molecular interactions and the macroscopic state of the system including the composition although for many purposes the composition dependence of thermodynamic properties can be represented by functional expansions about limiting compositions in the mixture.

Molecular distribution functions of different orders are related through density derivatives of the distribution functions. A first-order perturbation theory has been developed to relate the distribution functions of a real fluid to the similar functions in a hard sphere fluid through differences in the intermolecular potentials. The calculated radial distribution function for a Lennard-Jones 6-12 model agrees well with molecular dynamics results. A one-parameter corresponding states theory for the compressibility integral gives qualitative predictions for thermodynamic properties in subcritical systems.

Corresponding states correlations involving only a single characteristic parameter for each substance express the isothermal compressibility of pure liquids and the partial molar volumes of gases at infinite dilution as universal functions of the reduced solvent density. A generalized isothermal equation of state reproduces pressures and volumes in compression experiments of pure liquids up to high pressures.

The isothermal compressibility of liquid mixtures is described by a one-fluid theory with composition dependent parameters. A postulated linear variation of direct correlation function integrals between composition extremes gives accurate predictions of partial molar volumes and activity coefficients at intermediate compositions. The experimental triplet correlation functions in a representative subcritical system did not agree with the Percus-Yevick or HNC approximations.

An experimental determination of the volumetric and vapor-liquid equilibrium properties of gas-solvent mixtures is reported. Volumetric properties in the liquid phase are expressed by functional expansions in the solute mole fraction, with a one-fluid model for the solvent mixture. Generalized correlations are developed from experimental data to relate the activity coefficient parameters of H_2 and CH_4 in liquid solvents to the reduced solvent density. Several expressions relating the Henry's constant of a gas in a mixed solvent to those in the pure solvents are analyzed with experimental data. Vapor liquid equilibrium calculations show that some of these expressions with the generalized activity coefficients yield K-factors and bubble pressures in good agreement with experimental data.

CHAPTER 1

THERMODYNAMICS OF GAS-LIQUID SYSTEMS

Our everyday experience presents a panorama of processes in gas-liquid systems. They vary in nature from the complex transfer of oxygen into the blood stream of animals, to the simple dissolution of carbon dioxide in the ubiquitous coke bottle. A major effort of chemical and petroleum industries is contacting, treating and separating gas and liquid streams.

In all of these instances, the equilibrium distributions of material in the two phases follow simple thermodynamic relations. This is not to imply that equilibrium conditions obtain in these processes, for then there would be no transfer of materials. The equilibrium distributions reflect the thermodynamic constraints on the system. In the engineering domain, these equilibrium distributions are a key factor in the selection of processing conditions and the design of process equipment.

Thermodynamic properties of matter in bulk are the manifestation of the molecular interactions between the different species present in the system. Statistical mechanics provides the formal link between the molecular characteristics of a physical system and its bulk thermodynamic properties. This work describes the use of a statistical mechanical solution theory based on molecular distribution functions for correlating the thermodynamic properties of gas solvent systems.

1.1 Phase Equilibrium in Gas-Liquid Systems

Generally, for thermodynamic equilibrium between the phases of a

multicomponent system, the chemical potentials of each species are equal in all phases,[1] i.e.,

$$\mu_i^{(1)} = \mu_i^{(2)} = \mu_i^{(3)} \qquad \text{for all } i \tag{1.1}$$

$\mu_i^{(j)}$ is the chemical potential, or partial molar free energy of species i in phase j, and depends on temperature, pressure and composition of the phase.

For any phase, solid, liquid or gas, the chemical potential of the individual species can be expressed in terms of the fugacities, f_i, as[2]

$$\mu_i - \mu_i^o = RT\ln f_i/f_i^o \tag{1.2}$$

μ_i^o and f_i^o are the chemical potential and fugacity in the standard state. Of these two quantities, one can take on an arbitrary value, but they are not both independent. The fugacity, f_i, also depends on temperature, pressure, and composition. The fundamental equilibrium relation (1.1) reduces to

$$f_1^{(1)} = f_1^{(2)} = f_1^{(3)} \tag{1.3}$$

The central problem of phase equilibrium thermodynamics is the description of the component fugacities in terms of temperatures, pressures, and compositions. For vapor-liquid equilibrium, where the species are liquids at the temperature of the system, a suitable description of equation (1.3) is[2]

$$\phi_i^v y_i P = x_i \gamma_i (P^{ref}) \cdot f_i^{oL} \exp \int_{P^{ref}}^{P} \frac{\bar{v}_i^L}{RT}\, dP \tag{1.4}$$

which relates the vapor and liquid phase fugacities. ϕ_i^v is the vapor phase fugacity coefficient and represents the deviation from ideality of the individual components in the mixture, and the nonideality of mixing. For an ideal mixture of ideal gases, ϕ_i^v is unity. f_i^{oL} is the fugacity of the liquid in the standard state; this is the pure component at the temperature of the system, and under its own saturation pressure ($P^{ref} = P^{sat}$). $\gamma_i(P^{ref})$ is the activity coefficient in the liquid phase; it represents the composition dependence of the chemical potential at the reference pressure. (The importance of this quantity in the thermodynamics of liquids cannot be over emphasized.) For an ideal solution, $\gamma_i = 1$ at all x_i. In a nonideal mixture, $\gamma_i(P^{ref})$ is normalized such that

$$\gamma_i \to 1 \quad \text{as} \quad x_i \to 1 \tag{1.5}$$

The activity coefficient is unity when the component is in its standard state. The exponential term corrects for the change in fugacity of the liquid from the reference pressure to the pressure of the system.

The choice of the pure component as the standard state for fugacities serves very well in the description of liquid mixtures wherein each species can exist in the pure state at the system temperature. However, this definition is unsuitable in considering gas-liquid systems, for which the lighter components are supercritical at the mixture temperature. Here, the solute at infinite dilution in the solvent can be chosen as the standard state; the solvent may be a pure, or mixed, solvent. The liquid phase fugacity for the noncondensable components becomes[2]

$$f_i^L = x_i \gamma_i^*(P^{ref}) H_{i,m}(P^{ref}) \exp \int_{P^{ref}}^{P} \frac{\bar{v}_i^L}{RT} dP \qquad (1.6)$$

where the reference fugacity $H_{i,m}$, commonly called the Henry's constant, is

$$\lim_{x_i \to 0} \frac{f_i^L}{x_i} = H_{i,m}(P^{ref}) \qquad (1.7)$$

The activity coefficient $\gamma_i^*(P^{ref})$ is now normalized such that

$$\gamma_i^*(P^{ref}) \to 1 \quad \text{as} \quad x_i \to 0 \qquad (1.8)$$

where P^{ref} is usually the bubble pressure of the solvent at the temperature of the system. The product $x_i \gamma_i^*(P^{ref})\, H_{i,m}(P^{ref})$ describes the variation of the liquid phase fugacity with composition.

An important relation exists between the Henry's constant and activity coefficient of a gas dissolved in a mixed solvent and the corresponding quantities for the gas dissolved individually in each pure solvent. It is[3]

$$\ln H_{i,m} - \sum_{j=1}^{N} x_j \ln H_{ij} = \sum_{j=1}^{M} x_j (\lim_{x_i \to 1} \ln \gamma_{ij}^*) - \lim_{x_i \to 1} \ln \gamma_{im}^* \qquad (1.9)$$

where the multicomponent solvent mixture consists of N solvents with mole fraction x_j, j=1,...,N. $H_{i,m}$ and $H_{i,j}$ are the Henry's constants of the gas in the multicomponent solvent and the jth solvent, respectively; γ_{im}^* and γ_{ij}^* are the respective activity coefficients. Then if the solute interaction with the individual solvents is known, equation (1.9) can be used to calculate the solute nonideality in a

multicomponent solvent mixture from the Henry's constant, which is an ideal solution property. Conversely, if the solute nonideality in the multicomponent solvent can be approximated by some average of the nonideality in the individual solvents, the solubility in the multicomponent solvent can be determined from those in the individual solvents. However, one must recognize, the important and unavoidable assumption, made in equation (1.9), that the composition dependence of the activity coefficient as determined from dilute solution (or low concentration) behavior can be extrapolated to the physically unrealizable limit of $x_i = 1$.

1.2 Isothermal Pressure Dependence of Thermodynamic Properties

The fugacity of a component in a mixture depends on the temperature, pressure and composition. Its pressure dependence is given by the partial molar volume

$$\left(\frac{\partial \ell n f_i}{\partial P} \right)_{T,x} = \frac{\bar{v}_i}{RT} \tag{1.10}$$

The derivative is taken at constant temperature and composition; the volume changes to satisfy the general equation of state of the system. (The variance of the intensive quantities is, of course, determined by the phase rule.) For a finite pressure change,

$$\ell n\ f_i\Big]_{P_2} - \ell n\ f_i\Big]_{P_1} = \int_{P_1}^{P_2} \frac{\bar{v}_i}{RT}\, dP \tag{1.11}$$

In most liquid systems, the partial molar volume does not vary appreciably with pressure and (1.11) is simplified to

$$\ell n\ f_i\Big]_{P_2} - \ell n\ f_i\Big]_{P_1} = \frac{\bar{v}_i(P_2 - P_1)}{RT} \tag{1.12}$$

When the vapor and liquid phases are assumed ideal, and the partial molar volume is that at infinite dilution, we have

$$\frac{1}{x_i} = \frac{H_i(P^{ref} = 0)}{y_i P} \exp \frac{\bar{v}_i^{o} P}{RT} \tag{1.13}$$

which gives the pressure dependence of the solubility in an ideal liquid solution.

The effect of pressure changes on a fluid mixture is given by the isothermal compressibility, κ, which is defined as

$$\kappa = \frac{1}{\rho}\left(\frac{\partial \rho}{\partial P}\right)_{T,n} \tag{1.14}$$

where n denotes the constant composition of the system. In integrated form, equation (1.14) is

$$\Delta P = P_2 - P_1 = \int_{\rho_1}^{\rho_2} \frac{d\rho}{\rho\kappa} \tag{1.15}$$

Given κ as a function of density, this equation can be used to relate corresponding changes in pressure and density. Equation (1.15) is an isothermal equation of state.

REFERENCES FOR CHAPTER 1

1. K. G. Denbigh, Chemical Equilibrium, Cambridge University Press, Cambridge, 1966.

2. J. M. Prausnitz, Molecular Thermodynamics of Fluid Phase Equilibria, Prentice-Hall, Englewood Cliffs, 1969.

3. J. P. O'Connell, A.I.Ch.E.J., 17, 653 (1971).

CHAPTER 2

DISTRIBUTION FUNCTION SOLUTION THEORY

A distribution function solution theory for equilibrium properties of multicomponent fluid systems was first proposed by Kirkwood and Buff.[1] By rigorous statistical mechanical methods, they related thermodynamic properties of a mixture to volume integrals of the radial distribution functions. The shape of the radial distribution functions in a fluid mixture result from intermolecular attractions and depend in a complex, and, as yet, incompletely determined, way on the macroscopic variables of the system and on the intermolecular potentials of the different species present. Currently available theories for predicting the distribution functions,[2] albeit approximate, can provide an adequate basis for determining thermodynamic properties through the use of statistical mechanical relations to be presented here. The properties considered are the isothermal compressibility, the partial molar volume of each component, and the composition derivative of the chemical potentials.

2.1 Radial Distribution Function Solution Theory

The framework of the grand canonical ensemble is used in

the development of the solution theory. Relations are obtained between density fluctuations and integrals of the radial distribution functions, and again between density fluctuations and the composition dependence of the chemical potentials. Elimination of the density fluctuations leaves the desired relationships.

The system of interest, with volume V, is considered to be in a large heat bath and open with respect to molecules in the system. The bath provides a reservoir of heat at temperature T and of molecules at chemical potentials $\mu_1, \mu_2, \cdots, \mu_M$. The system is then characterized by the thermodynamic variables T, V, μ_i, i = 1, M. (M is the number of chemical species present.) There are fluctuations in the number of molecules, N_i, of each species within the system. The average singlet and pair densities and the fluctuations in the density of each species are related through equations of the form

$$\int \rho_\alpha^{(1)}(\underline{r}_1)d\underline{r}_1 = \langle N_\alpha \rangle_{av} \tag{2.1}$$

$$\iint \rho_{\alpha\beta}^{(2)}(\underline{r}_1,\underline{r}_2)d\underline{r}_1 d\underline{r}_2 = \langle N_\alpha N_\beta \rangle_{av} - \delta_{\alpha\beta}\langle N_\alpha \rangle_{av}\langle N_\beta \rangle_{av} \tag{2.2}$$

$$\iint \left[\rho_{\alpha\beta}^{(2)}(\underline{r}_1,\underline{r}_2) - \rho_\alpha^{(1)}(\underline{r}_1)\rho_\beta^{(1)}(\underline{r}_2)\right] d\underline{r}_1 d\underline{r}_2$$

$$= \left[\langle N_\alpha N_\beta \rangle_{av} - \langle N_\alpha \rangle_{av}\langle N_\beta \rangle_{av}\right] - \delta_{\alpha\beta}\langle N_\alpha \rangle_{av} \tag{2.3}$$

Here $\rho_{\alpha\beta}^{(2)}(\underline{r}_1,\underline{r}_2)$ is the average pair density for molecules of species α and β and $\rho_\alpha^{(1)}(\underline{r}_1)$ is the singlet density for molecules of type α, $\langle N_\alpha \rangle$ is the average number of molecules of species α within the volume V.

The radial distribution function $g^{(2)}_{\alpha\beta}(\underline{r}_1,\underline{r}_2)$ or $g_{\alpha\beta}(\underline{r})$, is simply related to the average pair and singlet densities:

$$\rho^{(2)}_{\alpha\beta}(\underline{r}_1,\underline{r}_2) = \rho^{(1)}_{\alpha}(\underline{r}_1)\rho^{(1)}_{\beta}(\underline{r}_2)g^{(2)}_{\alpha\beta}(\underline{r}_1,\underline{r}_2) \tag{2.4}$$

$$c_\alpha = \rho^{(1)}_{\alpha}(\underline{r}_1) = \langle N_\alpha \rangle_{av}/V \tag{2.5}$$

$$r = |\underline{r}_1 - \underline{r}_2| \tag{2.6}$$

c_α is the bulk concentration of species α; r is the scalar difference of $\underline{r}_1$ and $\underline{r}_2$. Equations (2.4) and (2.6) assume that $g^{(2)}_{\alpha\beta}(r)$ depends only on the relative distance between $\underline{r}_1$ and $\underline{r}_2$, and not on their exact locations within the system. $g^{(2)}_{\alpha\beta}(r)$ is generally a function of density, temperature, composition and the intermolecular forces between molecules of species α and β.

Equations (2.4) and (2.3) together yield the desired relation between density fluctuations in the grand ensemble and the integrals of the radial distribution functions

$$\int \{g^{(2)}_{\alpha\beta}(r) - 1\}d\underline{r} = V \frac{\langle N_\alpha N_\beta \rangle_{av} - \langle N_\alpha \rangle_{av}\langle N_\beta \rangle_{av}}{\langle N_\alpha \rangle_{av}\langle N_\beta \rangle_{av}} - \frac{\delta_{\alpha\beta}}{c_\alpha} \tag{2.7}$$

where the integral extends over all sets of relative coordinates of the pair α and β. It is instructive to note that $g^{(2)}_{\alpha\beta}(r)$ as written represents systems of monatomic fluids only, where the molecules have only translational degrees of freedom. If the system under study consists of molecules with structure, these must be accounted for in the expression for $g^{(2)}_{\alpha\beta}(r)$ and the integration extended over all possible

configurations. In the present discussion, $g^{(2)}_{\alpha\beta}(r)$ is considered to include the averaged effect of all degrees of freedom of the molecule.

In the grand canonical ensemble the relation between density fluctuations and the composition dependence of the chemical potentials is[3]

$$\langle N_\alpha N_\beta \rangle_{av} - \langle N_\alpha \rangle_{av} \langle N_\beta \rangle_{av} = |A_{\alpha\beta}|/|A| \tag{2.8}$$

where

$$A_{\alpha\beta} \equiv \frac{1}{kT} \left(\frac{\partial \mu_\alpha}{\partial N_\beta} \right)_{T,V,N_\gamma} \tag{2.9}$$

and $|A_{\alpha\beta}|$ is the cofactor of $A_{\alpha\beta}$ in the determinant det/A/; μ_α is the chemical potential per molecule of species α. Then, eliminating the density fluctuation between (2.8) and (2.7), we get

$$\frac{1}{kT} \left(\frac{\partial \mu_\alpha}{\partial N_\beta} \right)_{T,V,N_\gamma} = |B_{\alpha\beta}|/V|B| \tag{2.10}$$

where

$$B_{\alpha\beta} = c_\alpha \delta_{\alpha\beta} + c_\alpha c_\beta G_{\alpha\beta} \tag{2.11}$$

$$G_{\alpha\beta} = \int \{g^{(2)}_{\alpha\beta}(r) - 1\} d\underline{r} \tag{2.12}$$

Equation (2.10) deals with fluid mixtures at constant volume and temperature. To obtain relations at constant pressure, we use the Gibbs Duhem equation

$$\sum_{\alpha=1}^{M} N_\alpha \left(\frac{\partial \mu_\alpha}{\partial N_\beta} \right)_{T,P,N_\gamma} = 0 \tag{2.13}$$

and a mathematical relation[4]

$$\left(\frac{\partial \mu_\alpha}{\partial N_\beta} \right)_{T,V,N_\gamma} = \left(\frac{\partial \mu_\alpha}{\partial N_\beta} \right)_{T,P,N_\gamma} + \frac{\bar{v}_\alpha \bar{v}_\beta}{\kappa V} \tag{2.14}$$

where $\bar{v}_\alpha$ is the partial molar volume, per molecule, of species α, and κ is the isothermal compressibility of the mixture. Use of the additive property of the partial molar volumes

$$\sum_{\alpha=1}^{M} N_\alpha \bar{v}_\alpha = V \tag{2.15}$$

results in

$$\kappa kT = |B| / \sum_\alpha \sum_\beta c_\alpha c_\beta |B_{\alpha\beta}| \tag{2.16}$$

$$\bar{v}_\beta = \{ \sum_\alpha c_\alpha |B_{\alpha\beta}| \} / \sum_\alpha \sum_\beta c_\alpha c_\beta |B_{\alpha\beta}| \tag{2.17}$$

$$\left(\frac{\partial \mu_\alpha}{\partial N_\beta} \right)_{T,P,N_\gamma} = \frac{kT}{V|B|} \left[|B_{\alpha\beta}| - \frac{(\sum_\alpha c_\alpha |B_{\alpha\beta}|)(\sum_\beta c_\beta |B_{\alpha\beta}|)}{\sum_\beta \sum_\alpha c_\alpha c_\beta |B_{\alpha\beta}|} \right] \tag{2.18}$$

Equations (2.16), (2.17) and (2.18) are the key equations of the solution theory. For ease of manipulation, they are conveniently expressed in matrix form.[3] Redefining

$$G_{\alpha\beta} = \frac{N}{V} \int \{ g^{(2)}_{\alpha\beta}(\underline{r}) - 1 \} d\underline{r}$$

and further

$$d_{\alpha\beta} = \frac{N}{kT} \left(\frac{\partial \mu_\alpha}{\partial N_\beta} \right)_{T,P,N_\gamma}$$

$$a_{\alpha\beta} = \frac{N}{kT} \left(\frac{\partial \mu_\alpha}{\partial N_\beta} \right)_{T,V,N_\gamma}$$

equations (2.16), (2.17) and (2.18) are written as

$$v/\kappa RT = \underline{i}^t \underline{\underline{B}}^{-1} \underline{\underline{x}}\, \underline{i} \tag{2.19}$$

$$\rho \bar{v}_i = \sum_{j=1}^{M} B^{-1}_{ji} / \underline{i}^t \underline{\underline{B}}^{-1} \underline{\underline{x}}\, \underline{i} \tag{2.20}$$

$$\underline{\underline{x}}\, \underline{\underline{D}} = \underline{\underline{I}} - (\underline{\underline{x}}(\underline{\underline{B}}^{-1})^t \underline{i}\, \underline{i}^t)/\underline{i}^t \underline{\underline{B}}^{-1} \underline{\underline{x}}\, \underline{i} \tag{2.21}$$

where

$$\underline{\underline{B}} = \underline{\underline{I}} + \underline{\underline{x}}\, \underline{\underline{G}} \tag{2.22}$$

$\underline{\underline{A}}$, $\underline{\underline{D}}$ and $\underline{\underline{G}}$ are matrices with elements a_{ij}, d_{ij}, and G_{ij}, respectively, x is a diagonal matrix of mole fractions, $x_{ii} = N_i/N$, $\underline{i}$ is a unit column vector. The basic equation (2.10) relating chemical potentials to the radial distribution function integrals is

$$\underline{\underline{A}} = (\underline{\underline{B}}\, \underline{\underline{x}})^{-1} \tag{2.23}$$

2.2 Direct Correlation Functions

O'Connell has shown[5] that integrals of the direct correlation function may be used in the distribution function solution theory. The direct correlation function is related to the radial distribution function by the Ornstein-Zernike integral equation[2]

$$g(r) - 1 = c(r) + \rho \int c(\underline{r},\underline{r}')\{g(\underline{0},\underline{r}') - 1\}d\underline{r}' \tag{2.24}$$

Like g(r), c(r) is also a function of the intermolecular potential and the macroscopic variables of the system.

There is no conceptual advantage in relating thermodynamic properties to integrals of the direct correlation functions rather than to those of the radial distribution functions. However, on the molecular scale, as r, the distance between molecular centers increases,

the function c(r) goes to zero much more rapidly than the function g(r) - 1.[2,6] Hence, it may be possible that the integral $\int c(r)d\underline{r}$ can be calculated more accurately from a molecular theory than the corresponding integral $\int\{g(r) - 1\}d\underline{r}$. Anticipating these developments, the further results of the distribution function solution theory are presented in terms of integrals of direct correlation functions.

The spatially integrated form of the multicomponent Ornstein-Zernike integral equation is (Appendix A)

$$\underline{\underline{G}} = \underline{\underline{C}} + \underline{\underline{G}}\ \underline{\underline{x}}\ \underline{\underline{C}} \tag{2.25}$$

where
$$C_{ij} = \frac{N}{V}\int c_{ij}^{(2)}(\underline{r}_1,\underline{r}_2)d\underline{r}_2 \tag{2.26}$$

Then from (2.23) and (2.25) we have

$$\underline{\underline{x}}\ \underline{\underline{A}} = \underline{\underline{B}}^{-1} = \underline{\underline{I}} - \underline{\underline{x}}\ \underline{\underline{C}} \tag{2.27}$$

and the equations for thermodynamic properties become

$$\rho\bar{v}_i = \{1 - \sum_{j=1}^{M} x_j\, C_{ij}\}/\{1 - \sum_{j=1}\sum_{k=1} C_{jk}\, x_j x_k\} \tag{2.28}$$

and

$$1/\rho\kappa kT = \{1 - \sum_{j=1}\sum_{k=1} x_j x_k\, C_{jk}\} \tag{2.29}$$

$$\underline{\underline{x}}\ \underline{\underline{D}} = \left(\underline{\underline{I}} - \frac{\underline{\underline{x}}\ \underline{\underline{F}}\ \underline{i}\ \underline{i}^t}{\underline{i}^t\ \underline{\underline{F}}\ \underline{\underline{x}}\ \underline{i}}\right)\underline{\underline{F}} \tag{2.30}$$

where
$$\underline{\underline{F}} = \underline{\underline{I}} - \underline{\underline{x}}\ \underline{\underline{C}} \tag{2.31}$$

Equation (2.30) has elements of the form

$$\frac{N_i}{kT}\left(\frac{\partial \mu_i}{\partial N_j}\right)_{T,P,N_k} = \delta_{ij} - \frac{x_i\{1+C_{ij} - \sum_n x_n(C_{in}+C_{jn}) + \sum_n \sum_m x_n x_m (C_{in}C_{jm} - C_{ij}C_{nm}\}}{1 - \sum_n \sum_m x_n x_m C_{nm}} \tag{2.32}$$

In principle, one can use currently available theories for the distribution functions in the above expressions to calculate thermodynamic properties. However, the volume integrals of the direct correlation functions C_{ij}, (and the radial distribution functions G_{ij}), depend on the macroscopic variables of the system. Their composition dependence must be known before equations (2.32) or (2.18) can be integrated to obtain the Gibbs free energy of the mixture.

However, this restriction is by no means absolute. As in other branches of mathematical physics, one avenue of progress is via functional expansions about those limiting compositions in the mixture at which the distribution functions can be determined with some degree of certainty, e.g., the pure components. Then, within reasonably small ranges about these compositions, the thermodynamic properties can be evaluated by treating the distribution functions as independent of composition.

2.3 Taylor's Series Expansions for Thermodynamic Properties

The integrals C_{ij}, equations (2.25) - (2.32), are generally dependent on the system temperature, density, and the composition. The limiting composition dependence is determined from the behavior of the pure fluid (solvent component) and the infinitely dilute solution (solute component). To relate the discussions to the thermodynamics

of gases in mixed solvents, expansions are derived for the following physical systems:

i) Pure fluid, i.e, pure solvent,

ii) Solute gas in single solvent--binary system,

iii) Solute gas in binary solvent--ternary system.

Component 1 is the solute, 2 and 3 are solvents, superscripts ^{o} and $^{+}$ refer to solute at infinite dilution in single and mixed solvent, respectively. The general expressions will be derived first, i.e., case (iii), and the results for (ii) and (i) inferred as simplifications of the general case.

2.3.1 Solute Gas in Binary Solvent

The general form of functional expansion is:

$$W)_{x_1=x_1} = W)_{x_1=0} + x_1\left(\frac{\partial W}{\partial x_1}\right)_{x_1=0} + \frac{x_1^2}{2}\left(\frac{\partial^2 W}{\partial x_1^2}\right)_{x_1=0} + \ldots \tag{2.33}$$

where W is the thermodynamic property and x_1 is the solute mole fraction. The derivatives $\left(\frac{\partial W}{\partial x_1}\right)$, $\left(\frac{\partial^2 W}{\partial x_1^2}\right)$ are obtained from relations (2.28), (2.29) and (2.32), respectively. The integrals C_{ij} are functions of x_1, and the derivatives include integrals of higher order direct correlation functions. The relations between integrals of different orders are presented in Appendix B. The relation used here for the composition derivatives is equation (B.9). The final results are:

$$\ell n\gamma_1^* = - f_2^+(2x_1 - x_1^2) - f_3^+\left(\frac{3}{2}x_1^2 - x_1^3\right) + \ldots \tag{2.34}$$

where

$$2f_2^+ = -(1 - C_{11}^+) + \frac{(1 - t)^2}{(1 - D)} \tag{2.35}$$

$$3f_3^+ = -(1 - C_{11}^+ - C_{111}^+) + \frac{1 + C_{11}^+\{1 + u - \rho\bar{v}_1^+(1 - w)\}}{(1 - D)}$$

$$+ \rho\bar{v}_1^+[2(1 - 2t)(1 - \rho\bar{v}_1^+) - 3r + \rho\bar{v}_1^+\{3u + D - \rho\bar{v}_1^+(D + w)\}] \tag{2.36}$$

$$\rho\bar{v}_1 = \rho\bar{v}_1^+ + x_1\left\{2\rho\bar{v}_1^+(1 - \rho\bar{v}_1^+) + \frac{\{\rho\bar{v}_1^+[2u+t+D-\rho\bar{v}_1^+(D+w)]-C_{11}^+-r\}}{(1 - D)}\right\} + \cdots \tag{2.37}$$

$$\frac{1}{\rho\kappa RT} = (1 - D) + x_1[2(D - t) - u + w\rho\bar{v}_1^+ - D(1 - \rho\bar{v}_1^+)] + \cdots \tag{2.38}$$

where $D \equiv x_2^2C_{22}^+ + x_3^2C_{33}^+ + 2x_2x_3C_{23}^+$ (2.39)

$$t \equiv x_2C_{12}^+ + x_3C_{13}^+$$

$$u \equiv x_2^2C_{122}^+ + 2x_2x_3C_{123}^+ + x_3^2C_{133}^+$$

$$w \equiv x_2^2C_{222}^+ + 3x_2^2x_3C_{223}^+ + 3x_2x_3^2C_{233}^+ + x_3^3C_{333}^+$$

$$r \equiv x_2C_{112}^+ + x_3C_{113}^+$$

From equation (2.38) with $x_1 = 0$

$$\left(\frac{1}{\rho\kappa RT}\right)_{x_1=0} = (1 - D) \tag{2.40}$$

relating $(1 - D)$ to the compressibility of the solvent mixture. Again, from (2.37) with $x_1 = 0$

$$(\rho\bar{v}_1)_{x_1=0} = (\rho\bar{v}_1)^+ = \left(\frac{1 - t}{1 - D} \right) \tag{2.41}$$

Thus (1 - t) is related to the partial molar volume of the solute at infinite dilution in the solvent mixture.

2.3.2 Pure Component

Setting $x_1 = x_3 = 0$ in (2.38) gives

$$\left(\frac{1}{\rho\kappa RT} \right) = 1 - C_{22}^{o} \tag{2.42}$$

relating C_{22}^{o} directly to the isothermal compressibility of the pure solvent 2.

2.3.3 Gas in Single Solvent

Setting $x_3 = 0$ in (2.38) and (2.37) yields

$$\frac{1}{\rho\kappa RT} = (1 - C_{22}^{o}) + x_1[2(C_{22}^{o} - C_{12}^{o}) - C_{122}^{o} + C_{222}^{o}\,\rho\bar{v}_1^{o} - C_{22}^{o}(1 - \rho\bar{v}_1^{o})]$$

$$+ \ldots\ldots \tag{2.43}$$

$$\rho\bar{v}_1 = \rho\bar{v}_1^{o} + x_1 \frac{-C_{11}^{o} - C_{112}^{o} + 3\rho\bar{v}_1^{o}C_{12}^{o} + 2C_{122}^{o}\rho\bar{v}_1^{o} - \rho\bar{v}_1^{o}C_{22}^{o} - (\rho\bar{v}_1^{o})^2(C_{22}^{o} + C_{222}^{o})}{(1 - C_{22}^{o})}$$

$$+ \ldots\ldots \tag{2.44}$$

where

$$\rho\bar{v}_1^{o} = \frac{1 - C_{12}^{o}}{1 - C_{22}^{o}} \tag{2.45}$$

thus C_{12}^{o} is related to the partial molar volume of solute 1 at infinite dilution in solvent 2. Then, with $x_3 = 0$ in (2.35) and (2.36)

$$2f_2^{o} = -(1 - C_{11}^{o}) + \frac{(1 - C_{12}^{o})^2}{(1 - C_{22}^{o})} \tag{2.46}$$

$$3f_3^\circ = -(1 - C_{11}^\circ - C_{111}^\circ) + \frac{1 + C_{11}^\circ\{1 + C_{122}^\circ - \rho\bar{v}_1^\circ(1 - C_{222}^\circ)\}}{1 - C_{22}^\circ}$$

$$+ \rho\bar{v}_1^\circ[2(1 - 2C_{12}^\circ)(1 - \rho\bar{v}_1^\circ) - 3C_{112}^\circ + \rho\bar{v}_1^\circ\{3C_{122}^\circ + C_{22}^\circ - \rho\bar{v}_1^\circ(C_{22}^\circ + C_{222}^\circ)\}] \tag{2.47}$$

From (2.34)

$$\left(\frac{\partial \ell n \gamma_1^*}{\partial x_1}\right)_{x_1=0} = -2f_2^\circ \tag{2.48}$$

C_{11}° is contained in f_2°, and is thus related to the limiting slope of the composition dependence of the solute activity coefficient. Equations (2.42), (2.45) and (2.48) dictate a hierarchy for the determination of the direct correlation function integrals C_{22}°, C_{12}° and C_{11}° from experimental data. It is:

pure solvent isothermal compressibility gives C_{22}°.

C_{22}° and p.m.v.a.id. give C_{12}°.

C_{22}°, C_{12}° and limiting slope of activity coefficient give C_{11}°.

A similar hierarchy exists in the more general case of the solute in binary solvent. With experimental values of $(\partial \ell n \gamma_1^*/\partial x_1)$, $\rho\bar{v}_1$, $\frac{1}{\rho\kappa RT}$ one can calculate D, t and C_{11}^+ from equations (2.40), (2.41) and (2.35), respectively.

However, no such identification can be made between the thermodynamic properties and the three body integrals C_{ijk}° and C_{ijk}^+. This is a natural consequence of the Taylor's series expansion. The triplet functions result from the composition and density derivatives of two

body integrals in the composition dependent expressions for thermodynamic properties. Therefore, the C_{ijk} must be estimated from experimental data by truncating the expansions after a certain number of terms.

It is appropriate to make some general remarks about the expressions derived thus far. Being expansions about zero composition, they should be valid only in the range of small solute concentrations. To increase the composition range one must include terms from second and higher derivatives of the direct correlation function integrals; these will include triplet and higher order correlation function integrals.

The expressions for isothermal compressibility and partial molar volume indicate an important difference between these properties and the chemical potential. At small concentrations where the linear expressions in x_1 are valid, the chemical potential depends on two-body correlations only, i.e., f_2^o, whereas the compressibility and partial molar volume expressions include two and three-body terms.

Equation (2.42) has another important characteristic; C_{11}^o, which is related to the solute nonideality, appears in the linear term for the partial molar volume. It can be determined from the experimental partial molar volume in its linear range; i.e., from the slope at zero concentration. This presupposes a reliable method for determining the three-body integrals C_{112}^o and C_{122}^o. A generalized method for doing so is described in a later chapter. (One may be tempted to make the simple approximation of setting the $C_{ijk}^o = 0$, but this is not always physically realistic.)

2.4 Linear Composition Dependence of Direct Correlation Function Integrals

It is possible to relate the thermodynamic properties of the solute in the binary mixture to those of the solute in the pure solvents by postulating simple rules for the composition dependence of the quantities C_{ij}. The solution theory itself does not provide any such prescriptions. These must come from a molecular theory for mixtures. The simplest such rule is a linear variation of the form:

$$C_{ij}^{+} = C_{ij}^{*} + x_2(C_{ij}^{o} - C_{ij}^{*}) \tag{2.49}$$

where the superscript * refers to the solvent composition $X_3 = 1$, and the superscript ^{o} refers to the solvent composition $X_2 = 1$. A possible variation of the quantities C_{ij} according to the rule (2.49) is shown in Fig. 2-1. Quantities that can be determined from experimental binary data alone are shown circled. For example, isothermal compressibility of pure 2 gives C_{22}^{o}; C_{22}^{o} and partial molar volume of 3 at infinite dilution in 2 gives C_{32}^{o}; C_{22}^{o}, C_{32}^{o} and limiting slope of activity coefficient of 3 in 2 gives C_{33}^{o}. The quantities C_{13}^{o} and C_{12}^{*} are different from the two-body terms encountered thus far. C_{13}^{o} is the integral of the direct correlation function between one molecule each of 1 and 3 when both are entirely surrounded by a medium of type 2. It is not directly related to any thermodynamic property. A naive approximation for C_{13}^{o} is a mean of C_{12}^{o} and C_{32}^{o}, i.e., simply the arithmetic mean.

$$C_{13}^{o} = \frac{1}{2}(C_{12}^{o} + C_{32}^{o}) \tag{2.50}$$

A more appealing approximation is

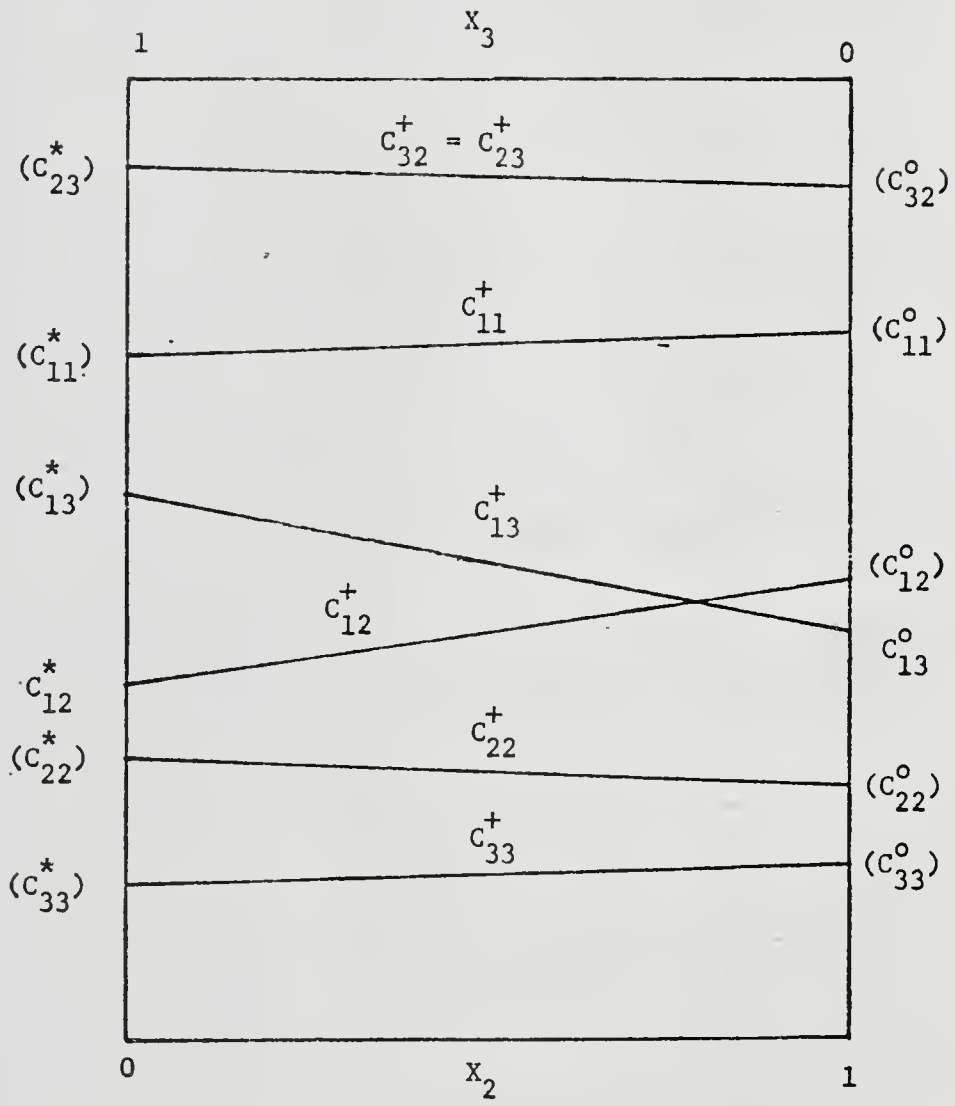

Fig. 2-1. Linear composition dependence of the integrals C^+_{ij} in system of solute in binary solvent. Circled quantities can be determined from binary data alone.

$$C^{o}_{13} = C^{*}_{13} \cdot v^{o}_{2}/v^{*}_{3} \tag{2.51}$$

and is arrived at by the following argument. C^{*}_{13} is the 1-3 interaction in an environment of type 3; C^{o}_{13} results when the environment is changed to type 2 and this is achieved macroscopically by changing the volume in the ratio of the pure component volumes. This assumes that the change in environment is accurately described by size effects. When the solvents 2 and 3 are chemically similar and are composed of nearly equal sized molecules, a realistic assumption is

$$C^{o}_{12} = C^{o}_{13} \tag{2.52}$$

From relationships of the type (2.49) we get

$$\frac{1}{\rho\kappa RT}^{+} = \frac{x_2^2}{\rho^{o}_{2}\kappa^{o}_{2}RT} + \frac{x_3^2}{\rho_3\kappa_3 RT} + 2x_2x_3(1 - x_3C^{*}_{23} - x_2C^{o}_{23})$$

$$- x_2x_3(x_2C^{*}_{22} - x_2C^{o}_{22} - x_3C^{o}_{33} + x_3C^{*}_{33}) \tag{2.53}$$

$$(\rho\bar{v}_1^{+}) = (\rho\kappa RT)^{+}\left[1 - x_2x_3(C^{*}_{12} + C^{o}_{13}) - x_2^2\left(1 - \frac{\bar{v}^{o}_{1}}{\kappa^{o}_{2}RT}\right) - x_3^2\left(1 - \frac{\bar{v}^{*}_{1}}{\kappa^{*}_{3}RT}\right)\right] \tag{2.54}$$

$$2f_2^{+} = x_2C^{o}_{11} + x_3C^{*}_{11} + \frac{(\rho\bar{v}^{*}_{1})^2}{(\rho\kappa RT)^{+}} - 1 \tag{2.55}$$

All quantities on the right side of these equations can be determined from binary experimental data.

The above expressions describe the thermodynamic properties of the solvent mixture over its entire composition range, i.e., from pure 2 to pure 3. The component activity coefficients are expressed in the symmetric convention, i.e.,

$$\mu_2 = \mu_2^{o} + RT\ell n\, x_2\gamma_2 \tag{2.56}$$

The superscripts ^{o} and * again refer to pure 2 and pure 3, respectively. Then

$$\frac{1}{RT}\left(\frac{\partial\mu_2}{\partial x_2}\right)_{N_3,T,P} = \frac{1}{x_2} + \left(\frac{\partial \ell n\gamma_2}{\partial x_2}\right)_{N_3,T,P} \tag{2.57}$$

Using the relation

$$\left(\frac{\partial\mu_2}{\partial x_2}\right)_{N_3} = \left(\frac{\partial\mu_2}{\partial N_2}\right)_{N_3}\left(\frac{\partial N_2}{\partial x_2}\right)_{N_3} = \left(\frac{\partial\mu_2}{\partial N_2}\right)_{N_3}\left(\frac{N_2 + N_3}{x_3}\right) \tag{2.58}$$

in equation (2.32) leads to

$$\left(\frac{\partial \ell n\gamma_2}{\partial x_2}\right)_{N_3} = \frac{1}{x_3} - \frac{1}{x_3\alpha}\left[1 + C_{22} - 2x_2C_{22} - 2x_3C_{23} + x_3^2(C_{23}C_{23} - C_{22}C_{33})\right] \tag{2.59}$$

where

$$\alpha = 1 - x_2^2C_{22} - x_3^2C_{33} - 2x_2x_3C_{23} \tag{2.60}$$

At the compositions of 2 and 3 at infinite dilution in each other, we get

$$\left(\frac{\partial \ell n\gamma_3}{\partial x_3}\right)\Bigg|_{x_3=0} = -\frac{C_{33}^{o} + C_{22}^{o} - 2C_{23}^{o} - (C_{22}^{o}C_{33}^{o} - C_{23}^{o}C_{23}^{o})}{(1 - C_{22}^{o})} \tag{2.61}$$

$$\equiv -e_3$$

and

$$\left(\frac{\partial \ell n\gamma_2}{\partial x_2}\right)\Bigg|_{x_2=0} = -\frac{C_{22}^{*} + C_{33}^{*} - 2C_{23}^{*} - (C_{22}^{*}C_{33}^{*} - C_{23}^{*}C_{23}^{*})}{(1 - C_{33}^{*})} \tag{2.62}$$

$$\equiv -e_2$$

From equation (2.28)

$$\frac{1 - C_{23}^{o}}{1 - C_{22}^{o}} = (\rho \bar{v}_3)^{o} \tag{2.63}$$

$$\therefore \quad C_{23}^{o} = 1 - \bar{v}_3^{o}/\kappa_2^{o}RT \equiv \beta_2 \tag{2.64}$$

Similarly

$$C_{23}^{*} = 1 - \bar{v}_2^{*}/\kappa_3^{*}RT \equiv \beta_3 \tag{2.65}$$

Finally from equation (2.42)

$$C_{33}^{*} = 1 - 1/\rho_3^{*}\kappa_3^{*}RT \equiv \alpha_3 \tag{2.66}$$

$$C_{22}^{o} = 1 - 1/\rho_2^{o}\kappa_2^{o}RT \equiv \alpha_2 \tag{2.67}$$

Then for a linear composition dependence of the C_{ij} we get

$$C_{22} = \alpha_3 x_2(1 - \alpha_2) + x_3(\alpha_3 - \alpha_3 e_2 - (1 - \beta_3)^2) \tag{2.68}$$

$$C_{33} = \alpha_2 x_3(1 - \alpha_3) + x_2(\alpha_2 - \alpha_2 e_3 - (1 - \beta_2)^2) \tag{2.69}$$

$$C_{23} = x_2\beta_2 + x_3\beta_3 \tag{2.70}$$

And, substituting in equations (2.29), (2.28) and (2.59), we get

$$\alpha = \frac{1}{\rho\kappa RT} = 1 - x_2^3\alpha_3(1 - \alpha_2) - x_2^2x_3(\alpha_3 - \alpha_3 e_2 - \overline{1 - \beta_3}^{\,2}) - x_2^3\alpha_2(1 - \alpha_3)$$

$$- x_3^2x_2(\alpha_2 - \alpha_2 e_3 - \overline{1 - \beta_2}^{\,2}) - 2x_2x_3(x_3\beta_3 + x_2\beta_2) \tag{2.71}$$

$$\rho\bar{v}_2 = [1 - x_2^2\alpha_3(1 - \alpha_2) - x_2x_3[\alpha_3 - \alpha_3 e_2 - (\overline{1 - \beta_3})^2] - x_3(x_3\beta_3 + x_2\beta_2)]/\alpha$$

(2.72)

and

$$\left(\frac{\partial \ell n \gamma_2}{\partial x_2}\right) = \frac{1}{x_3} - \frac{1}{\alpha x_3}\,[1 + (1 - 2x_2)\{\alpha_3 x_2(1 - \alpha_2) + x_3[\alpha_3 - \alpha_3 e_2 - (\overline{1 - \beta_3^2})]\} - 2x_3(x_3\beta_3 + x_2\beta_2) + x_3^2\{(x_3\beta_3 + x_2\beta_2)^2 - [\alpha_3 x_2(1 - \alpha_2) + x_3[\alpha_3 - \alpha_3 e_2 - (\overline{1 - \beta_2})^2]]\}\{\alpha_2 x_3(1 - \alpha_3) + x_2(\alpha_2 - \alpha_2 e_3 - \overline{1 - \beta_2^2})\}]] \qquad (2.73)$$

These expressions are used in Chapter 5 to study the thermodynamic properties of liquid-liquid systems.

REFERENCES FOR CHAPTER 2

1. J. G. Kirkwood and F. P. Buff, J. Chem. Phys., 19, 774 (1951).

2. J. S. Rowlinson, Liquids and Liquid Mixtures, Plenum Press, New York, 1969.

3. T. L. Hill, Statistical Mechanics, McGraw-Hill, New York, 1956, p. 113.

4. N. Davidson, Statistical Mechanics, McGraw-Hill, New York, 1962, p. 274.

5. J. P. O'Connell, Mol. Phys., 20, 27 (1971).

6. J. K. Percus in Classical Fluids, edited by H. L. Frisch and J. L. Lebowitz, Benjamin, New York, 1964.

CHAPTER 3

PERTURBATION THEORY FOR MOLECULAR DISTRIBUTION FUNCTIONS OF DENSE FLUIDS

The molecular distribution functions in a real fluid are quite complex functions of its molecular interactions and the macroscopic variables of the system. No complete theory presently exists which can accurately predict the radial distribution function (RDF) in a real fluid in terms of its intermolecular potential and the temperature and bulk density of the system. This situation is even more complex, and hopeless from the point of view of prediction, in a fluid with many chemical species, and hence different molecular interactions.

The problem of describing the RDF and relating it to the intermolecular potential has traditionally been approached in two distinct ways. The first method is the postulation of theories relating the direct correlation function (DCF), the RDF and intermolecular potential. These theories are postulated or derived by techniques such as the diagrammatic methods (HNC theory) or by functional differentiation (Percus Yevick).[1] They provide a relation between $g(r)$, $c(r)$ and $\phi(r)$, where $g(r)$ and $c(r)$ depend on the temperature and density of the system, whereas $\phi(r)$ is assumed independent of the macroscopic conditions. These theories are moderately successful in describing the dense liquid state.[1,2,3]

The other approach to the problem at hand is perturbation theory. In this method the real fluid is modelled as a perturbed state about a reference state[3,4] whose properties can be well determined; the perturbation is usually in the intermolecular potential, and the RDF is

determined as a function of the perturbation parameters. These theories have been quite successful in determination of thermodynamic properties;[5] however, for close agreement, second order terms in the perturbation parameters must be included.

In the present study we have derived a simple, but rigorous, first order perturbation theory for a real fluid. For computational convenience, the base fluid is taken to be the hard sphere fluid, though this is not a requirement of the theory. A first order density expansion is obtained relating the RDF's and DCF's in the real and hard sphere fluids. Combined with the Ornstein-Zernike equation for the real fluid, the perturbation expression provides a scheme for determining the real fluid distribution functions. To reduce the solution of an integral equation to that of computing a numerical integration, an intuitive approximation is made about the nature of the real fluid distribution function. The validity of this approximation is borne out by the close agreement of the calculated RDF to that resulting from computer experiments. The DCF of the real fluid is then calculated from the known intermolecular potential and calculated RDF. It is also numerically integrated to yield $\int c(r)d\underline{r}$, which has earlier been shown to be related to the isothermal compressibility of the pure fluid. The integral is computed as a function of reduced temperature and density giving a table of values of the reduced compressibility integral.

In multicomponent systems, the DCF and its integral depends on the composition, and no theory is yet available to describe this dependence accurately. Empirically, the composition dependence of the

DCF integral is represented as being through the macroscopic volume of the system which depends on the composition. Then, using representative molecular parameters for the different intermolecular attractions present, the DCF integrals in the mixture can be evaluated at any liquid density. This method is used to determine the thermodynamic properties in several mixtures of subcritical components for the infinitely dilute composition states. The agreement between calculated and experimental values is good enough to classify this theory as acceptable, for the purposes for which it is used. Further work in this regard is clearly warranted.

3.1 First-Order Perturbation Theory

The perturbation expression is derived by the method of functional differentiation described by Percus;[6] it is based on the recognition that the molecular distribution functions are functional derivatives of the molecular density at any point in the fluid with respect to a change in potential on the fluid. This provides a precise relation (hierarchy) between molecular distribution functions of different orders.

Details of the derivation are presented in Appendix C. The resulting integral equation is:

$$g^{rf}(r) - 1 + \frac{g^{rf}(r)\exp[\beta\phi^{rf}(r)]}{g^{hs}(r)\exp[\beta\phi^{hs}(r)]} - 1 - g^{hs}(r) - c^{hs}(r)$$

$$= \int \left\{ \frac{-g^{rf}(s)\exp[\beta\phi^{rf}(s)-\beta\phi^{hs}(s)]}{g^{hs}(s)} + 1 - g^{hs}(s) + c^{hs}(s) \right\} \cdot$$

$$[g^{rf}(r') - 1] \; d\underline{r}' \qquad (3.1)$$

where $s = |\underline{r} - \underline{r}'|$. Now making the approximation that for terms within the integral we can write

$$g^{rf}(r) = g^{hs}(r) \tag{3.2}$$

we get

$$y^{rf}(r) - d^{rf}(r) - 1 = \rho \int_0^a [f^{hs}(s)y^{hs}(s) + d^{hs}(s)][e^{-\beta\phi^{hs}(r')}y^{hs}(r') - 1]d\underline{r}'$$

$$+ \rho \int_a^\infty [d^{hs}(s) + 1 - e^{\beta\phi^{rf}(s)}][y^{hs}(\underline{r}') - 1]\ d\underline{r}' \tag{3.3}$$

where we are using Rowlinson's notation[1]

$$y(r) = g(r)e^{\beta\phi(r)}\ ;\quad c(r) = f(r)y(r) + d(r)\ ;\quad f(r) = e^{-\beta\phi(r)} - 1 \tag{3.4}$$

Given an intermolecular potential function, and a value of the reduced hard sphere diameter, $a^* = a/\sigma$, where σ is the distance of zero potential, the real fluid distribution functions can be calculated for any thermodynamic state.

Calculations for the Lennard-Jones 6-12 potential have been made at two thermodynamic states in the dense liquid region. The hard sphere diameter was determined by the Barker-Henderson[3] prescription, and the hard sphere distribution function by the Walts and Henderson[7] modification of the Percus-Yevick equation. The resulting RDF's are shown in Fig. 3-1 and compared with molecular dynamics values[8] of Verlet. For one of the two states, we also show the RDF determined from the usual first order Percus-Yevick theory. As anticipated, the calculated $g^{rf}(r)$ follows the molecular dynamics result closely out to

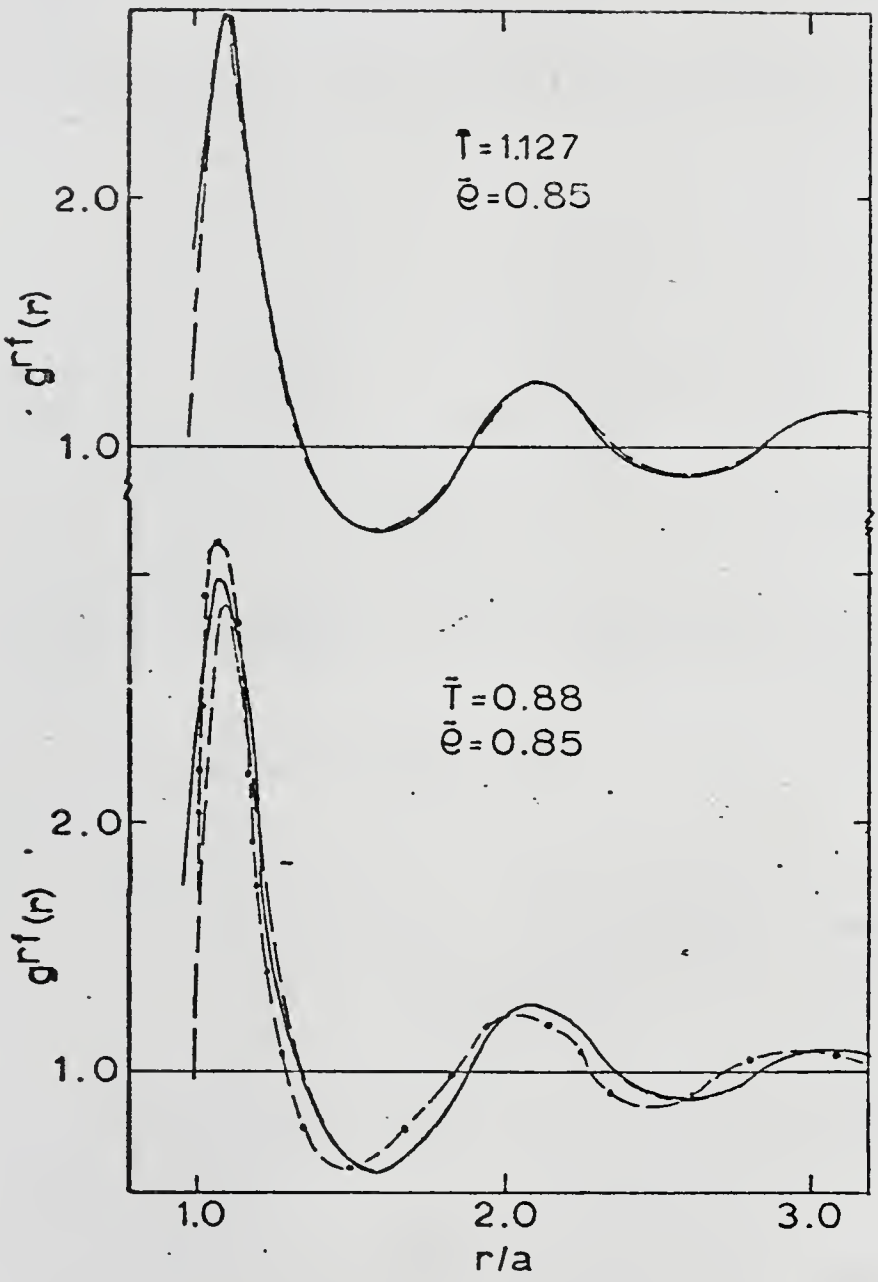

Fig. 3-1. Radial distribution function for Lennard-Jones 6-12 fluid.

large reduced distances in both magnitude and phase, and is clearly an improvement over the Percus-Yevick result. The calculated first peak of $g^{rf}(r)$, which is most important in the determination of thermodynamic properties is also much closer to the molecular dynamics peak than is the Percus-Yevick peak. This indicates that thermodynamic properties determined from the $g^{rf}(r)$ calculated from (3.3) should agree more closely with experimental (computer) results than do those determined from the Percus-Yevick theory.

To obtain improved solutions of $g^{rf}(r)$, equation (3.3) could be used in an iterative solution scheme. It is expected that this procedure will yield results in even closer agreement with molecular dynamics values. In the same fashion, varying the hard sphere diameter in ways other than that of the Barker-Henderson prescription could lead to improved results.

3.2 Reduced DCF Integrals

The agreement obtained between the calculated RDF and Monte Carlo results indicates that the perturbation theory developed here is a satisfactory, if not completely accurate, model of the molecular interactions in a Lennard-Jones 6-12 fluid. We now postulate that within the limits of accuracy, the Lennard-Jones 6-12 potential represents the interactions in a real fluid.

In spherically symmetric intermolecular potentials, the compressibility equation of state, or equation (2.42) is

$$\frac{1}{\rho\kappa RT} = 1 - 4\pi \int_0^\infty c(r)r^2 dr \qquad (3.5)$$

In terms of the reduced variables

$$\tilde{\rho} = \rho\sigma^3, \quad \tilde{T} = \frac{kT}{\varepsilon}, \quad d = \frac{a}{\sigma}, \quad \tilde{r} = \frac{r}{a} \tag{3.6}$$

we have

$$\tilde{\kappa} = \kappa \frac{\varepsilon}{\sigma^3} = \frac{(1 - \tilde{\rho}\,\tilde{C})^{-1}}{\tilde{\rho}\, d^3\, \tilde{T}} \tag{3.7}$$

$$\tilde{C} = 4\pi d^3 \int_0^\infty c(\tilde{r})\, \tilde{r}^2 d\tilde{r} \tag{3.8}$$

The integral $\tilde{C}$ has been calculated for state points covering the entire liquid region, using the perturbation theory developed earlier. Fig. 3-2 shows the variation of this quantity with reduced density at several values of the reduced temperature including the critical temperature and the triple point. At a fixed reduced density, this integral is not a strong function of temperature, and in the dense liquid region, it may be taken as approximately constant. It does vary strongly with reduced density along an isotherm. This is not surprising since the direct correlation function $c(\tilde{r})$, especially at small $\tilde{r}$, is a strong function of density.

It is now a simple matter to calculate the isothermal compressibility of the fluid at a given thermodynamic state. All that is required are appropriate values of the potential parameters σ and ε/k. However, before establishing a general rule for determining these from some known macroscopic property such as a second virial coefficient or shear viscosity, it is advantageous to examine further macroscopic implications of the graphs shown in Fig. 3-2.

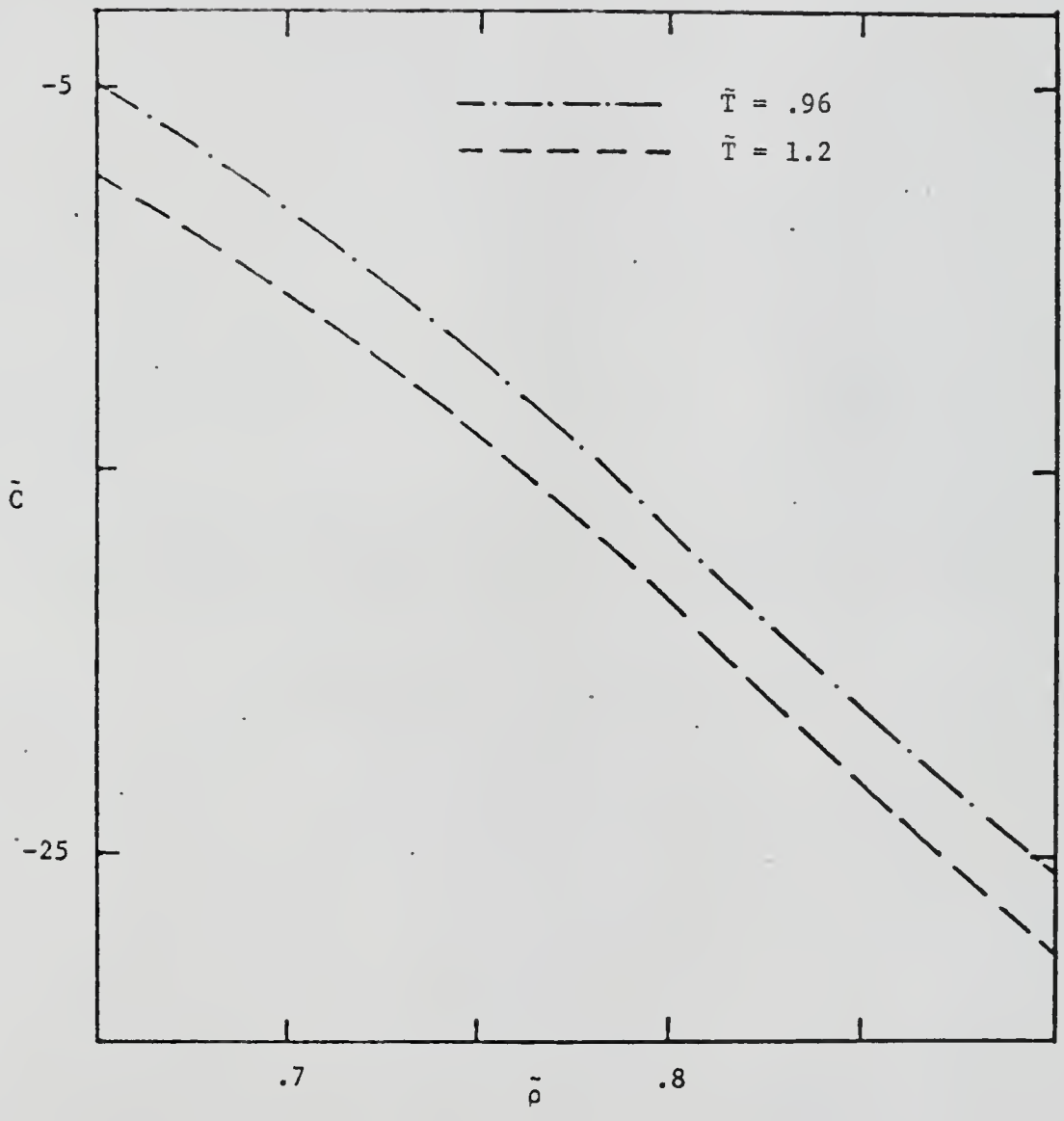

Fig. 3-2. Reduced direct correlation function integral for Lennard-Jones 6-12 fluid from perturbation theory.

The reduced compressibility $\tilde{\kappa}$ can be re-expressed as

$$1 + \frac{1}{\rho\kappa RT} = 1 + \frac{1}{\tilde{\rho}} \tilde{\kappa} \tilde{T} \tag{3.9}$$

Since we know from macroscopic evidence that $\tilde{\kappa}$ depends on $\tilde{\rho}$ and $\tilde{T}$, we expect that $1 + \frac{1}{\tilde{\rho}} \tilde{\kappa} \tilde{T}$ also depends on $\tilde{\rho}$ and $\tilde{T}$. The calculated quantity $1 + \frac{1}{\tilde{\rho}} \tilde{\kappa} \tilde{T}$, where $\tilde{\kappa}$ is obtained from (3.7), is shown in Fig. 3-3. Over the entire liquid range it does not vary with temperature by more than 10% at a fixed reduced density, and may be considered constant. This assumption makes isochoric lines on a P-T plot linear.

The constancy of the reduced compressibility over the temperature range provides the microscopic verification for a macroscopic correlation of the isothermal compressibility of pure fluids. The development of the macroscopic correlation will be discussed in detail later. The general result for pure liquids is that $(1 + \frac{1}{\rho\kappa RT})$ is a universal function of a reduced density and is independent of temperature. The reducing density is close to the critical density for nonpolar liquids, and larger than the critical for polar liquids. These correlating densities are used as the source of molecular parameters in the microscopic theory. Existence of the correlation asserts that macroscopic corresponding states is valid for this property, and the representation of all molecular interactions is equivalent to postulating corresponding states on the microscopic level. Then taking Argon as the prototype or reference substance, i.e., as satisfying both macroscopic and microscopic corresponding states, the molecular parameters for the other fluids are determined from the relation

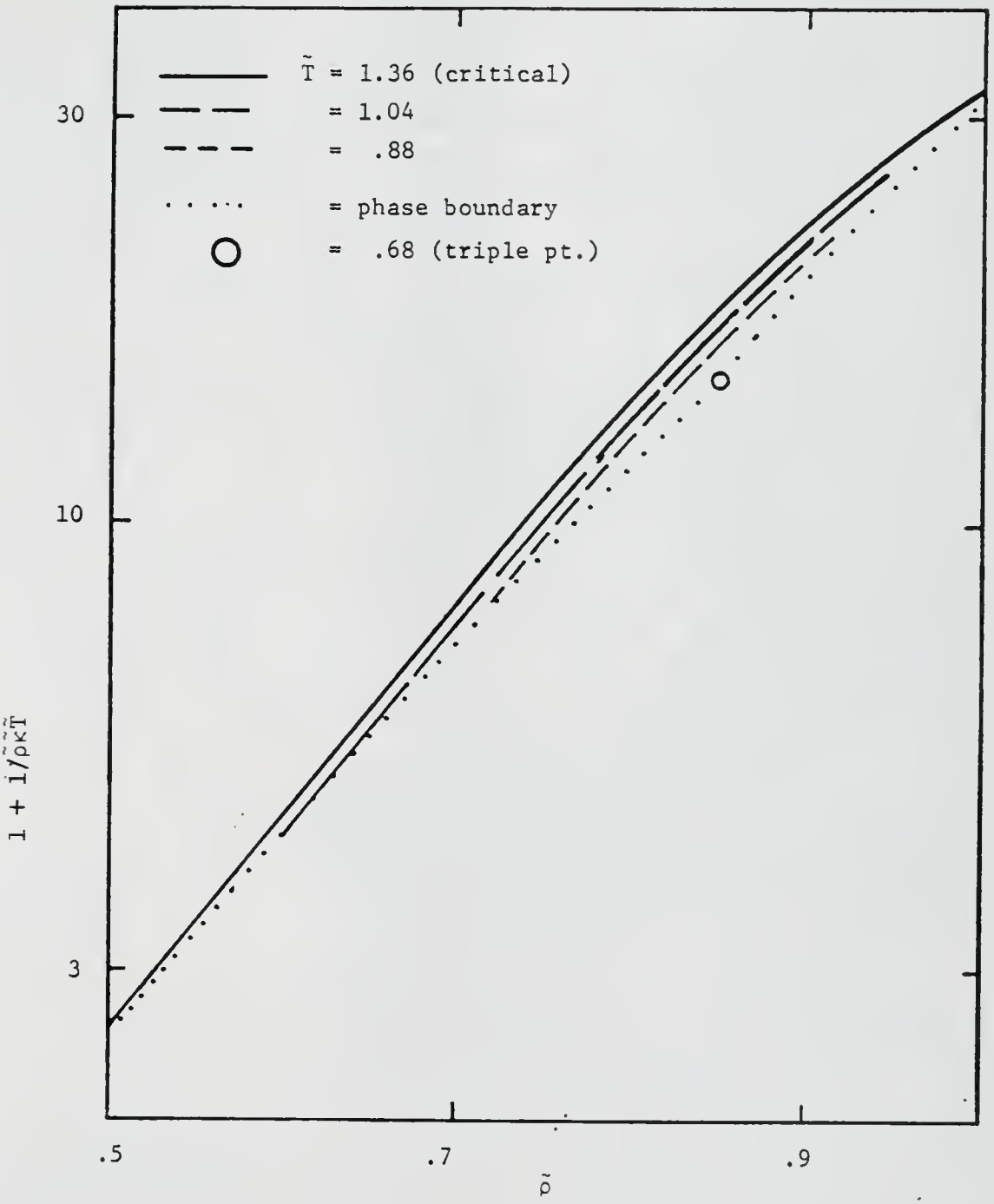

Fig. 3-3. Microscopic correlation of isothermal compressibility for Lennard-Jones 6-12 fluid.

$$\sigma = \sigma_{Ar}\left(\frac{v^*}{v^*_{Ar}}\right)^{1/3} \tag{3.10}$$

where v^* is the reciprocal reducing density for the macroscopic correlation. Values of σ for some substances are shown in Table 3-1.

TABLE 3-1

INTERMOLECULAR PARAMETERS FOR SIMPLE FLUIDS

Substance →	Ar	CH_4	N_2	O_2	CO	C_2H_4
v^* cc/mole →	74.57	99.5	90.1	73.4	93.1	127.3
σ Å →	3.405[+]	3.749	3.627	3.387	3.666	4.069

H_2O	CCl_4	C_6H_6	SO_2	C_3H_8	nC_4H_{10}
46.4	276.0	255.0	115.0	200.0	255.0
2.907	5.267	5.130	3.934	4.752	5.130

CS_2	CH_3OH	NH_3	Cyclohexane
165.0	101.5	65.18	311.0
4.437	3.774	3.756	5.481

[+]From second virial coefficient data

The value of σ_{Ar} is taken from second virial coefficient data. For other substances, the value calculated from (3.10) is generally smaller than that obtained from second virial coefficients. The highly polar substances, water and methanol, have relatively much smaller values of σ.

The function $\tilde{C}$ is assumed temperature independent at a fixed reduced density and no temperature related molecular parameter is necessary to characterize the microscopic state of the fluid. $\tilde{C}$ at a given $\tilde{\rho}$ is determined from Fig. 3-1.

3.3 Multicomponent Systems

In a mixture the quantities C_{ij} depend on the molecular interactions and the macroscopic state of the system. No present day molecular theory can describe the composition dependence accurately. (The multicomponent perturbation theory of Barker-Henderson-Smith[10] is a first attempt at describing the composition dependence of the multicomponent radial distribution function.)

An intuitive method is proposed here to represent the dependence of C_{ij} on the system variables. It is based on two postulates, which are:

1. All molecular interactions in the mixture, ϕ_{ij}, are of the same type; i.e., they are representable by a unique reduced potential function, the Lennard-Jones 6-12 potential.

2. The composition dependence of the C_{ij} is completely described by the macroscopic density of the system, which is composition dependent. This assumption neglects the effects on C_{ij} of composition changes at constant density but emphasizes that the most significant parameter for determining C_{ij} is the macroscopic density.

On the basis of these two postulates, the general reduced integral $\tilde{C}_{ij}$ may be written as

$$\tilde{C}_{ij} = F(\tilde{\rho}_{ij}) = F(\tilde{\rho}_{ij})_{\tilde{T}=1} = F(\rho\sigma_{ij}^3)_{\tilde{T}=1} \tag{3.11}$$

where σ_{ij} is the size parameter for the i-j interaction. Here, it is calculated from the arithmetic mean rule

$$\sigma_{ij} = \frac{1}{2} (\sigma_{ii} + \sigma_{jj}) \tag{3.12}$$

These equations form a method for determining the integrals C_{ii}, C_{jj} and C_{ij} at any given liquid density from which the thermodynamic properties can be calculated. The calculated thermodynamic properties for some binary systems are shown in Table 3-2 and compared with experimental values as available. The composition dependent integrals C_{ij} have been calculated only at the state of infinite dilution of component 1 in component 2. For all systems of simple molecules Ar, O_2 and N_2, there is good agreement between calculated and experimental isothermal compressibilities and partial molar volumes at infinite dilution. This indicates that the molecular representation assumed by the theory is quite valid for these systems. For the other systems of more complex molecules, the agreement is only qualitative, although the trends of all calculated quantities are in the direction of the experimental values.

Comparison of the calculated C^{o}_{ij} with the experimental values, where these are available, indicates that the calculated C^{o}_{ij} are not negative enough, e.g., C^{o}_{22} in the n-pentane systems. The larger negative values necessary are obtained only by calculating the quantities at larger reduced densities (i.e., the σ values are too small), or by introducing a temperature dependent parameter into the formulation of the theory, which would then allow somewhat larger negative C^{o}_{ij}. However, it is more likely that the assumptions of conformal solutions

TABLE 3-2

THERMODYNAMIC PROPERTIES IN SUBCRITICAL SYSTEMS FROM PERTURBATION THEORY[+]

System 1	System 2	T °K	v_2^o cc/mole	C_{11}^o	C_{22}^o	C_{12}^o	$\frac{1}{\rho\kappa RT}$ Calc	$\frac{1}{\rho\kappa RT}$ Expt	$\bar{v}_1^o$ cc/mole Calc	$\bar{v}_1^o$ cc/mole Expt	$\left(\frac{\partial \ln \gamma_1}{\partial x_1}\right)_{x_1=0}$ Calc	$\left(\frac{\partial \ln \gamma_1}{\partial x_1}\right)_{x_1=0}$ Expt
N_2	Ar	83.78	28.19	-30.0	-19.5	-26.0	20.5	21.2	37.1	35.4	-4.56	-
Ar	O_2	83.78	27.30	-22.0	-21.0	-21.0	22.0	23.5	27.3	28.7	1.0	-
Ar	O_2	90.0	28.05	-20.0	-18.0	-19.0	19.0	18.6	29.5	29.5	- .053	-
C_6H_6	nC_5H_{12}	288.	114.41	- 8.5	-21.0	-14.0	22.0	24.8	78.0	89.1	- .73	-
nC_5H_{12}	C_6H_6	288.	88.33	-34.0	-26.0	-30.0	27.0	42.6	101.0	115.1	- .59	-
nC_4H_{10}	nC_6H_{14}	298.	132.0	- 6.0	-23.0	-12.0	24.0	31.6	71.5	104.9	- .04	-
nC_4H_{10}	C_6H_6	298.	89.0	-25.5	-25.5	-25.5	26.5	37.2	89.0	105.0	.00	-
C_6H_{12}	nC_5H_{12}	288.	114.41	-22.0	-21.0	-21.5	22.0	24.8	117.0	107.3	-1.01	-
nC_5H_{12}	cyclohex	288.	107.51	-25.5	-25.9	-25.8	26.9	43.5	107.11	113.5	- .20	-
C_6H_6	cyclohex	298.	108.7	-11.1	-25.03	-18.0	26.0	38.5	79.43	91.7	-1.77	-.0247
cyclohex	C_6H_6	298.	89.0	-36.7	-27.7	-34.0	28.7	37.2	108.5	111.2	-4.98	-.0247
C_6H_6	cyclohex	343.	115.1	- 7.5	-21.3	-14.0	22.3	22.6	77.4	97.6	-1.59	-.0175
cyclohex	C_6H_6	343.	94.75	-30.5	-20.8	-26.0	21.8	22.1	117.35	118.0	-1.94	-.0175

[+]Sources of experimental data in Tables 4-1, 4-2, 4-3, 5-1, 5-5.

(potentials) and pairwise additivity break down for complex molecules in dense systems.

Nevertheless, the above theory provides a basis for the qualitative, and often quantitative, understanding of the state dependence of the direct correlation functions and their integrals. Two valid conclusions can be drawn:

1. The calculated integrals C^{o}_{11}, C^{o}_{22} and C^{o}_{12} are approximately in the correct ratio to one another.

2. When the calculated integral C^{o}_{22} is within 5-10% of the experimental value, the calculated C^{o}_{12} and C^{o}_{11} are also within this range of the corresponding experimental quantity. When the theory is inadequate in predicting experimental data, it is due to the poor modelling of the pure solvent state.

REFERENCES FOR CHAPTER 3

1. J. S. Rowlinson, Rept. Progr. Phys., 28, 169 (1965).
2. J. S. Rowlinson, Mol. Phys., 10, 533 (1966).
3. J. A. Barker and D. Henderson, J. Chem. Phys., 47, 2856 (1967).
4. J. D. Weeks et al., J. Chem. Phys., 54, 5237 (1971).
5. J. A. Barker and D. Henderson, J. Chem. Phys., 47, 4714 (1967).
6. J. K. Percus in Classical Fluids, edited by H. L. Frisch and J. L. Lebowitz, Benjamin, New York (1964).
7. R. O. Watts and D. Henderson, Mol. Phys., 16, 217 (1969).
8. L. Verlet, Physical Review, 165, 201 (1968).
9. F. Mandel et al., J. Chem. Phys., 52, 3315 (1970).
10. W. R. Smith and D. Henderson, Mol. Phys., 19, 411 (1970).

CHAPTER 4

MACROSCOPIC STATE DEPENDENCE OF DIRECT CORRELATION FUNCTION INTEGRALS

In the preceding chapter we studied a molecular theory for the state dependence of the DCF integrals. Although the generalized microscopic method gave some adequate results for thermodynamic properties, there are still areas of uncertainty in the molecular approach, and no real clues are provided for improvements to the molecular theory. In this chapter we study the available macroscopic data to determine the state dependence of the DCF integrals.

A definite hierarchy exists in the calculation of C_{22}^{o}, C_{12}^{o} and C_{11}^{o} from experimental data, and this order is followed in searching for macroscopic correlations. Generalized equations for the temperature variation of the pure solvent saturation pressure and liquid volumes are combined with the previously derived correlations to derive the temperature and pressure dependence of the C_{ij}.

4.1 Corresponding States Correlations for C_{22}^{o} and C_{12}^{o}

The DCF integral C_{22}^{o} is related to the isothermal compressibility, κ, of a pure fluid by the equation

$$1 - C_{22}^{o} = \frac{1}{\rho_2^{o}\kappa_2^{o}RT} \tag{4.1}$$

It is experimentally derived from P-V-T measurements of compression experiments. Commonly, the compression data are filled to analytic and fitted expressions such as the Tait Equation (for most liquids) and the

Huddleston equation (liquid hydrocarbons).[1] Experimentally, κ for a pure liquid is found to be a strong function of temperature, and very weakly dependent on pressure. As the temperature approaches the critical, the isothermal compressibility of the saturated liquid becomes very large.

In Fig. 4-1, the experimental quantity $1 + 1/\rho\kappa RT$ is shown as a function of ρ for several simple liquids; the plot for n-decane is along an isotherm (358°K), i.e., a compressed liquid, while the others are along the liquid vapor saturation line. The curves are all similar in shape and one concludes that there exists a general correlation of the form

$$\left(1 + \frac{1}{\rho\kappa RT}\right) = F(\tilde{\rho}) = F(\rho v^*) \tag{4.2}$$

Experimental compressibility data for Ar, O_2, N_2, CH_4, CCl_4, $nC_{10}H_{22}$, $nC_{12}H_{26}$, $nC_{14}H_{30}$ and $nC_{16}H_{34}$ are used to derive an analytical expression for this general relationship. The first five of these substances are chosen among the primary set because they are simple molecules. Further, their characteristic volumes can be taken as the critical volumes to yield a set of curves for $\left(1 + \frac{1}{\rho\kappa RT}\right)$ that are coincident within experimental error. The function $\left(1 + \frac{1}{\rho\kappa RT}\right)$ then has a limiting value of unity as $\tilde{\rho} = \rho v^* \to 1$; however, detailed experimental data are not available in this lower reduced density range. The reduced density range for this set of substances extends over $1.5 \leq \tilde{\rho} \leq 2.9$. The long chain hydrocarbons are included in the primary set to extend the reduced density range of the correlation to larger

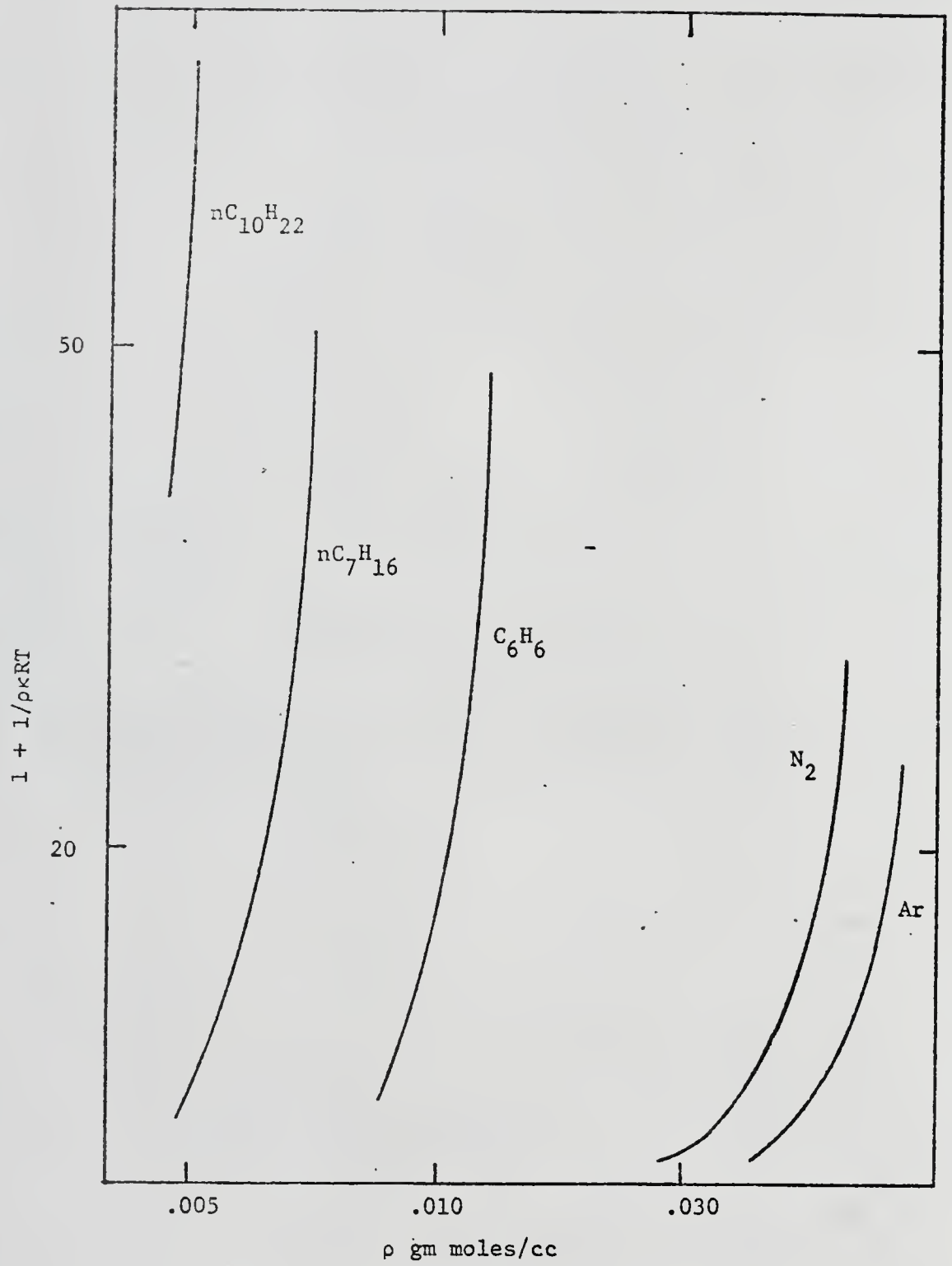

Fig. 4-1. Isothermal compressibilities of pure liquids.

values; their compressibilities are reported to be of a high degree of accuracy ($\pm$ 1%). The characteristic volumes for these hydrocarbons are obtained by matching the experimental data to the curve for simple substances in the region of overlap. The algebraic expression obtained to represent the experimental data over the range $1.5 \leq \tilde{\rho} \leq 3.7$ is

$$2 - C_{22}^{o} = 1 + \frac{1}{\rho \kappa RT} = \exp[-.42704(\tilde{\rho} - 1) + 2.089(\tilde{\rho} - 1)^2 - .42367(\tilde{\rho} - 1)^3] \tag{4.3}$$

Fig. 4-2 is the graphical representation of equation (4.3) and shows some representative experimental data to indicate the average error of prediction. For all substances other than those listed above, the characteristic volumes were obtained by fitting experimental compressibility data to equation (4.3). For nonpolar substances, the fitted characteristic volumes are estimated to be within the errors of experimental and predictive methods for the critical molar volume. Thus, in the absence of experimental compressibility data, the critical volume of a nonpolar substance or a weakly polar substance may be used as the characteristic volume. For polar substances, however, e.g., water and methanol, v^* as fitted from equation (4.3) is found to be less than v_c. (On the molecular scale, v^* is related to the distance parameter in the angle averaged or effective spherical potential.) There is no clear and lucid explanation of this relationship, however, that would permit the determination of v^* from other macroscopic data. Therefore, this parameter must be obtained from at least one experimental point.

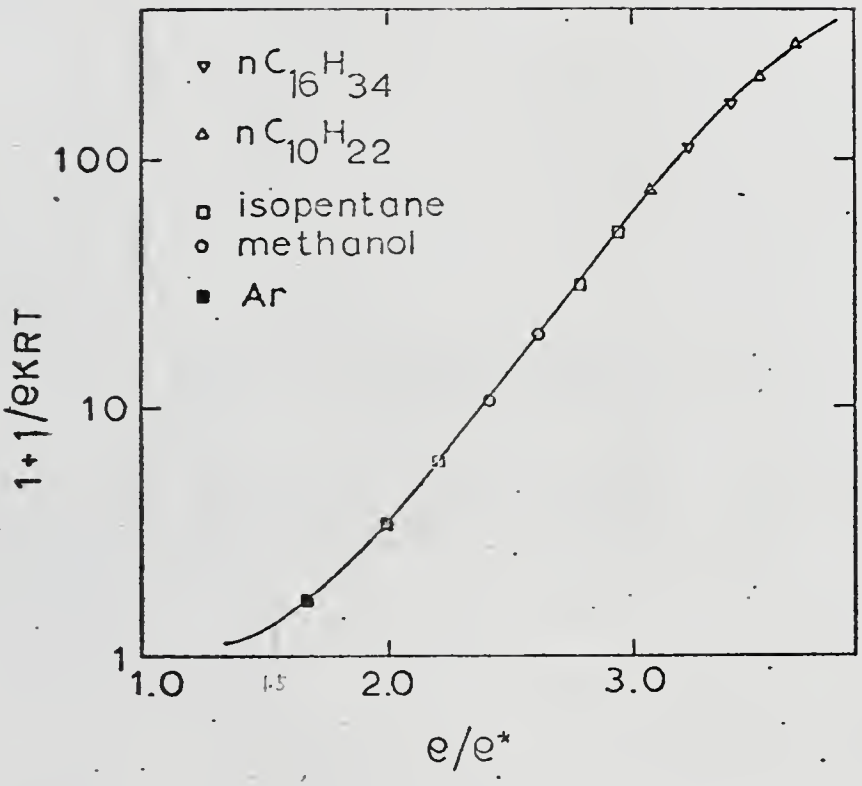

Fig. 4-2. Generalized correlation for isothermal compressibility of liquids.

The results of compressibility calculations with equation (4.3) are shown in Table 4-1 for nine representative substances. δ, the fractional root-mean-square deviation in $1 + \frac{1}{\rho\kappa RT}$, is always less than 0.08; the largest single error in $1 + \frac{1}{\rho\kappa RT}$ encountered over an aggregate of 70 state points is 11%. Characteristic volumes for all the substances included in the correlation are presented in Table 4-2; the list contains liquids of all types, polar, nonpolar, long chain and branched hydrocarbons, alcohols, esters, inorganic liquids, etc. In general, for substances with known characteristic parameters, both polar and nonpolar, equation (4.3) provides a value of κ with an average deviation of 6-8% at $\tilde{\rho}$ greater than 1.5.

In a binary solution, C_{12}^{o} is related to the partial molar volume of component 1 at infinite dilution in component 2. (When component 1 is a gas, whose critical temperature is appreciably lower than the temperature of the solution, the infinitely dilute state is a thermodynamically conceptualized state.) The partial molar volume is determined experimentally by observing the change in volume of the mixture as the component composition is changed. It is then extracted from the experimental volume by the general procedure for partial molar properties and extrapolated to zero composition. If the solution is assumed to be ideal, the partial molar volume at infinite dilution (pmv aid) can be obtained from the change in solute solubility with pressure. Eqn. (2.45) is

$$\rho\bar{v}_1^{o} = (1 - C_{12}^{o})/(1 - C_{22}^{o}) \tag{4.4}$$

$$\therefore \quad \bar{v}_1^{o} = v_2^{o}(1 - C_{12}^{o})/(1 - C_{22}^{o}) \tag{4.5}$$

C_{12}^{o} was calculated from equations (4.5) and (4.3) with experimental

TABLE 4-1

GENERALIZED CORRELATION FOR LIQUID COMPRESSIBILITY

Substance	Temp. Range °K	# Data Points	v^* cc/g mole	v^*/v_c	RMS Deviation %	Data Reference
Argon	81 - 140	9	74.57	1.0	4.4	1
CH_4	90.66- 100	11	99.5	1.0	5.8	1
N_2	63.18- 120	7	90.1	1.0	3.1	1
O_2	60 - 150	9	73.4	.986	6.4	1
$C_{10}H_{22}$	298 - 358	10	602	1.0	3.5	2
$C_{40}H_{82}$	423 - 573	4	2575	1.016+	2.6	3
Benzene	278 - 473	7	255	.981	4.8	1
PSU 88‡	311 - 408	3	1530	-	3.8	4
Water	273 - 573	10	46.4	.828	6.9	1

+Critical volume estimated by Lyderson's method. See reference 5.

‡Complex hydrocarbon. See reference 4 for formula.

TABLE 4-2-a

REDUCING VOLUMES FROM ISOTHERMAL COMPRESSIBILITIES[a]

Substance	Temp. Range °K	# Data Points	RMS Dev. %	v^* cc/g mole	Data Reference
CCl_4	250 - 343	11	4.7	276[b]	1
$nC_{12}H_{26}$	298 - 358	5	6.0	730	2
$nC_{14}H_{30}$	318 - 358	4	5.0	845	2
$nC_{16}H_{34}$	298 - 358	4	5.8	970	2
C_3H_8	310 - 327	6	5.5	200[b]	6
nC_4H_{10}	310 - 344	6	8.6	255[b]	7
nC_5H_{12}	273 - 344	5	6.2	309	3
iso C_5H_{12}	223 - 298	4	3.5	308[b]	11
nC_6H_{14}	273 - 444	6	6.1	369[b]	3
nC_7H_{16}	273 - 473	7	3.1	425[b]	1
nC_8H_{18}	403 - 553	6	3.2	489	3
nC_9H_{20}	303 - 473	5	2.9	541[b]	3
$nC_{11}H_{24}$	298 - 473	3	5.75	670	3
$nC_{13}H_{28}$	323 - 473	3	2.9	783[b]	3
$nC_{15}H_{32}$	333 - 408	3	2.5	915	4
$nC_{17}H_{36}$	323 - 523	3	3.6	1035[b]	3
$nC_{18}H_{38}$	333 - 408	3	2.58	1100[b]	4
$nC_{20}H_{42}$	323 - 573	6	3.4	1225	3
$nC_{30}H_{62}$	373 - 573	3	2.82	1880	3
$C_6H_5CH_3$	223 - 298	4	3.7	312	11
$C_6H_5NO_2$	298 - 358	4	3.3	321	8
$C_6H_5NH_2$	298 - 358	4	2.78	285	8
C_6H_5Cl	298 - 358	4	1.0	306	8
C_6H_5Br	298 - 358	4	2.68	321	8
O-xylene	298	2	3.3	363.5	9
m-xylene	298	2	2.6	362.5	9
Cumene	298	2	2.1	298	9

[a] Also for use in partial molar volume correlation

[b] Within .5% of experimental or predicted critical volume.

TABLE 4-2-a (Continued)

Substance	Temp. Range °K	# Data Points	RMS Dev. %	v^* cc/g mole	Data Reference
Mesitylene	298	2	1.9	423	9
Tetrahydronaphthalene	298	2	3.0	430.2	9
CH_2Cl_2	303 - 323	2	.06	168.8	10
$C_2H_5OOCH_3$	303 - 323	2	7.5	283	10
$CHCl_3$	298	2	.55	219.6	9
Cyclohexane	298 - 348	4	1.21	311	12
Isopropyl ether	323	1	-	415.8	10
Tetrahydrofuran	303 - 323	2	6.9	237	10
Ethyl Ether	273 - 413	8	6.5	281.2	15
$(CHCl_2)_2$	298	1	-	286.7	13
$(CCl_2)_2$	298	1	-	303.6	13
$(CH_2Cl)_2$	298	1	-	226	13
$CHCl\ CCl_2$	298	1	-	258.9	13
$(CHCl)_2$	298	1	-	208.6	13
CH_3CHCl_2	298	1		233	13
CH_3COCH_3	298	1		200.2	13
PSU 25[c]	310 - 408	4	3.6	1550	14
PSU 19[c]	310 - 408	4	2.7	1465	14
PSU 174[c]	352 - 408	4	3.7	1332	14
PSU 528[c]	333 - 408	4	8.3	785	14
PSU 532[c]	333 - 408	5	5.9	933	14
PSU 537[c]	333 - 408	5	5.1	1116	14
PSU 175[c]	333 - 408	3	1.1	1452	14
PSU 12[c]	333 - 408	3	1.8	1368	14
PSU 574[c]	333 - 408	3	3.7	800	14
PSU 575[c]	333 - 408	3	5.4	873	14
PSU 122[c]	373 - 408	3	.75	1708	14
CS_2	298 - 358	4	2.0	165	14

[c] Complex hydrocarbon. See reference 14 for formula.

TABLE 4-2-a (Continued)

Substance	Temp. Range °K	# Data Points	RMS Dev. %	v^* cc/g mole	Data Reference
Methanol	273 - 323	3	2.7	101.5	9
Propanol	298	4	2.5	160.3	9
NH_3	253 - 313	16	8.8	65.18	17

TABLE 4-2-b

CHARACTERISTIC VOLUMES DETERMINED FROM PARTIAL MOLAR VOLUMES AT INFINITE DILUTION[a,b]

Substance	# Data Points	# Solvents	v^* cc/g mole
CO	10	3	93.1[c]
CO_2	6	2	80
H_2	19	5	51.5[d]
C_2H_6	4	4	158
CF_4	2	2	139
C_2H_4	3	3	127
C_2H_2	3	3	112.6[c]
$(CH_3)_2O$	3	3	169.7
CH_3Cl	3	3	136.5
SO_2	3	3	115

[a] Also for use in compressibility correlation.

[b] Sources of experimental data quoted in Table 4-3.

[c] Assigned to be critical volume.

[d] Effective critical volume. See reference 28.

data on a wide variety of solute (1) and solvent (2) pairs. In cases where the total experimental pressure had not been reported, the volume of the pure solvent was taken as that of the saturated liquid. Hypothesizing a general dependence of the DCF integrals on the reduced solvent density, the variation of C_{12}^{o} was found to be similar, but not identical, for all solute-solvent pairs. A factor accounting for the relative molecular sizes, as represented by the ratio of the characteristic volumes, was introduced. The empirical relationship obtained for C_{12}^{o} is shown in Fig. 4-3, with some representative systems. The analytic expression for this relationship is

$$\ell n \left(-C_{12}^{o} \left[\frac{v_2^*}{\bar{v}_1^*} \right]^{.62} \right) = -2.4467 + 2.12074\ \tilde{\rho}_2^{o} \ ; 2.0 \leq \tilde{\rho}_2^{o} \leq 2.785$$

$$= 3.02214 - 1.87085\ \tilde{\rho}_2^{o} + .71995\ \tilde{\rho}_2^{o2} ; 2.785 \leq \tilde{\rho}_2^{o} \leq 3.2 \qquad (4.6)$$

Calculation of $\bar{v}_1^{o}$ for a solute-solvent pair of known characteristic parameters thus requires only a knowledge of v_2^{o}, the pure solvent volume. C_{12}^{o} is obtained from (4.6), C_{22}^{o} from (4.3) and $\bar{v}_1^{o}$ from (4.5). $\tilde{\rho}_2^{o}$ is the reduced solvent density and is used in both correlations.

The numerical coefficients in equation (4.6) were generated using $\bar{v}_1^{o}$ for seven gases in different solvents. For Ar, N_2, O_2 and CH_4 the characteristic parameters had been determined earlier from compressibility measurements. For CO and C_2H_2, the choice of the critical volume as the characteristic parameter proved satisfactory; similarly the effective critical volume was chosen for H_2.

Equation (4.6) provides a satisfactory representation of

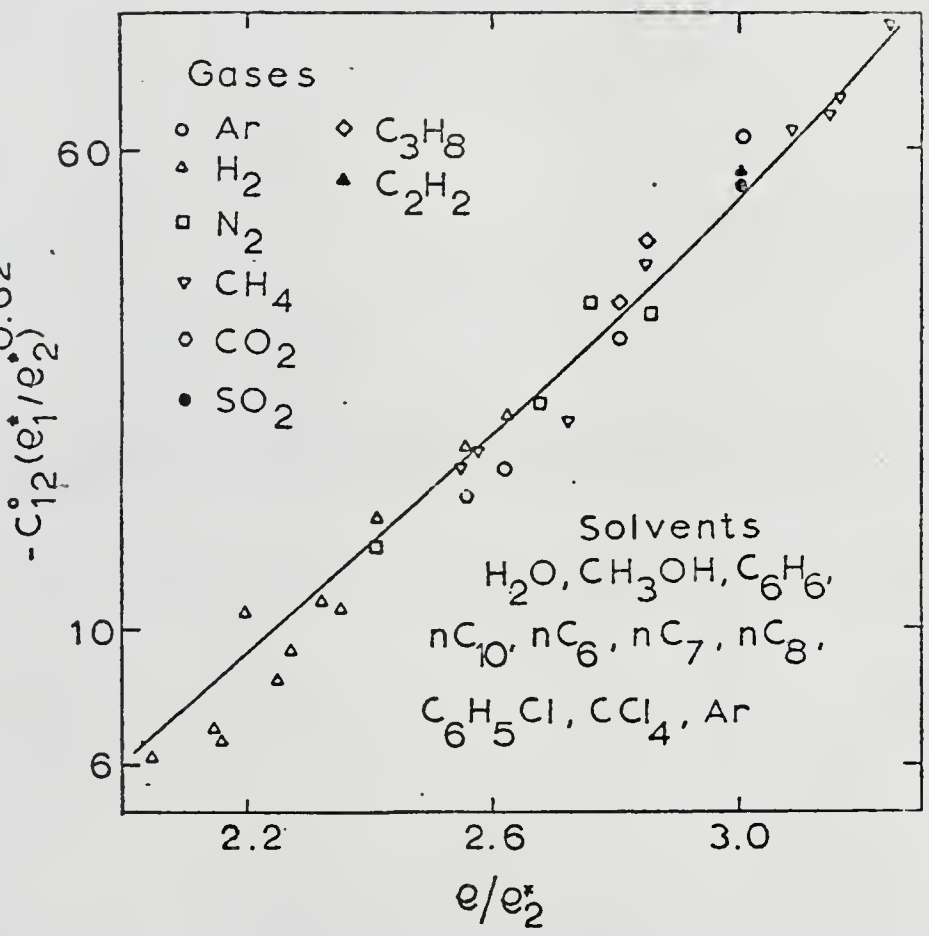

Fig. 4-3. Generalized correlation for partial molar volumes of gases at infinite dilution in liquids.

experimental partial molar volumes. Since the experimental variable in the correlation is the solvent density, which is a function of both temperature and pressure, the variation of the volumetric properties with pressure is partially accounted for by equation (4.6). Partial molar volumes for varied gas-solvent systems as calculated from equation (4.6) are shown in Table 4-3, and compared with experimental data. Also shown are volumes calculated from the generalized correlation of Lyckman,[29] which is based on a cohesive energy density for the solvent. The accuracy of the two correlations is similar for saturated systems at low temperatures. However, since the correlation of equation (4.6) is based on the reduced solvent density which is a function of both temperature and pressure, it can account for the pressure effect on volumetric properties to some extent, and for the rapid change in solvent volume at temperatures approaching the critical. This is clearly seen in the hydrogen-benzene system where a 30% change in partial molar volume with pressure is well predicted, and the high temperature value is correlated closely.

The characteristic parameters for several substances other than the seven previously listed, were obtained by fitting experimental partial molar volumes to equation (4.6). In each case, $\bar{v}_1^o$ for the gas in several different solvents was used. They are shown in Table 4-2-b.

4.2 Generalized Isothermal Equation of State for Liquids

Macroscopic experimental evidence, equation (4.3), shows that the function $1 + \frac{1}{\rho\kappa RT}$ is a universal function of reduced density for all liquids. Substituting for $\rho\kappa$ from equation (4.3) into equation (1.15)

TABLE 4-3

PARTIAL MOLAR VOLUMES OF GASES AT INFINITE DILUTION

Solute	Solvent	T,°K	$\tilde{\sigma}$	$\bar{v}_1^o$ cc/gm mole			Data Reference
				Calculated	Experiment	Lyckman	
CH_4	nC_7	300	2.86	56.6	55.4	58.2	17
CF_4	CCl_4	300	2.845	69.1	79.7	66.3	
CF_4	nC_7	300	2.86	88.7	86.4	73.7	
H_2	C_6H_6	298	2.865	31.1	35.0	37.1	18
		403	2.496	57.4	58.3	52.7	
			2.521	53.9	53.7		
			2.55	51.4	49.7		
		433	2.375	66.9	72.1	60.6	
			2.412	63.0	64.0		
			2.443	56.7	57.5		
		473	2.197	92.9	104.4	64.7	
			2.251	81.6	85.6		
			2.296	69.0	72.5		
H_2	nC_8	403	2.646	68.4	63.6	59.8	
			2.683	62.8	58.0		
			2.716	57.55	53.3		
		473	2.355	104.6	110.3	67.9	
			2.422	86.2	87.6		
			2.474	77.1	72.7		
CH_4	nC_6	298	2.776	59.1	60.2	62.5	19
C_2H_6				76.8	67.9	72.	
C_3H_8				88.8	93	93.2	
nC_4				102.5	104.9	107.3	
Ar				50.4	51.5	53.4	
N_2				55.8	62.8	59.1	
O_2				49.7	55.7	52.7	
H_2	CCl_4	298	2.838	33.6	38	39.2	20
Ar				41.8	44	43.5	
CH_4	CCl_4	298	2.838	49.2	52.4	51.2	21
C_2H_6				64.7	65.9	67.1	
N_2				43.1	53.0	48.3	
C_2H_4				57.1	60.8	61.7	22
C_2H_2				53.0	53.6	57.3	
$(CH_3)_2O$				67.9	66.7	63.2	

TABLE 4-3 (Continued)

Solute	Solvent	T, °K	$\tilde{\rho}$	$\overline{v_1^o}$ cc/gm mole			Data Reference
				Calculated	Experiment	Lyckman	
CH_3Cl				59.4	54	58.8	
SO_2				53.6	53.2	61.4	
C_2H_6	C_6H_5Cl	298	3.033	57.4	63.4	63.3	22
C_2H_4				54.6	57.8	58.0	
C_2H_2				47.0	49.3	53.8	
$(CH_3)_2O$				60.1	65.3	73.0	
CH_3Cl				52.9	52.8	63.2	
SO_2				47.7	47	57.6	
C_2H_6	C_6H_6	298	2.865	60.1	66.1	64.7	22
C_2H_4				56.9	60.4	59.3	
C_2H_2				49.4	50.3	54.9	
$(CH_3)_2O$				62.8	67.1	74.3	
CH_3Cl				55.2	54.1	64.6	
SO_2				49.8	46.8	58.9	
CH_4				43.2	52.0	48.8	21
N_2				43.1	52.6	45.9	
CH_4	nC_{10}	323	2.998	58.4	53.0	59.1	23
		273	3.162	52.6	49.0	-	
		248	3.242	46.1	46.0	-	
CH_4	nC_8	223	3.257	40.8	43.0	52.6	23
		248	3.172	48.4	47.0	58.0	
		273	2.726	75.2	59.0	87.6	
CH_4	nC_7	233	3.156	46.2	44.0	55.2	23
CH_4	nC_6	223	3.094	44.5	45.5	54.1	23
		248	3.00	47.9	48.0	59.8	
		298	2.812	56.2	53.5	73.3	
H_2	CH_3OH	273	2.566	35.1	35.	28.2	24
N_2				48.6	47.	25.3	
CO_2				45.4	40.	39.5	
CO				49.6	47.	37.2	
O_2				43.2	42.	31.7	

TABLE 4-3 (Continued)

Solute	Solvent	T,°K	$\tilde{\rho}$	$\overline{v}_1^o$ cc/gm mole			Data Reference
				Calculated	Experiment	Lyckman	
CH_4				51.6	47.	39.4	
H_2	CH_3OH	298	2.500	39.1	35.	30.4	24
N_2				54.0	52.	26.8	
CO_2				50.5	43.	41.8	
CO				55.1	51.	39.5	
O_2				48.0	45.	34.0	
CH_4				57.3	52.	41.7	
H_2	CH_3OH	323	2.428	44.2	42.	32.9	24
N_2				60.7	54.	28.7	
CO_2				56.7	46.	44.5	
CO				61.9	56.	42.2	
O_2				54.0	50.	36.6	
CH_4				64.4	55.	44.4	
H_2	H_2O	273	2.577	24.9	24.	21.2	24
N_2				34.8	41.	29.4	
CO_2				32.4	32.	32.2	
CO				35.5	37.	30.0	
O_2				30.8	31.	24.6	
CH_4				37.0	36.	32.2	
H_2	H_2O	298	2.569	25.2	26.	21.8	24
N_2				35.2	40.	30.1	
CO_2				32.8	33.	32.9	
CO				36.0	36.	30.7	
O_2				31.2	31.	25.3	
CH_4				37.4	37.	32.9	
H_2	H_2O	323	2.547	26.1	34.	22.7	24
N_2				36.4	38.	30.9	
CO_2				34.0	33.	33.8	
CO				37.2	32.	31.5	
O_2				32.3	32.	26.1	
CH_4				38.7	38.	33.7	

TABLE 4-3 (Continued)

Solute	Solvent	T, °K	$\tilde{\rho}$	$\overline{v_1^o}$ cc/gm mole			Data Reference
				Calculated	Experiment	Lyckman	
CO	nC_8H_{18}	426	2.501	109.3	99.6	80.5	27
		455	2.374	138.4	128.8	88.2	
		483	2.218	189.9	175.0	94.9	
		512	2.029	292.0	267.3	99.6	
N_2	Ar	83.78	2.671	40.7	35.4	35.6	25
N_2	O_2	77	2.765	30.1	35.6	31.1	25
Ar	O_2	83.78	2.689	32.0	28.7	31.0	25
		90	2.617	35.7	29.5	34.2	
CH_4	Cyclo-hexane	298	2.858	37.0	53.0	53.3	26
		310.9	2.819	52.3	57.0	55.5	
		344	2.697	65.2	65.0	62.7	
N_2	NH_3	273	2.448	48.8	43.6	-	28

$$\Delta P = \int_{\rho_1}^{\rho_2} \frac{d\sigma}{\rho<} = \sigma^* \int_{\tilde{\rho}_1}^{\tilde{\rho}_2} d\tilde{\rho} RT[f(\tilde{\rho}) - 1] \tag{4.7}$$

$$\therefore \quad \frac{(P_2 - P_1)}{RT} v^* = \int_{\tilde{\rho}_1}^{\tilde{\rho}_2} [f(\tilde{\rho}) - 1] d\tilde{\rho} \tag{4.8}$$

where

$$f(\tilde{\rho}) = \exp[-.42704(\tilde{\rho} - 1) + 2.019(\tilde{\rho} - 1)^2 - .42367(\tilde{\rho} - 1)^3] \tag{4.9}$$

Equation (4.8) relates the isothermal pressure change corresponding to a density change, and holds over the same reduced density range as (4.3). For calculational convenience, the definite integral is re-expressed as

$$(P_2 - P_1) \frac{v^*}{RT} = \int_{\tilde{\rho}_o}^{\tilde{\rho}_2} [f(\tilde{\rho}) - 1] d\tilde{\rho} - \int_{\tilde{\rho}_o}^{\tilde{\rho}_1} [f(\tilde{\rho}) - 1] d\tilde{\rho} \tag{4.10}$$

where $\tilde{\rho}_o$ is an arbitrary base density. The integral from $\tilde{\rho}_o$ to $\tilde{\rho}$ has been numerically evaluated, and is shown in Table 4-4. (The integrals are tabulated at integrals of $\Delta\tilde{\rho} = 0.1$; they were evaluated for $\Delta\tilde{\rho} = 0.002$.)

Equation (4.8) can be used to determine unknown densities or pressures. Given P_1, ρ_1 and ρ_2, P_2 is found easily from the difference of the integrals of equation (4.10). Given P_1, P_2 and ρ_1, one looks for a reduced density ρ_2 such that the corresponding integral of Table 4-4 satisfies equation (4.10).

The characteristic parameters used in the following calculations were those obtained from the experimental compressibility data. Considerable manipulation of the experimentally measured volumes is

TABLE 4-4

REDUCED INTEGRALS FOR ISOTHERMAL EQUATION OF STATE

$\tilde{\rho}$	1.4	1.5	1.6	1.7	1.8	1.9
$\int_{\rho_o}^{\tilde{\rho}} [f(\tilde{\rho}-1)]d\tilde{\rho}$	0	.0214	.0603	.1237	.2209	.3641
$\tilde{\rho}$	2.0	2.1	2.2	2.3	2.4	2.5
$\int_{\rho_o}^{\tilde{\rho}} [f(\tilde{\rho}-1)]d\tilde{\rho}$	.5705	.8631	1.2739	1.8469	2.6423	3.7427
$\tilde{\rho}$	2.6	2.7	2.8	2.9	3.0	3.1
$\int_{\tilde{\rho}_o}^{\tilde{\rho}} [f(\tilde{\rho}-1)]d\tilde{\rho}$	5.2596	7.3427	10.1895	14.0564	19.2680	26.2246
$\tilde{\rho}$	3.2	3.3	3.4	3.5	3.6	
$\int_{\tilde{\rho}_o}^{\tilde{\rho}} [f(\tilde{\rho}-1)]d\tilde{\rho}$	35.4028	47.3454	62.6364	81.8564	105.5160	

necessary before compressibilities are extracted, e.g., fitting to an equation of state such as the Tait equation. Thus the use of these characteristic parameters in the integrated relation to predict volumes constitutes a severe test of both the accuracy of the parameter and the validity of the generalized equation of state. Also, the integral in Table 4-4 increases very rapidly at high reduced densities.

The results of compression calculations on liquids with equation (4.8) are reported in Tables 4-5 and 4-6. In most cases, the initial state corresponds to the saturated liquid. Then given either the volume or pressure of the compressed state, the other is calculated. Where Tait equation parameters were available, calculations were made using this equation too. The Tait equation is a two-parameter equation[1] usually written in the form

$$v_2 = v_1 \left[1 - C \ln \left(\frac{B + P_2}{B + P_1} \right) \right] \qquad (4.11)$$

The constant C generally has a value of .11 for all liquids, whereas B varies with temperature.

Volumes calculated from equation (4.8) agree to within 1% for all the substances considered, over the entire pressure and temperature range. The Tait equation with one fixed constant C (as for NH_3) gives results which are slightly improved over those of equation (4.8). However, when both Tait contants B and C are varied with temperature and fitted to experimental data as for $nC_{10}H_{22}$, the Tait equation gives decidedly better results than the generalized one-parameter equation (4.8).

TABLE 4-5

VOLUMES OF COMPRESSED LIQUIDS

Substance	T °K	P_1 atm	P_2 atm	v_1 cc/mole	v_2 cc/mole Calc.	Exp.	δ_v% exp-calc / exp	Tait Equation v_2 Calc cc/mole	Tait Equation δ %	Tait Parameters	
CH_4	114.53	8.83	308.89	38.259	36.279	36.220[a]	-.16				
	134.34	6.80	306.23	41.331	38.143	38.143	.00				
	158.23	22.60	300.61	46.443	40.608	40.865	+.63				
	172.72	26.57	309.33	52.900	42.109	42.534	+1.0				
$nC_{10}H_{22}$	288.15	1.0	2310.	196.01	172.33	172.66[b]	.18	172.72	.03	.08743	797.5[b]
	318.15	1.0	3701.	200.23	167.32	167.70	.22	167.76	-.03	.08779	691.5
	338.15	1.0	4837.	204.68	164.65	165.00	.21	164.98	-.01	.08809	601.1
	358.15	1.0	6473.	209.41	160.73	161.63	.56	161.59	.02	.08832	526.4
Water	273.15	1.0	900.	18.018	17.363	17.294[c]	-.40				
	293.15	1.0	1000.	18.047	17.364	17.321	-.25				
	323.15	1.0	1000.	18.231	17.542	17.525	-.10				
	373.15	1.0	1000.	18.792	18.001	18.009	.04				
	471.15	50.0	1000.	20.783	19.388	19.489	.52				
NH_3	253.15	2.0	1400.	25.563	23.651	23.526[d]	-.5	23.551	-.10	.1101	1336.8[d]
	273.15	4.5	1400.	26.622	24.197	24.120	-.3	24.129	-.04	.1101	1036.4
	293.15	10.0	1400.	28.200	24.878	24.808	-.3	24.874	-.27	.1101	714.4
	313.15	16.0	1400.	29.337	25.276	25.349	+.3	25.409	-.24	.1101	567.1

Pressure calculations are shown in Table 4-6. The errors of calculation of equation (4.8) and the Tait equation are of the same order of magnitude, but generally the Tait equation gives better agreement with the experimental pressure.

Where extensive volumetric data for a specific liquid are available, it is preferable to extract the Tait constants and use equation (4.11) for compression calculations. Equation (4.8), however, has the appeal both of generality and a firm basis in molecular theory. Its dependence on a single characteristic parameter reinforces the simplicity of use. Where there is limited experimental data, the use of equation (4.8) will give results of adequate accuracy for compression calculations. Further, it is equally possible, although it remains uninvestigated, that a characteristic parameter extracted directly from volumetric data, i.e., equation (4.8) rather than from compressibilities, will yield results of accuracy equivalent to those of a particular equation of state such as the Tait or Huddleston equations.

4.3 Temperature and Pressure Dependence of DCF Integrals

The corresponding states correlations for C_{22}° and C_{12}° describe their variation with the reduced solvent density. The solvent density, however, is a unique function of the system temperature and pressure. Knowledge of the temperature and pressure behavior of the DCF integrals directly yields the state dependence of the related thermodynamic properties. We have, in the 1-2 binary,

$$1 + \frac{1}{\rho\kappa RT} = 2 - C_{22}^{\circ} = F_1(\tilde{\rho}_2) \qquad (4.12)$$

TABLE 4-6

PRESSURES OF COMPRESSED LIQUIDS

Substance	T °K	v_1 cc/mole	v_2 cc/mole	P_1 atm	P_2 atm Exp	Calc	δ%	Tait Eqn. P_2 atm	δ%
NH_3	253.15	25.563	23.526	2.0	1400.[a]	1537	9.7	1424.	1.7
	273.15	26.622	24.120	4.5	1400.	1471	5.1	1408.	.55
	298.15	28.200	24.808	10.0	1400.	1388	- .82	1445	3.23
	313.15	29.337	25.349	16.0	1400.	1294	-7.6	1454.	3.8

Taking a derivative w.r.t temperature at constant pressure

$$-\left(\frac{\partial C_{22}^{o}}{\partial T}\right)_P = \left(\frac{\partial F_1}{\partial \rho_2^{o}}\right)_P \left(\frac{\partial \rho_2^{o}}{\partial T}\right)_P \tag{4.13}$$

$$= \left(\frac{\partial F_1}{\partial \rho_2^{o}}\right)_P \left(-\left(\frac{\partial \rho_2^{o}}{\partial P}\right)_T \left(\frac{\partial P}{\partial T}\right)_{\rho_2^{o}}\right) \tag{4.14}$$

Now $$\left(\frac{\partial \rho_2^{o}}{\partial P}\right)_T = \rho_2^{o}\kappa_2^{o} = \frac{1}{RT}/(F_1 - 1) \tag{4.15}$$

$$\left(\frac{\partial C_{22}^{o}}{\partial T}\right)_P = \left(\frac{dF_1}{d\rho_2^{o}}\right)\left(\frac{1}{RT}/[F_1 - 1]\right)\left(\frac{\partial P}{\partial T}\right)_{\rho_2^{o}} \tag{4.16}$$

Now, writing the isothermal equation of state, equation (4.8), with P_2^s, the saturation pressure of the solvent as the base pressure,

$$\frac{P - P^s}{RT\rho_2^*} = \int_{\tilde{\rho}_2^s}^{\tilde{\rho}_2} [F_1(\tilde{\rho}_2) - 1]d\tilde{\rho}_2 \tag{4.17}$$

$$= \int_{\tilde{\rho}_2^o}^{\tilde{\rho}_2} [F_1(\tilde{\rho}_2) - 1]d\tilde{\rho} - \int_{\tilde{\rho}_2^o}^{\tilde{\rho}_2^s} [F_1(\tilde{\rho}_2) - 1]d\tilde{\rho} \tag{4.18}$$

$$= F_6(\tilde{\rho}_2) - F_6(\tilde{\rho}_2^s) \tag{4.19}$$

then

$$\frac{1}{RT\rho_2^*}\left(\left(\frac{\partial P}{\partial T}\right)_{\rho_2} - \frac{dP^s}{dT}\right) - \frac{P - P^s}{RT^2\rho_2^*} = \left(\frac{\partial F_6}{\partial T}\right)_{\rho_2} - \frac{\partial}{\partial T}[F_6(\tilde{\rho}_2^s)]_{\rho_2} \tag{4.20}$$

$$\therefore \quad \frac{1}{RT\rho_2^*}\left[\left(\frac{\partial P}{\partial T}\right)_{\rho_2^o} - \frac{dP^s}{dT}\right] - \frac{P - P^s}{RT^2\rho_2^*} = -\frac{dF_6(\tilde{\rho}_2^s)}{dT} \tag{4.21}$$

$$\left(\frac{\partial P}{\partial T}\right)_{\rho_2^o} = RT\rho_2^*\left[\frac{P - P^s}{RT^2\rho_2^*} - \frac{dF_6(\tilde{\rho}_2^s)}{dT}\right] + \frac{dP^s}{dT} \tag{4.22}$$

Substituting (4.34) in (4.29)

$$\left(\frac{\partial C_{22}^o}{\partial T}\right)_P = \left(\frac{dF_1}{d\rho_2^o}\right)\left[\frac{1}{RT}/[F_1(\tilde{\rho}_2) - 1]\right]\left[RT\rho_2^*\left(\frac{P - P^s}{RT^2\rho_2^*} - \frac{dF_6(\tilde{\rho}_2^s)}{dT}\right) + \frac{dP^s}{dT}\right] \tag{4.23}$$

Then, to determine the temperature derivative of C_{22}^o, we need

(i) the compressibility correlation, equation (4.3)

(ii) an equation (relation) for the saturation pressure for the solvent as a function of temperature; we shall use one of the generalized equations suggested by Reid and Sherwood,[5] e.g., Antoine equation, or Miller-Thodos equation.

(iii) an equation for the density of saturated liquid; here we use the generalized Rackett equation.[32]

(iv) the generalized isothermal equation of state, equation (4.8).

Differentiating (4.12) w.r.t. pressure

$$-\left(\frac{\partial C_{22}^o}{\partial P}\right)_T = \frac{dF_1(\tilde{\rho}_2)}{d\rho_2^o}\left(\frac{\partial \rho_2^o}{\partial P}\right)_T \tag{4.24}$$

$$= -\frac{dF_1(\tilde{\rho}_2)}{d\rho_2}\frac{1}{RT}/[F_1(\tilde{\rho}_2^o) - 1] \tag{4.25}$$

Similar expressions can be obtained for the state dependence of C_{12}^{o}

$$- C_{12}^{o} \left(\frac{v_2^*}{v_1^*} \right)^{.62} = F_2(\tilde{\rho}_2) \tag{4.26}$$

$$\therefore \quad \left(\frac{\partial C_{12}^{o}}{\partial T} \right)_P = \left(\frac{dF_2}{d\rho_2} \right) \left(\frac{v_1^*}{v_2^*} \right)^{.62} \frac{1}{RT} / [F_1(\tilde{\rho}_2) - 1] \left(\frac{\partial P}{\partial T} \right)_{\rho_2} \tag{4.27}$$

$$\text{and} \quad \left(\frac{\partial C_{12}^{o}}{\partial P} \right)_T = - \left(\frac{dF_2}{d\rho_2} \right) \left(\frac{v_1^*}{v_2^*} \right)^{.62} \frac{1}{RT} / [F_1(\tilde{\rho}_2) - 1] \tag{4.28}$$

We can now write the pressure and temperature variation of the isothermal compressibility and partial molar volumes using equations (4.23) through (4.28).

$$\left(\frac{\partial \kappa_2}{\partial T} \right)_P = \frac{\kappa_2}{(1 - C_{22}^{o})} - \frac{\kappa_2}{T} - \frac{\kappa_2}{\rho_2} \left(\frac{\partial \rho_2}{\partial T} \right)_P \tag{4.29}$$

$$\left(\frac{\partial \kappa_2}{\partial P} \right)_T = \frac{\kappa_2}{(1 - C_{22}^{o})} \left(\frac{\partial C_{22}^{o}}{\partial P} \right)_T - \frac{\kappa_2}{\rho_2} \left(\frac{\partial \rho_2}{\partial P} \right)_T \tag{4.30}$$

$$\left(\frac{\partial \bar{v}_1^{o}}{\partial P} \right)_T = \frac{\bar{v}_1^{o}}{(1 - C_{22}^{o})} \left(\frac{\partial C_{22}^{o}}{\partial P} \right)_T - \frac{1}{\rho_2^{o}(1 - C_{22}^{o})} \left(\frac{\partial C_{12}^{o}}{\partial P} \right)_T - \frac{\bar{v}_1^{o}}{\rho_2^{o}} \left(\frac{\partial \rho_2}{\partial P} \right)_T \tag{4.31}$$

$$\left(\frac{\partial \bar{v}_1^{o}}{\partial T} \right)_P = \frac{\bar{v}_1^{o}}{(1 - C_{22}^{o})} \left(\frac{\partial C_{22}^{o}}{\partial T} \right)_P - \frac{1}{\rho_2^{o}(1 - C_{22}^{o})} \left(\frac{\partial C_{12}^{o}}{\partial T} \right)_P - \frac{\bar{v}_1^{o}}{\rho_2^{o}} \left(\frac{\partial \rho_2}{\partial T} \right)_P \tag{4.32}$$

The quantity $\left(\frac{\partial \rho_2}{\partial T} \right)$ is obtained from $\frac{dF_6(\tilde{\rho}_2^{s})}{dT}$ in equation (4.23). The details of this derivation are in Appendix D.

Calculations for general gas-solvent systems are shown in Table 4-7. These are order-of-magnitude estimates of the pressure and temperature derivatives of the compressibility and partial molar volume. Ultimate accuracy of prediction depends on close correlation of C_{22}^{o} and C_{12}^{o}.

TABLE 4-7

TEMPERATURE AND PRESSURE DERIVATIVES OF THERMODYNAMIC PROPERTIES[+]

System 1	System 2	I °K	P atm	C_{22}^{o} eqn.(4.3)	$10^4\kappa$ $(atm)^{-1}$	$10^4\left(\frac{\partial\kappa}{\partial P}\right)_T$ $(atm)^{-2}$	$10^4\left(\frac{\partial\kappa}{\partial T}\right)_P$ $(atm°K)^{-1}$	C_{12}^{o} eqn.(4.6)	$\bar{v}_1^{o}$ cc/mole	$\left(\frac{\partial\bar{v}_1^{o}}{\partial P}\right)_T$ cc/mole/atm	$\left(\frac{\partial\bar{v}_1^{o}}{\partial T}\right)_P$ cc/mole/°K
H_2	C_6H_6	413	140.	-11.14	2.47 (1.91)	-.006 (-.007)	.029	- 6.53	63.13 (51.6)	-.08 (-.09)	.46 (.26)
H_2	nC_8H_{18}	413	140.	-20.49	2.51 (2.73)	-.006 (-.011)	.024	- 6.24	61.6 (59.7)	-.075 (-.11)	.38 (.26)
N_2	nC_8H_{18}	413	140.	-20.49	2.51	-.006	.024	- 8.83	83.7	-.098	.49
H_2	C_6H_6	298	1.0	-36.78	.97 (.98)	-.009 (-.008)	.008	-12.79	32.61 (35.1)	-.01	.15
N_2	C_6H_6	298	1.0	-36.78	.97	-.009	.008	-18.08	45.14 (52.6)	-.02	.21
H_2	CCl_4	298	1.0	-35.66	1.08 (1.09)	-.0016 (-.0014)	.008	-11.91	34.2 (38.0)	-.015	.16
N_2	CCl_4	298	1.0	-35.66	1.08	-.0016	.008	-16.85	47.3 (53.0)	-.02	.21

[+]Experimental values in parentheses.

REFERENCES FOR CHAPTER 4

1. J. S. Rowlinson, Liquids and Liquid Mixtures, Plenum Press, New York, 1969.

2. P. S. Snyder and J. Winnick, "The Pressure, Volume and Temperature Properties of Liquid n-Alkanes at Elevated Pressures," 5th Symposium on Thermophysical Properties, ASME (1970).

3. A. K. Doolittle and B. Doolittle, AIChE.J., 6, 157 (1960).

4. W. G. Cutler et al., J. Chem. Phys., 29, 727 (1959).

5. R. C. Reid and T. K. Sherwood, The Properties of Gases and Liquids, McGraw-Hill, New York (1966).

6. B. H. Sage et al., I.E.C., 26, 1218 (1934).

7. W. B. Kay, I.E.C., 32, 358 (1940).

8. R. E. Gibson and O. H. Loeffler, J. Am. Chem. Soc., 61, 2877 (1939).

9. P. W. Bridgman, Proc. Am. Acad. Arts & Sci., 69, 389 (1934).

10. L. G. Schornack and C. A. Eckert, J. Phys. Chem., 74, 3014 (1970).

11. F. I. Mopsik, J. Chem. Phys., 50, 2559 (1969).

12. G. A. Holder and E. Whalley, Trans. Far. Soc., 58, 2095 (1962).

13. D. W. Newitt and K. E. Weale, J. Chem. Soc., London, 3092 (1951).

14. D. A. Lowitz et al., J. Chem. Phys., 74, 3014 (1970).

15. J. S. Rowlinson, Liquids and Liquid Mixtures, Butterworths, London (1958).

16. K. Kumagai and T. Toriumi, J. Chem. Engr. Data, 16, 293 (1971).

17. R. H. Schum and O. L. I. Brown, J. Am. Chem. Soc., 75, 2520 (1953).

18. J. F. Connolly and G. A. Kandalic, C. E. P. Symposium Series, 59, 8 (1963).

19. Y. Ng and J. Walkley, J. Phys. Chem., 73, 2274 (1969).

20. J. E. Jolly and J. H. Hildebrand, J. Am. Chem. Soc., 80, 1050 (1958).

21. J. C. Gjalbaek and J. H. Hildebrand, J. Am. Chem. Soc., 72, 1072 (1950).

22. J. Horiuti, Scientific Papers of Institute of Physical and Chemical Research, 17, 125 (1931).

23. J. P. Kohn, "Volumetric and Phase Equilibria of Methane-Hydrocarbon Binary Systems," A.I.Ch.E. Meeting, Houston (1967).

24. I. Kritchevsky and A. Illinskaya, Acta Physicochemica U.R.S.S., 20, 327 (1945).

25. S. D. Chang and B. C. Lu, Can. J. Chem. Engr., 48, 261 (1970).

26. V. Berry and B. H. Sage, J. Chem. Engr. Data, 4, 204 (1959).

27. M. Orentlicher and J. M. Prausnitz, Can. J. of Chem., 45, 595 (1967).

28. J. M. Prausnitz, Molecular Thermodynamics of Fluid Phase Equilibria, Prentice-Hall, Englewood Cliffs (1969).

29. E. C. Lyckman et al., Chem. Engr. Sci., 20, 685, 703 (1965).

30. A. V. Itterbeek et al., Physica, 29, 742 (1963).

31. E. H. Amagat, Ann. de Chim et Phys., 29, 68-136, 505-574 (1893).

32. C. F. Spencer and R. P. Danner, J. Chem. Engr. Data, 17, 236 (1972).

CHAPTER 5

SOLUTION THEORY FOR SUBCRITICAL SYSTEMS

In previous sections we discussed the pressure and temperature dependence of thermodynamic properties, and of the corresponding DCF integrals for systems of constant composition, either pure solvent or a solute at infinite dilution. Here, we consider the prediction of thermodynamic properties in subcritical systems of variable composition. The temperature or pressure of the systems may be fixed or variable in accordance with the Gibbs phase rule.

The corresponding states correlations for the DCF integrals derived earlier for limiting compositions can be extended to mixtures by the concept of a pseudo pure fluid, analogous to a one-fluid macroscopic theory. Here the mixture properties are represented by those of a pure fluid whose critical parameters depend on the composition of the mixture. This rule is similar in concept to Kay's rule[1] of pseudo criticals, and Prausnitz and Chueh's[2] mixing rule. The mixing rules for the critical parameters are necessarily empirical, unless they are based on a rigorous molecular theory. This approach will be used to study the compressibilities of binary and ternary liquid mixtures.

Finally, when faced with a lack of experimental data in the mid-composition range of a solution, one can postulate (on the basis of empirical knowledge) rules for the composition dependence of the DCF integrals. Two of the simple rules are the linear arithmetic mean and the linear harmonic mean. Expressions for the thermodynamic properties with the linear rule have been presented earlier.

5.1 One-Fluid Theory

Leland and Chappelear[1] discuss several methods of applying corresponding states theory to mixtures. The microscopic principle rests on the specification of the parameters of a pure fluid pair potential function which generates the properties of the mixture at the same temperature, pressure and density. On the macroscopic level, the problem becomes one of defining a relation between the critical properties of the pure components and the pseudocritical properties of the hypothetical pure fluid. One of the simplest examples of these is Kay's rule,[1] and an equally simple rule is used here.

It is postulated that the properties of the fluid mixture correspond to those of a pseudo pure fluid, whose characteristic parameters depend on the composition of the mixture. The pseudo pure fluid follows macroscopic states and its thermodynamic properties are described by the correlations derived earlier.

The macroscopic correlation for compressibility, equation (4.3), contains only one characteristic parameter for each substance, the characteristic volume. For the mixture, this is defined to be the simple mole fraction average of the pure component volumes

$$v^*_{mix} = \Sigma\, x_i v^*_i \tag{5.1}$$

Then, for the mixture

$$\left(1 + \frac{1}{\rho\kappa RT}\right)_{mixture} = F(\tilde{\rho}_{mix}) \tag{5.2}$$

where $F(\tilde{\rho}_{mix})$ is the same generalized function of $\tilde{\rho}$ as equation (4.3).

Equation (5.2), with the rule of (5.1), has been used to determine the isothermal compressibilities of the binary mixtures of benzene-cyclohexane, methyl acetate-water, nitrobenzene-aniline, and of the ternary mixture n-hexane, n-heptane, n-octane. The results are shown in Tables 5-1 and 5-2. In all systems, there is good agreement between the calculated and experimental compressibilities over the entire composition range. This clearly demonstrates the efficacy of the approximations and the composition mixing rules of (5.2) and (5.1). In the binaries of the hydrocarbons, and of nitrobenzene-aniline, there is a small, but consistent deviation between the experimental and calculated compressibilities. However, this probably results from an incorrect prediction of the pure compressibilities by equation (4.3) and should not be immediately attributed to a failure of the mixing rule. A possible remedy is to adjust the characteristic parameters of the pure components such that equation (4.3) predicts their experimental compressibilities correctly. The results of such calculations are shown in Table 5-3, and reveal marked improvements in the benzene-cyclohexane and aniline-nitrobenzene systems. This stratagem has a mixed effect in the water-methyl acetate system, which is a possible reflection of the complex interactions in this mixture.

The volume of the binary mixture is required in all of the above calculations and has been assumed an experimentally accessible quantity. This may not always be the case and the simplest approximation under these conditions is one of ideal mixing. The effects of this assumption on the predictions of the one-fluid theory are shown in Figs. 5-4 and 5-5.

TABLE 5-1

ISOTHERMAL COMPRESSIBILITIES OF BINARY LIQUID MIXTURES CALCULATED BY PSEUDO PURE FLUID APPROXIMATION

System 1	System 2	T	x_1	v_{mix} exprtl. cc/mole	v^*_{mix}	$\tilde{\rho}_{mix}$	$10^4 \kappa$ (atm^{-1}) Calc.	$10^4 \kappa$ (atm^{-1}) Exprt.	Data Reference
nC_8H_{18}	nC_7H_{16}	333	0	154.030	425.0	2.759	1.93	1.89	8
			.220	157.886	439.1	2.781	1.85	1.82	
			.413	161.255	451.43	2.799	1.79	1.76	
			.654	165.466	466.84	2.821	1.72	1.68	
			.827	168.503	477.95	2.836	1.67	1.62	
			1.0	171.524	489.0	2.851	1.62	1.57	
nC_7H_{16}	nC_6H_{14}	333	0.0	138.211	369.0	2.670	2.29	2.22	8
			.319	143.262	386.88	2.701	2.15	2.11	
			.657	148.609	405.81	2.731	2.03	2.00	
			1.0	154.030	425.0	2.759	1.93	1.89	
nC_8H_{18}	nC_6H_{14}	333	0	138.211	369.0	2.670	2.29	2.22	8
			.338	149.477	409.58	2.740	1.99	1.89	
			.615	158.692	442.78	2.790	1.81	1.85	
			1.0	171.524	489.0	2.851	1.62	1.57	
$C_6H_5NH_2$	$C_6H_5NO_2$	298	0	102.651	321.00	3.127	.48	.50	5,6
			.431	98.101	305.48	3.114	.48	.49	
			.684	95.251	296.37	3.111	.47	.49	
			.798	93.910	292.26	3.112	.46	.48	
			.891	92.787	288.93	3.114	.75	.47	
			1.0	91.416	285.00	3.118	.44	.47	

TABLE 5-1 (Continued)

System 1	System 2	T	x_1	v_{mix} exprtl. cc/mole	v^*_{mix}	$\tilde{\rho}_{mix}$	$10^4 \kappa$ (atm^{-1}) Calc.	$10^4 \kappa$ (atm^{-1}) Exprt.	Data Reference
C_6H_6	C_6H_{12}	298	0.0	108.80	311.0	2.858	1.13		3,4
			.25	103.89	297.0	2.859	1.09	1.06	
			.50	99.30	283.0	2.850	1.04	1.02	
			.75	94.36	269.0	2.851	.99	.98	
			1.0	89.00	255.0	2.865	.90		
C_6H_6	C_6H_{12}	323	0.0	112.05	311.0	2.775	1.47		3,4
			.25	107.03	297.0	2.775	1.30	1.29	
			.50	102.26	283.0	2.767	1.24	1.25	
			.75	97.15	269.0	2.770	1.19	1.19	
			1.0	92.25	255.0	2.764	1.16		
Methyl-water acetate		293	0.0						7
			.1016	23.66	64.54	2.728	.36	.40	
			.1484	26.256	72.90	2.776	.35	.40	
			.1780	27.909	78.19	2.801	.35	.40	
			1.0	79.357	225.	2.835	.90	.87	

TABLE 5-2

ISOTHERMAL COMPRESSIBILITY OF TERNARY LIQUID MIXTURES

System	T °K	v_{mix} expt. cc/mole	v^*_{mix}	$\tilde{\rho}_{mix}$	$10^4 \kappa$ Calc.	$10^4 \kappa$ Expt.+
35.26% C_6H_{14}	273	142.53	426.39	2.992	1.08	1.17
31.72% C_7H_{16}	298	147.034	426.39	2.900	1.34	1.42
33.02% C_8H_{18}	313	149.995	426.39	2.843	1.54	1.60
	333	154.228	426.39	2.765	1.90	1.89
19.11% C_6H_{14}	273	146.067	439.73	3.010	1.05	1.16
41.16% C_7H_{16}	298	150.776	439.73	2.918	1.30	1.41
39.73% C_8H_{18}	313	153.703	439.73	2.861	1.50	1.58
	333	157.957	439.73	2.784	1.84	1.85

+Reference 8

TABLE 5-3

ISOTHERMAL COMPRESSIBILITIES OF FLUID MIXTURES

System (1)	System (2)	T °K	v_1^* cc/mole	v_2^* cc/mole	x_1	v_{mix}^*	v_{mix}^{exprtl}	$\tilde{\rho}_{mix}$	$1/\rho\kappa RT$ Calc(1)	$1/\rho\kappa RT$ Exprt	$1/\rho\kappa RT$ Calc(2)
Aniline	Nitrobenzene	339	283.001	319.271	.431	303.632	101.475	2.929	58.76	58.42	62.94
					.684	294.454	98.546	2.988	58.05	58.89	62.41
					.798	290.312	97.182	2.987	57.93	58.66	62.39
					.891	286.959	96.038	2.988	58.05	58.17	62.60
Benzene	Cyclohexane	298	252.617	309.735	.2893	298.211	103.550	2.832	36.44	37.32	39.02
					.5498	278.331	98.518	2.825	35.75	36.71	38.80
					.7856	264.863	93.656	2.828	36.04	36.53	38.52
n-Octane	n-Heptane	333	490.765	426.047	.2204	440.934	157.886	2.793	32.36	31.77	31.20
					.413	453.245	161.255	2.811	34.19	33.61	32.90
					.6537	368.630	165.466	2.832	36.50	36.05	35.28
					.8273	479.726	168.503	2.847	38.18	37.98	36.93
Methyl Acetate	Water	293	225.683	46.398	.1016	64.613	23.660	2.731	26.73	24.73	27.04
					.1484	73.004	26.256	2.780	31.16	27.51	30.17
					.1780	78.311	27.909	2.806	33.69	29.32	33.08

(1) Adjusted pure component parameters

(2) Unadjusted pure component parameters

5.2 Rules for Composition Dependence of DCF Integrals

The thermodynamic properties of a binary system are completely defined by the three integrals C_{11}, C_{12} and C_{22} though the expressions

$$\frac{1}{\rho\kappa RT} = 1 - x_1^2 C_{11} - x_2^2 C_{22} - 2x_1 x_2 C_{12} \tag{5.3}$$

$$\frac{\rho \bar{v}_1}{\rho\kappa RT} = (1 - x_1 C_{11} - x_2 C_{12}) \tag{5.4}$$

and

$$\left(\frac{\partial \ell n \gamma_1}{\partial x_1} \right)_{T,P} = \frac{1}{x_2} - \frac{1 + C_{11} - 2x_1 C_{11} - 2x_2 C_{12} + x_2^2 (C_{12} C_{12} - C_{11} C_{22})}{1 - x_1^2 C_{11} - x_2^2 C_{22} - 2x_1 x_2 C_{12}} \tag{5.5}$$

The quantities C_{11}, C_{12} and C_{22} vary with the composition of the mixture. At any composition, they can be determined only through a simultaneous knowledge of all three thermodynamic properties.

However, experimental data are often available only at the composition extremes, and the variation of the C_{ij} over the composition range must be hypothesized to calculate mixture properties at other compositions. Equations describing this composition dependence may be proposed and the calculated thermodynamic properties compared with experimental data. Good agreement for a wide range of systems is evidence for the accuracy of the composition rules which can then be (confidently) applied to other systems. The two composition rules studied are the arithmetic mean (5.6) and the reciprocal mean (5.7)

$$C_{ij} = C_{ij}^* + x_1 (C_{ij}^o - C_{ij}^*) \tag{5.6}$$

$$\frac{1}{C_{ij}} = \frac{x_1}{C^*_{ij}} + \frac{1 - x_1}{C^\circ_{ij}} \tag{5.7}$$

The superscripts * refer to quantities at $x_2 = 0$, while $^\circ$ refers to quantities at $x_1 = 1$. The above relations are then substitution into equations (5.3), (5.4) and (5.5) to yield expressions for thermodynamic properties of the mixture in terms of DCF integrals at the limiting compositions, which in turn are calculated as follows

$$\frac{1}{\rho_1^\circ \kappa_1^\circ RT} = 1 - C^\circ_{11} \tag{5.8}$$

$$\frac{\bar{v}_2^\circ}{v_1^\circ} = \frac{1 - C^\circ_{12}}{1 - C^\circ_{11}} \tag{5.9}$$

$$\left(\frac{\partial \ell n \gamma_2}{\partial x_2} \right)^\circ_{T,P} = (1 - C^\circ_{22}) - \frac{(1 - C^\circ_{12})^2}{(1 - C^\circ_{11})} \tag{5.10}$$

where the symbols have their usual meaning. Similar expressions relate C^*_{11}, C^*_{12} and C^*_{22} to properties at the compositions $x_2 = 1$.

The benzene-cyclohexane and aniline-nitrobenzene systems were studied initially. Complete thermodynamic data are available for these systems.[3,4,9,5,6,10] The composition dependent C_{11}, C_{12} and C_{22} in the benzene-cyclohexane system were determined by simultaneous solution of equations (5.3), (5.4) and (5.5) and are shown in Fig. 5-1. Although this binary system is not very nonideal, the experimental C_{ij}'s show a quadratic dependence on composition. This is consistent with the quadratic and higher order composition dependence of the thermodynamic properties.

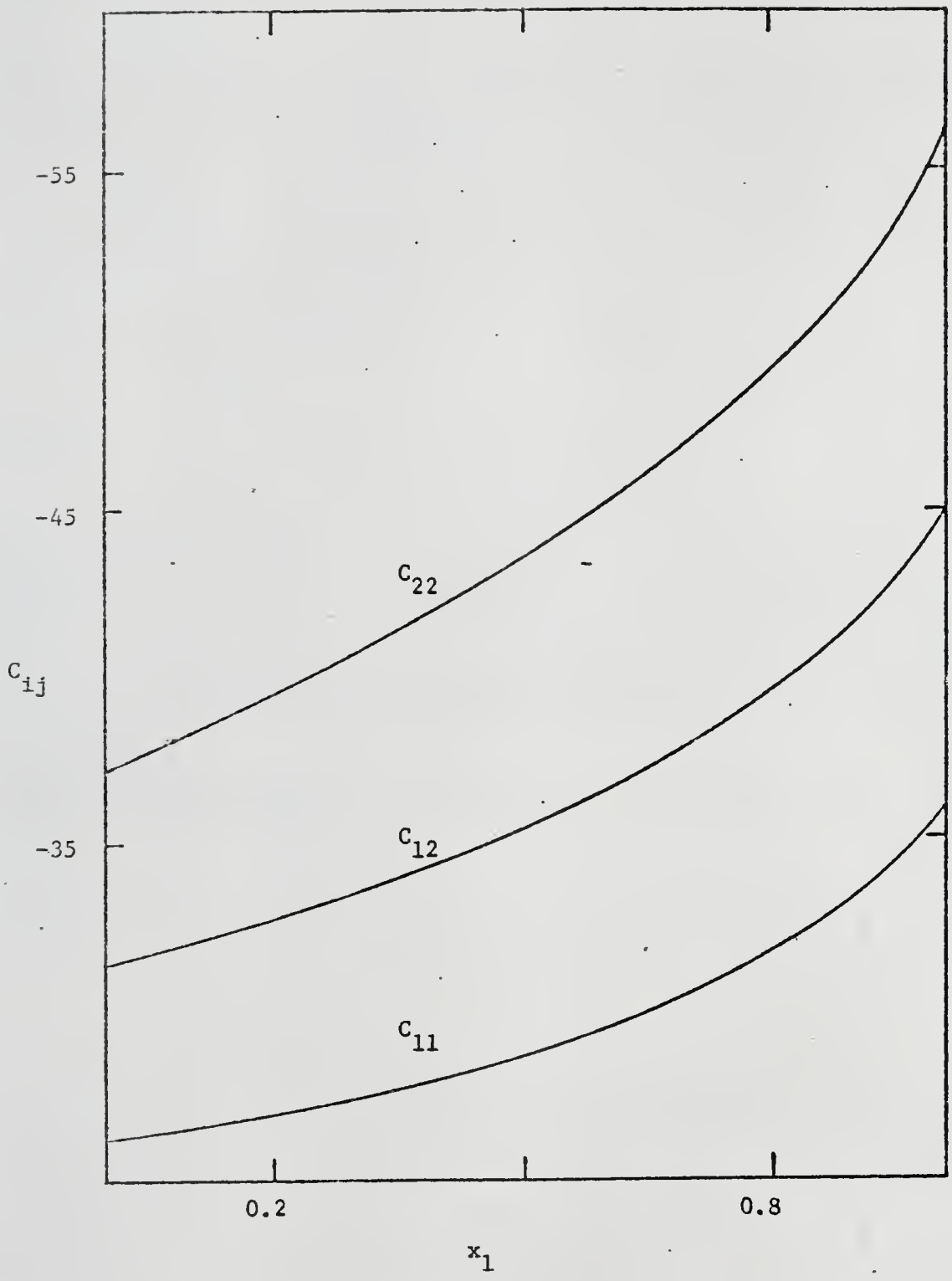

Fig. 5-1. Experimental DCF integrals in benzene (1) - cyclohexane (2) system at 298°K.

The third-order correlation function integrals C_{111}, C_{112}, C_{122} and C_{222} of the system can be obtained from the complete composition dependence of C_{11}, C_{12} and C_{22}. The triplet and pair correlation function integrals are related by the recurrence relations (Appendix B)

$$\left(\frac{\partial C_{ij}}{\partial x_1} \right)^*_{T,P,N_2} = C^*_{ij}(1 - \rho\bar{v}^*_1) + C^*_{ij1} - \rho\bar{v}^*_1 C^*_{ij2} \qquad (5.11)$$

$$i,j=1,2$$

$$\left(\frac{\partial C_{ij}}{\partial x_2} \right)^o_{T,P,N_1} = C^o_{ij}(1 - \rho\bar{v}^o_1) + C^o_{ij2} - \rho\bar{v}^o_2 C^o_{ij1} \qquad (5.12)$$

$$i,j=1,2$$

These provide three relations between the four quantities C_{ijk} at each composition extreme. The fourth relation is obtained from the density derivative of the pure liquid compressibility (Appendix B)

$$C_{iii} = \rho_i \left(\frac{\partial C_{ii}}{\partial \rho_i} \right)_{T,P,N_j} - C_{ii} \qquad (5.13)$$

The corresponding states correlation, equation (4.3), was used to determine the density derivative $\left(\frac{\partial C_{ii}}{\partial \rho_i} \right)$. The composition derivatives were evaluated analytically by fitting the experimental C_{ij}'s to quadratics. The derived C_{ijk}'s are shown in Table 5-4. They all have large negative values, much more so than the C_{ij}'s. This is in total contradiction to the HNC assumption for mixtures which requires all $C_{ijk} = 0$ (Appendix F). Interestingly enough, there is a consistent relation of the form

$$C^3_{iij} = C^2_{iii} C_{jjj}$$

TABLE 5-4

SECOND AND THIRD ORDER DCF INTEGRALS IN THE BENZENE-CYCLOHEXANE SYSTEM

T °K	$x_{benzene}$	C_{11}	C_{12}	C_{22}	C_{111}	C_{112}	C_{122}	C_{222}	$(C_{111}^2 C_{222})^{1/3}$	$(C_{111} C_{222}^2)^{1/3}$
298	0	-26.41	-31.56	-37.61	-187.7	-227.5	-273.8	-327.0	-225.8	-271.8
	1	-36.05	-45.29	-56.79	-312.6	-380.0	-459.9	-553.9	-378.3	-457.8
343	0	-15.19	-18.17	-21.61	-127.1	-145.5	-164.9	-184.6	-143.9	-163.0
	1	-21.18	-26.61	-33.30	-177.8	-220.9	-273.5	-337.5	-220.2	-272.6

which is analogous to the relation often used for the cross third virial coefficients in gas mixtures.[11]

The essentially quadratic composition dependence of the C_{ij} indicates that the linear rule can only be a first order approximation. Thermodynamic properties calculated with equations (5.6) and (5.7) are shown in Table 5-5. Although the hypothetical and experimental C_{ij}'s in the benzene-cyclohexane system differ by more than 10% at some compositions, the resulting thermodynamic properties are in much closer agreement with experimental data. Figs. 5-2 and 5-3 show comparisons of the isothermal compressibility and partial molar volumes with experiment. The calculated partial molar volumes agree very well with the experiment over the complete composition range. The isothermal compressibility is not as well predicted and the calculated curve is of a different shape than the experimental. The maximum error occurs near the mid-composition range and is about 8%. Fig. 5-2 also shows the isothermal compressibility calculated from the one-fluid theory with nonadjusted and adjusted pure component characteristic parameters. Isothermal compressibilities calculated from the one-fluid theory show the same composition dependence as the experimental data.

For calculations of the aniline-nitrobenzene system, the partial molar volumes at infinite dilution were assumed equal to the pure component molar volumes, i.e., ideal mixing. The composition dependences of the activity coefficient, calculated with equations (5.6) and (5.7), follow the experimental result quite closely and are shown in Fig. 5-4. The calculated isothermal compressibility is of the

TABLE 5-5

RULES FOR COMPOSITION DEPENDENCE OF DCF INTEGRALS - CALCULATIONS

System (1)	System (2)	T °K	x_1	C_{22}	C_{12}	C_{11}
Benzene	Cyclohexane	298	0.0	(-37.46)	(-31.45)	(-26.35)
			.2893	-43.12 (-40.64)	-35.50 (-32.43)	-29.17 (-29.41)
			.5498	-48.21 (-47.35)	-39.16 (-33.63)	-31.75 (-31.31)
			.7856	-52.82 (-76.55)	-42.46	-34.08
			1.0	(-57.03)	(-45.47)	(-36.20)
Aniline	Nitrobenzene	338	0.0	(-60.36)	(-53.70)	(-47.37)
			.25	-63.31	-56.39	-49.87
			.50	-66.27	-59.09	-52.37
			.75	-69.22	-61.78	-54.88
			1.0	(-72.17)	(-64.48)	(-57.38)

[+] Experimental values in parentheses.

OF THERMODYNAMIC PROPERTIES IN SUBCRITICAL SYSTEMS[+]

$\frac{1}{\rho\kappa RT}$	$\rho\bar{v}_1$	$\rho\bar{v}_2$	$\left(\frac{\partial \ln \gamma_1}{dx_1}\right)_{T,P,N_2}$	$\left(\frac{\partial \ln \gamma_2}{\partial x_2}\right)_{T,P,N_1}$
(38.47)	(.84)	(1.0)	(- .0247)	(0.0)
39.82	.871	1.053	- .0212	- .0086
(37.32)	(.872)	(1.052)	(- .0175)	
39.75	.908	1.113	- .0116	- .0142
(36.71)	(.909)	(1.112)	(- .0111)	
38.76	.951	1.179	- .0072	- .0265
(37.20)	(1.0)	(1.249)	(0.0)	(- .0247)
(61.36)	(.892)	(1.0)	(- .394)	(0.0)
60.88	.916	1.028	- .277	- .092
60.21	.942	1.058	- .170	- .170
59.36	.971	1.089	- .077	- .231
(58.38)	(1.0)	(1.122)	(0.0)	(- .271)

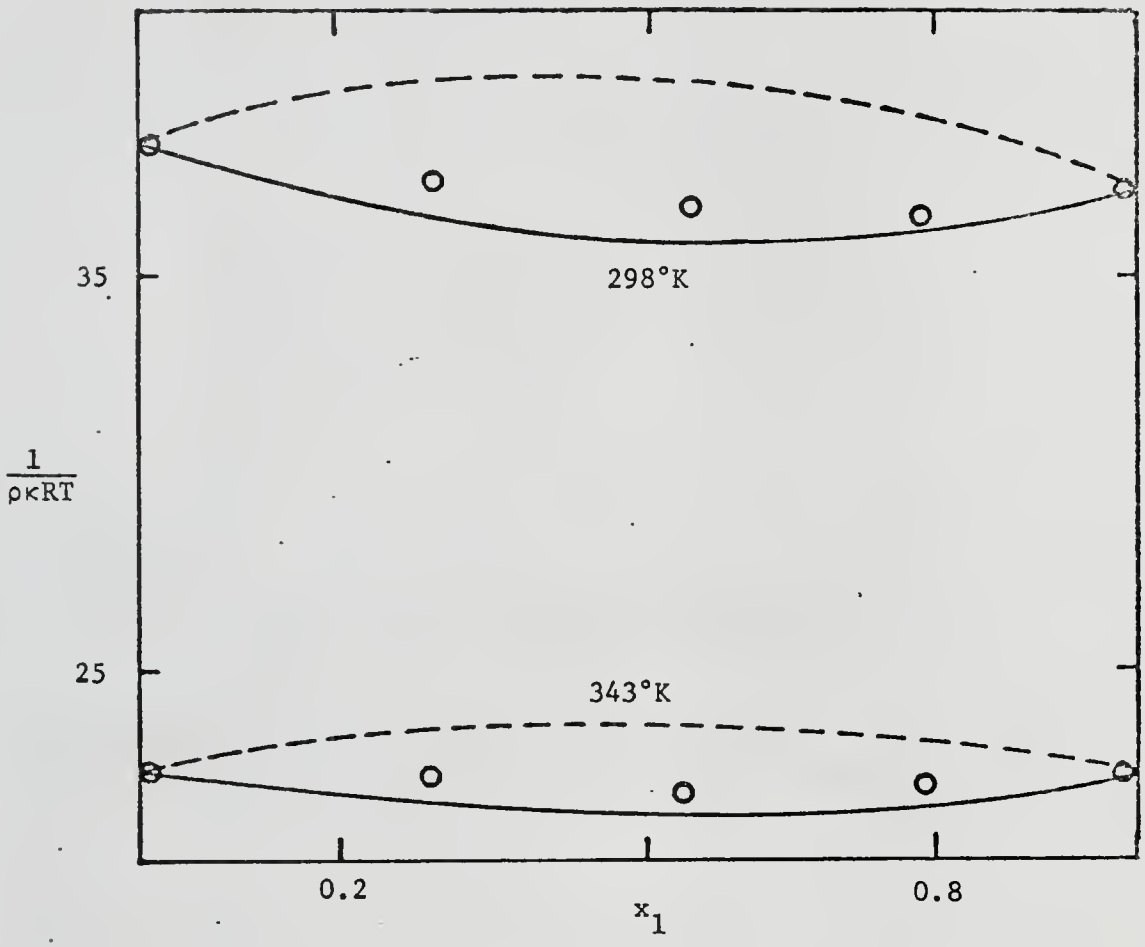

Fig. 5-2. Isothermal compressibility function of benzene (1) - cyclohexane (2) mixtures.

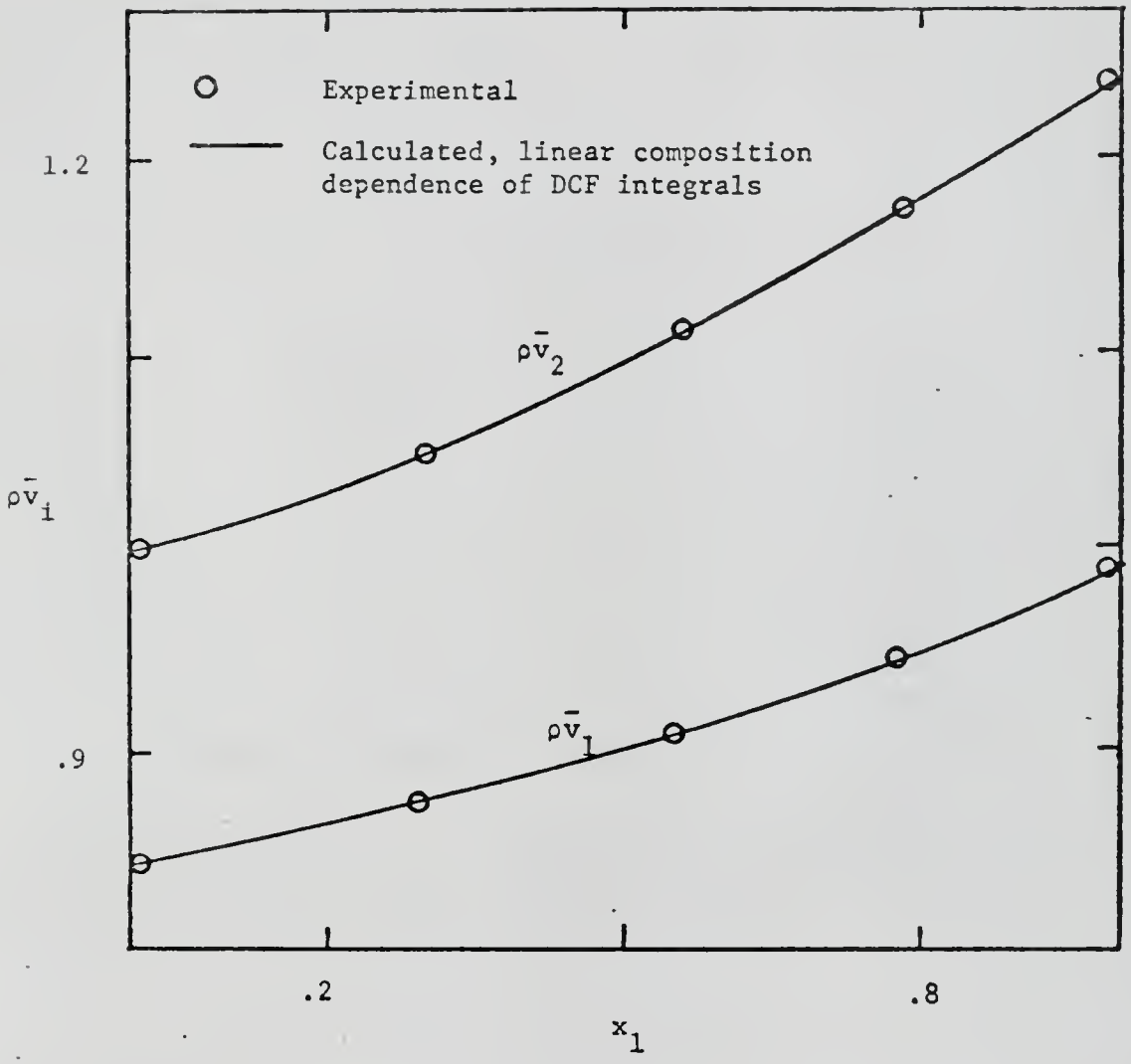

Fig. 5-3. Partial molar volumes in benzene (1) - cyclohexane (2) system at 298°K.

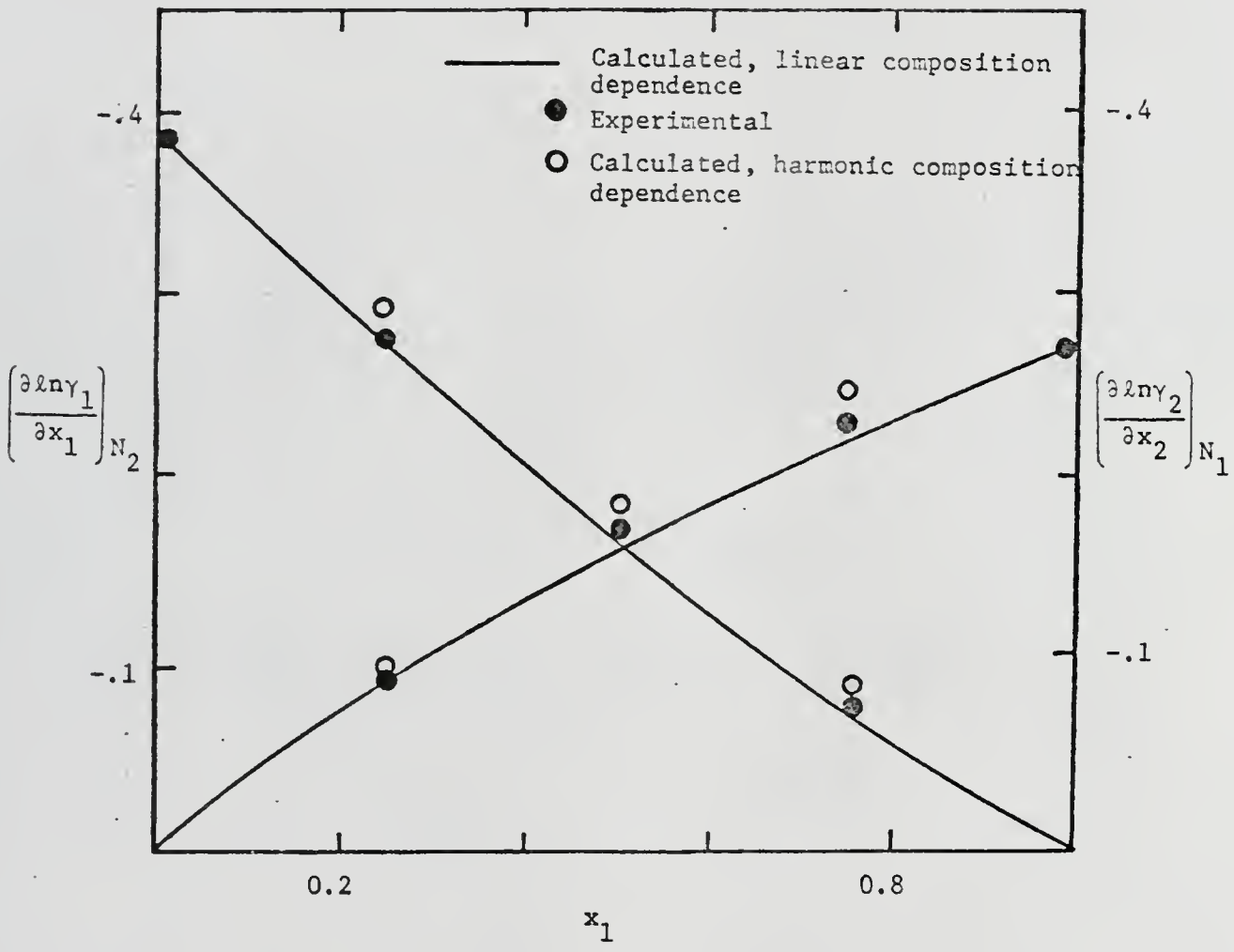

Fig. 5-4. Activity coefficients in aniline (1) - nitrobenzene (2) system at 338°K.

same form as in the benzene cyclohexane system and deviates from the experimental value at the mid-composition range (Fig. 5-5). The predictions of the one-fluid theory with adjusted parameters, on the other hand, agrees well with the experimental data. From the limited study of the two binary systems, one can only speculate on the efficacy of the linear composition rule for the DCF integrals in calculating thermodynamic properties. However, the results for these systems indicate that with a knowledge of the six limiting values of the DCF integrals, the partial molar volume can be estimated to within 5% at any composition, and the logarithm of the activity coefficient at infinite dilution to about 10%. The isothermal compressibility is best determined from the one-fluid theory with adjusted parameters, using an ideal mixing rule for the volume of the mixture if this is unknown.

In some situations, one may not have all the thermodynamic information necessary to calculate the six DCF integrals at the limiting compositions. Under these circumstances, the only alternative to total surrender is a reasonable and realistic approximation to relate the C_{ij}'s at each composition. The experimental C_{ij}'s in the benzene-cyclohexane system (Fig. 5-1) provide a clue in this direction. Over the entire composition range, C_{12} is approximately the arithmetic mean of C_{11} and C_{22}, and this assumption is made in subsequent calculations. We now propose to determine activity coefficients in the binary mixture from the molar volumes and isothermal compressibilities of the pure components and their partial molar volumes at infinite dilution in the other. C^{o}_{11}, C^{o}_{12}, C^{*}_{22} and C^{*}_{12} are calculated as in equations (5.8) and

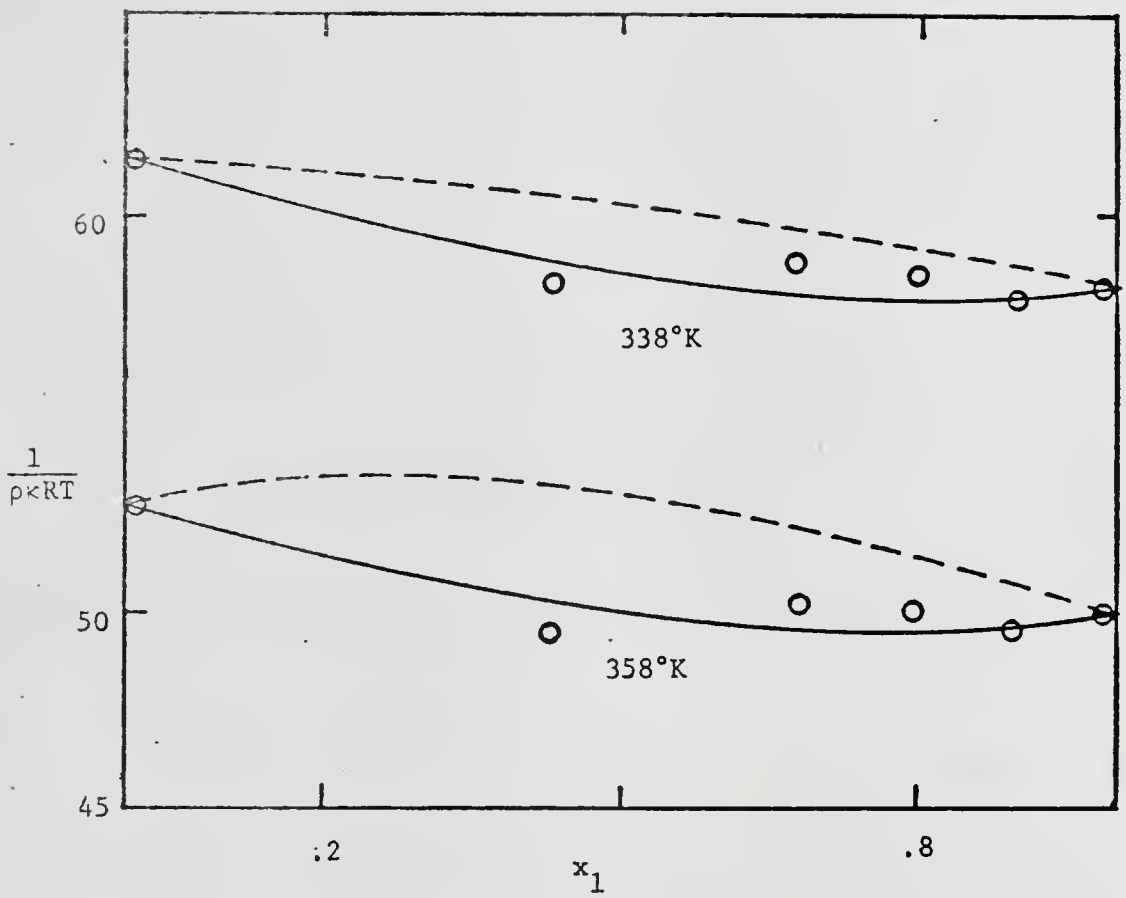

Fig. 5-5. Compressibility function of aniline (1) - nitrobenzene (2) mixtures.

(5.9). C_{11}^{*} and C_{22}^{o} are evaluated from

$$C_{11}^{*} = 2C_{12}^{*} - C_{22}^{*} \tag{5.14}$$

$$C_{22}^{o} = 2C_{12}^{o} - C_{11}^{o} \tag{5.15}$$

The linear composition rules are used to determine C_{ij} at intermediate compositions. The calculated composition derivatives of the activity coefficients are integrated to yield activity coefficients at infinite dilution.

$$\ell n\gamma_1\Big]_{x_1=0} = \ell n\gamma_1^{o} + \int_1^{o} \left(\frac{\partial \ell n\gamma_1}{\partial x_1} \right)_{T,P,N_2} dx_1$$

$$= 0 - \int_o^{1} \left(\frac{\partial \ell n\gamma_1}{\partial x_1} \right)_{T,P,N_2} dx_1 \tag{5.16}$$

The infinite dilution activity coefficients in some binary mixtures are shown in Table 5-6. The agreement with experimental data is satisfactory only in the acetone-benzene system. In other systems, the calculated slope of the activity coefficient has too large a negative value. This slope is calculated as a small difference of large numbers, and is accurate only when the C_{ij}'s at the composition extremes are precisely known. Evidently, equations (5.14) and (5.15) do not yield values of C_{22}^{o} and C_{11}^{*} which satisfy this criterion. The calculation for aniline-nitrobenzene at 338°K illustrates this point. The deviation of C_{12} from the arithmetic mean is designated δ_{12}, i.e.,

$$\delta_{12} = \frac{2C_{12}}{C_{11} + C_{22}} - 1 \tag{5.17}$$

TABLE 5-6

ACTIVITY COEFFICIENTS IN BINARY LIQUID MIXTURES[+]

System (1)	System (2)	T °K	γ_1 x_1=.5	γ_1 x_1=0	γ_2 x_2=.5	γ_2 x_2=0	Data Reference
acetone	CCl_4	298	1.255	2.371	1.241	2.482	12
benzene	cyclohexane	298	1.241 (1.005)	1.919 (1.020)	1.174 (1.005)	2.402 (1.020)	3, 4, 9
		343	1.1304 (1.007)	1.443 (1.029)	1.094 (1.007)	1.646 (1.029)	
aniline	nitrobenzene	338	1.1068 (1.037)	1.4668 (1.204)	1.100 (1.047)	1.502 (1.159)	5, 6, 10
		358	1.105 (1.021)	1.369 (1.207)	1.080 (1.043)	1.499 (1.100)	
acetone	benzene	318	1.124 (1.079)	1.165 (1.126)	1.736 (1.607)	1.654 (1.355)	13, 14

[+]Experimental values in parentheses.

The experimental values of δ^{o}_{12} and δ^{*}_{12} as determined from Table 5-5 are - .0246 and - .0030, respectively. These values of δ_{12} in conjunction with the linear rules yield slopes of the activity coefficients which are in close agreement with experiment (Fig. 5-5). However, when $\delta^{*}_{12} = \delta^{o}_{12} = 0$, equations (5.14) and (5.15), the resulting activity coefficients differ by more than 20% from experiment.

A possible correction for this shortcoming is to include information on the limiting activity coefficient of one component in the other, e.g., a polar solute at infinite dilution in a non-polar solvent. This would provide the precise knowledge of the C_{ij}'s, and hence δ_{12}, at the pure solvent composition. Then, assuming a constant value for δ_{12}, the C_{ij}'s at the pure solute composition can be calculated. In all likelihood, the calculated activity coefficient for the nonpolar solvent at infinite dilution in the polar solute will be in closer agreement with experiment than that calculated by the assumptions of equations (5.14) and (5.15).

REFERENCES FOR CHAPTER 5

1. J. M. Prausnitz, Molecular Thermodynamics of Fluid Phase Equilibria, Prentice Hall, Englewood Cliffs (1969).

2. T. W. Leland and P. S. Chappelear, in Applied Thermodynamics, American Chemical Society, New York (1968).

3. S. E. Wood and A. E. Austin, J. Am. Chem. Soc., 67, 480 (1945).

4. G. A. Holder and E. Whalley, Trans. Far. Soc., 58, 2095 (1962).

5. R. E. Gibson and O. H. Loeffler, J. Am. Chem. Soc., 61, 2877 (1939).

6. R. E. Gibson and O. H. Loeffler, J. Am. Chem. Soc., 61, 2515 (1939).

7. S. E. Richards and J. Chadwell, J. Am. Chem. Soc., 47, 2283 (1925).

8. H. E. Eduljee et al., J. Chem. Soc., London, 3086 (1951).

9. G. N. Lewis and M. Randall, Thermodynamics, 2nd Ed., McGraw-Hill, New York (1961).

10. G. W. Holtzlander and J. W. Riggle, A.I.Ch.E.J., 1, 312 (1955).

11. M. Orentlicher and J. M. Prausnitz, Canadian J. of Chemistry, 45, 373 (1967).

12. K. E. Bachman and E. L. Simons, I.E.C., 44, 202 (1952).

13. I. Brown and F. Smith, Austr. J. of Chem., 15, 9 (1962).

14. E. Hala et al., Vapor-Liquid Equilibrium Data at Normal Pressures, Pergamon Press, London (1968).

CHAPTER 6

DETERMINATION OF EXPERIMENTAL THERMODYNAMIC PROPERTIES OF GAS-LIQUID SYSTEMS

The experimental method of Kay[1] and coworkers, and Connolly and Kandalic,[2] was used to determine the P-V-T relationships of constant composition fluid mixtures. A small precisely measured amount of the constant composition fluid sample is contained over mercury in an inverted capillary tube, sealed at the top. The tube is mounted on a steel block, within a constant temperature bath. Pressure is exerted on the fluid through the mercury. The volume of the sample at a fixed temperature and pressure is determined by measuring the length of the liquid column with a cathetometer; the cross-sectional area of the tube is accurately calibrated.

6.1 Description of Apparatus

The apparatus is divided into pressure and vacuum sections.

A symbolic drawing of the vacuum section is shown in Fig. 6-1. The glass manifold M, approximately 100 cm long, 4 cm in diameter, is connected to a mechanical vacuum pump through the stopcock H (4 mm bore), and a cold trap with liquid nitrogen. Stopcocks D, E, F, G and I are 2 mm bore. A tilting Mcleod gauge, reading to 1 micron Hg, is connected at D and indicates the ultimate vacuum obtained in the manifold. A Texas Instruments pressure gauge is connected at G. (The Texas gauge has interchangeable pressure measuring Bourdon capsules for different pressure ranges.) J, B and C are 4 mm bore vacuum stopcocks, and K is a ball and socket joint. The entire

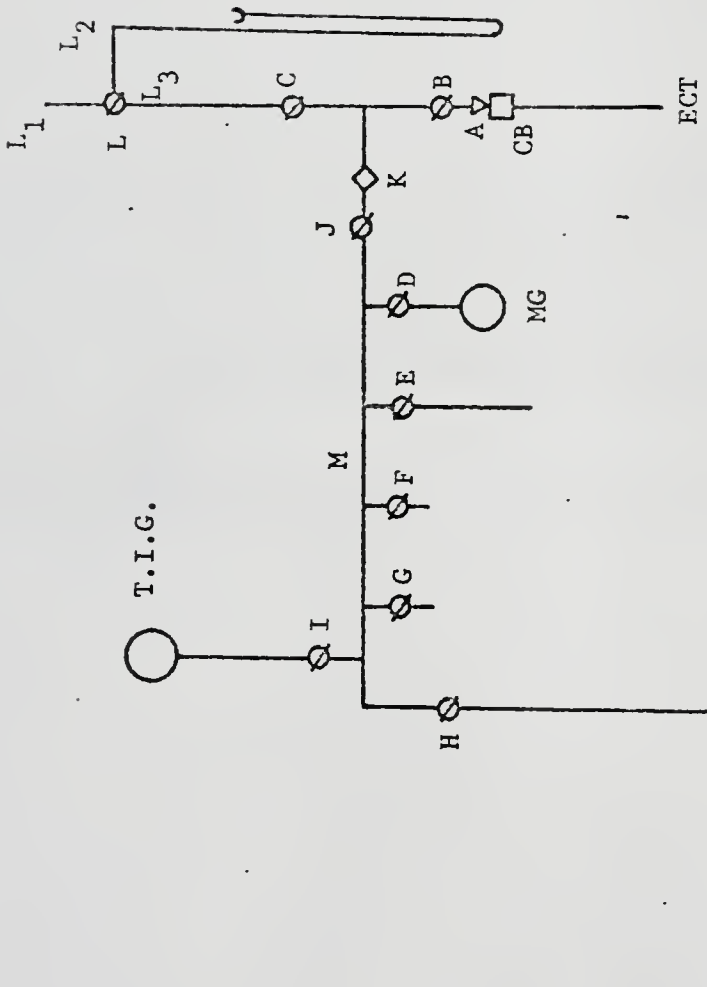

Fig. 6-1. Experimental apparatus - vacuum section.

apparatus, to the right of K, can be swivelled through 180° for use during calibration. A is a Cajon Ultra Torr stainless steel fitting that provides a vacuum connection between the glass tubing and the stainless steel compression block (CB) which holds the experimental capillary tube ECB. L is a three-way glass stopcock through which mercury may flow into the system. The length of the glass column from L to A is approximately 80 cms.

The pressure section of the apparatus is shown in Fig. 6-2. The double walled glass jacket (VJ) is supported on the base of the compression block. The annular space in the jacket is permanently evacuated. T_1 and T_2 are temperature probes for a Hewlett Packard quartz thermometer (HPT). The connecting lines in the pressure section are 1/8" O.D. stainless steel tubing. Valves 1 through 10 are high pressure stainless steel needle valves. SG is a thick walled plexiglass tube. It is used as a sight glass up to 8 atm pressure to indicate the level of mercury in the system, and is shut off during operation at higher pressures. MLI is a high pressure mercury level indicator, made out of stainless steel. It is constructed by connecting three pieces of insulated copper wire through pressure seals 1-1/2" apart. The wires are led to lamps through a 6-Volt battery. When the mercury in the system rises to the level of each wire, the corresponding lamp is lit. HG and BG are Bourdon-type pressure gauges. The former is a Heise gauge reading up to 600 psi, and was calibrated with a dead weight tester. The latter gauge reads up to 6000 psi and is used as an indicator. DWG is a Ruska Instrument dead weight pressure tester and gauge; its pressure range is 0.4 to

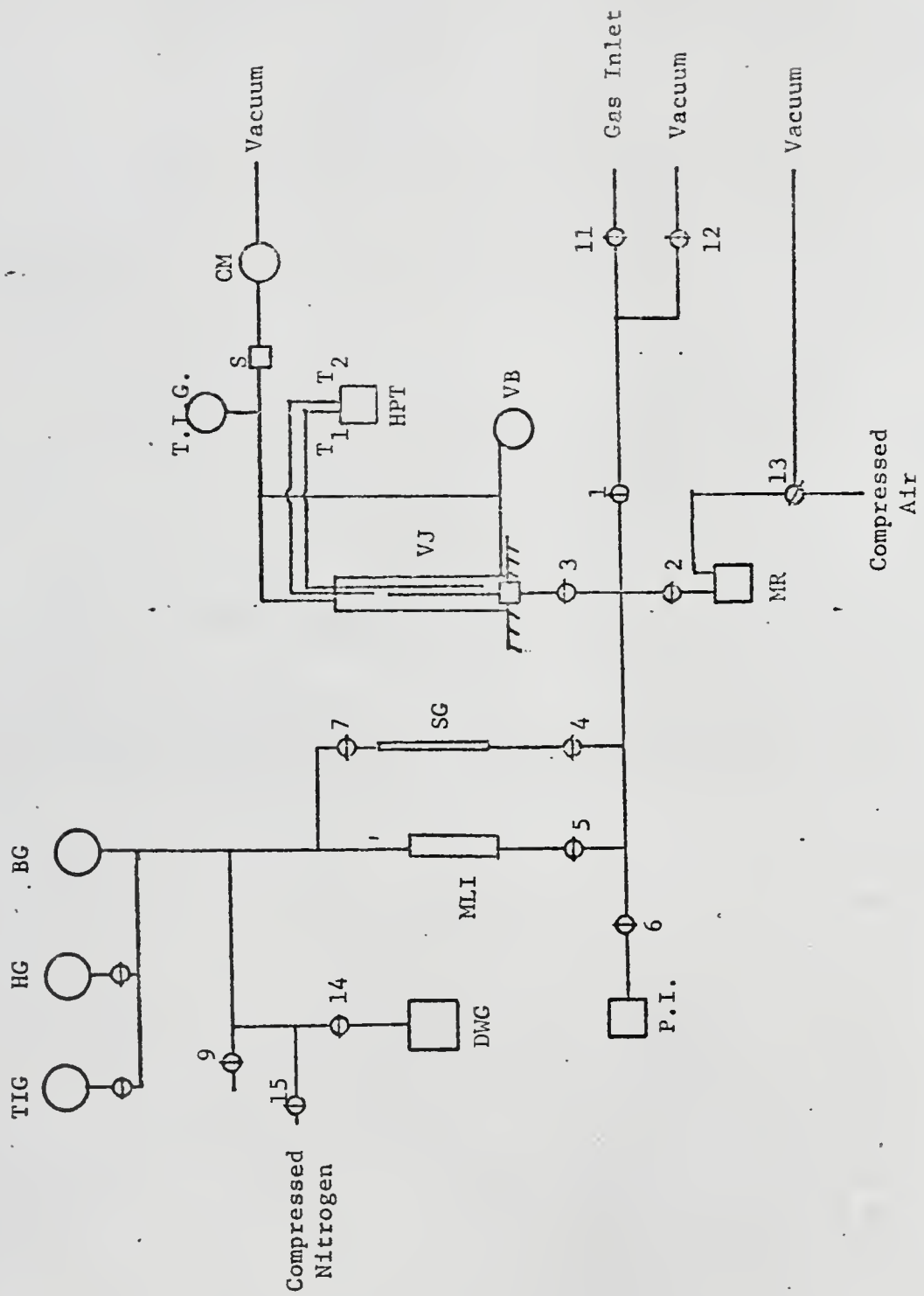

Fig. 6-2. Experimental apparatus - pressure section.

170 kgm/cm^2. PI is a piston-type pressure intensifier manufactured by High Pressure Co.; it can produce pressures up to 10,000 psi.

6.2 Experimental Procedure

The materials used were spectrograde quality benzene, n-octane, and carbon tetrachloride of certified purity +99 mole %. H_2 and N_2 gases were prepurified grade 99.95%. The densities of the liquid samples were determined by measuring the volumes in a standard 5 ml pycnometer at 25%, and then measuring the mass on a Sartorius balance.

The liquid sample was transferred into a clean dry glass tube and attached by clear rubber tubing at stopcock E. The clean experimental capillary tube (ECT), with a small stainless steel ball, 2 mm diameter, dropped into it,was mounted on the compression block, and connected at A. C was closed, with clean mercury above it. The system, with E closed, was evacuated for several hours, the ultimate vacuum obtained was about 50 u Hg. At this point, E was opened and air in contact with the liquid, together with some liquid, exhausted. E was closed and the system evacuated again. On attaining the ultimate vacuum, H was closed off and a liquid N_2 flask held around the ECT. On opening E some of the liquid volatilized into the ECT which was at liquid nitrogen temperature. E was closed and the system partially evacuated with the liquid nitrogen flask in place. D was then closed, and C opened, dropping some mercury onto the frozen liquid sample. The flask of liquid nitrogen was quickly removed. With the sample still frozen, the compression block was disconnected and mounted upright on its base on the pressure section. Valves 9, 11 and

2 were closed and the pressure system evacuated with the vacuum pump. When the lower section of the frozen mercury column began to thaw, pumping was stopped, valves 1 and 12 shut and 2 opened. Mercury from the reservoir (MR) was forced up into the system by pressurizing with compressed air, usually the level was raised up to the middle copper probe of the MLI. Valve 2 was then shut. The system was now loaded and ready for measurement. The vapor jacket (VJ) was mounted on its base, around the ECT, and connected to the cartesian manostat (CM) through a separation tube. The manostat controlled the pressure in the vapor jacket to within $\pm$ .1 mm Hg. The bath heater was turned on, and the temperature stabilized in the vapor jacket in about 30-40 minutes. Ethylene glycol was used as the fluid in the vapor bath. The bath temperature was measured at the upper and lower ends of the vapor jacket.

For system pressures up to 8 atmospheres, the mercury level was read in the sight glass SG. For higher pressure operation, it was shut off through valves 4 and 7. Pressures up to 600 psi gauge were read on the Heise gauge. Higher pressures were measured with the Ruska dead weight tester. The system pressure was adjusted by introducing compressed nitrogen gas from the cylinder at desired delivery pressures up to 1500 psi. By manipulating the pressure intensifier (PI), the level of mercury in the MLI was maintained quite constant as indicated by the lamps of the MLI. The level of mercury in the ECT was read on the Wild Herbregg cathetometer.

After completing measurements on the liquid sample, the pressure was released through valve 9, and the vapor jacket removed.

Two small metal cups were mounted on the ECT. Each had a hole in the bottom somewhat larger than the diameter of the ECT with retaining O-rings. Both cups C1 and C2 were placed lower than the mercury level in the ECT. Liquid N_2 was poured into C2, the lower cup. When the mercury froze, valve 1 was opened, 11 shut and the system evacuated through valve 12. The frozen mercury at C1 kept the liquid sample isolated from the vacuum. After evacuating to 500 μ Hg, valves 12, 4, 5 and 6 were shut, and valve 11 opened to introduce gas into the system up to C2. Valve 3 was shut, 4, 5 and 12 opened and the system evacuated once more. Finally, after evacuating at 500 μ Hg for 10 minutes, 12 and 1 were shut, 2 opened, and mercury from the reservoir raised up into the system and the ECT, sealing off the gas between it and the mercury frozen at C2. Valve 2 was then closed and liquid nitrogen poured into C1 freezing the mercury in its vicinity; this mercury was kept frozen throughout the following operation. Nitrogen gas from the cylinder forced the mercury further up into the ECT below the trapped gas. There was also a visible mercury head in SG. The mercury at C2 was then allowed to thaw; as it thawed and warmed to room temperature, the gas expanded to about twice its original volume and pushed the mercury downward. The system pressure was adjusted such that the mercury level was just visible above the compression block CB. The length of the gas column, the mercury levels in the ECT and SG, and the pressure at HG and TIG were noted. This gave a measurement of the gas volume at room temperature.

Valves 4 and 5 were then shut and the mercury at C1 allowed to thaw. Cups C1 and C2 were removed, and the system pressurized up

to 100 psig, as read on the Heise gauge. The mercury column separating the gas and liquid was broken by moving the steel ball (placed inside initially) through it with a powerful magnet. The two components were mixed, and stirred with the steel ball for about 10 minutes. The system was again ready for P-V-T measurements.

The system was pressurized in regular increments of 20 psi, with vigorous stirring between pressure changes. The bubble pressure of the system was reached when the last bubble of gas disappeared on stirring. By reducing and increasing the pressure around the bubble pressure, it could be reproduced to within $\pm$ 1 psi for all systems except the CCl_4 system for which this range was $\pm$ 2 psi. When reducing the pressure, the bubble pressure was indicated by the appearance of the first gas bubble. For pressures above the bubble pressure, P-V-T measurements were conducted as described earlier for the liquid system.

The mixed solvent could not be volatilized into the vacuum manifold, due to the differences in volatility of the components. It was made up in the desired composition by mixing measured amounts of the pure components in a clean measuring bottle, and then injected into the ECT through a syringe. The ECT was mounted on the compression block, and then connected at A. The liquid nitrogen flask was attached, and the system evacuated while the liquid mixture was frozen. B was then closed, the nitrogen flask removed, and the mixture thawed. The freeze and thaw procedure was repeated until no gas bubbles appeared on thawing. No losses of material could be detected by the cathetometer in this sequence of operations. After

the last thawing operation, in all cases, the level of liquid in the ECT was the same (as detected by the cathetometer) as when first introduced into the ECT. The procedure from this point onwards was the same as for the pure liquid solvents.

The ECT was calibrated on the vacuum section. The limb on the right of joint K was swivelled through 180°, so that the ECT was mounted upright. The system was evacuated to the ultimate vacuum. The mercury level was raised up in the limb CL until it stood a little below C. The system was pumped out for another 2 hours. Stopcock J was then closed and the mercury raised up all the way into the ECT with the levelling bulb. A weighing bottle was held under L; L_1 and L_3 were connected and a small amount of mercury collected in the weighing bottle. The amount of mercury was weighed and its value determined from the known density. The mercury level in the ECT was noted. The procedure was repeated in steps until the ECT was completely drained. A calibration curve was made of the volume of mercury collected corresponding to a given level in the ECT.

6.3 Treatment and Analysis of Experimental Data

The densities of the liquid samples were measured at 25°C in a pycnometer. These are reported in Table 6-1, and compared with values from the literature. The measured density of pure octane is 4% larger than the literature value; all the other densities agree to within .05%.

The mass of liquid in the experimental capillary was determined from the measured volume (in situ) and the known density. The virial

TABLE 6-1

DENSITIES OF PURE AND MIXED SOLVENTS AT 25°C

Solvent Components			Density, gms/cc	
1	2	x_1	Measured	Literature
Benzene		1.0	.8736	.8737[3]
Benzene	CCl_4	0.5	1.2443	1.2420[3]
CCl_4		1.0	1.5850	1.5844[3]
Benzene	Octane	0.5	.7662	-
Octane		1.0	.7047	.7019[4]

equation of state, up to the second virial coefficient, was used with the measured volume to determine the moles of gas added to the system.

Table 6-2 contains a key indicating the compositions of the mixture studied. The bubble pressures measured for each gas composition are also shown in this table. These were reproducible in both increasing pressure and decreasing pressure to ± 1 psia for the benzene-octane systems and to ± 2 psia for the benzene-carbon tetrachloride systems. The bubble pressures are used later to derive Henry's constants and activity coefficients.

Experimental volumes were measured to a precision of ± .25% and pressures to ± .6%. The volumes of constant composition liquid mixtures were fitted to equations of the form

$$v(T,P) = a + \frac{b}{P} + cP + dP^2 \qquad (6.1)$$

at each isotherm. A least squares fitting program was used for this purpose. Wherever possible, the three-parameter equation, with d = 0, was used. The fitted constants a, b, c, d are reported in Table 6-3. δ is the sum of squares of the relative error in representing the experimental volume by equation (6.1).

The isothermal compressibility from equation (6.1) is

$$\kappa = \frac{b/P^2 - c - 2dP}{a + b/P + cP + dP^2} \qquad (6.2)$$

and

$$\frac{1}{\rho\kappa RT} = \frac{[a + b/P + cP + dP^2]^2}{RT[b/P^2 - c - 2dP]} \qquad (6.3)$$

The uncertainty in determining κ from the experimental volumes is ± 10%.

TABLE 6-2

MEASURED BUBBLE PRESSURES OF GAS-SOLVENT SYSTEMS

System	Run #	x_{gas}	Bubble Pressure atm 298°K	378°K	418°K
N_2-benzene	A2	.0063	14.98	11.98	13.89
	A3	.0129	31.45	22.60	23.28
	A4	.01971	49.56	33.96	33.08
	A5	.0272	-	46.79	44.20
	A6	.0330	-	57.03	52.96
N_2-benzene octane	B2	.0052	4.580	5.94	8.63
	B3	.0112	9.92	11.13	13.84
	B4	.0191	17.20	18.09	20.80
	B5	.0267	24.52	24.93	27.62
	B6	.0379	35.87	35.29	37.90
N_2-octane	C2	.01065	7.08	7.08	8.03
	C3	.02113	14.16	13.61	14.30
	C4	.0436	30.22	27.64	27.64
	C5	.06335	45.20	40.16	39.48
N_2-CCl_4	U2	.0073	11.71	11.44	14.02
	U3	.0132	21.38	19.06	21.24
	U4	.02078	34.45	29.14	30.50
	U5	.0278	47.11	37.97	39.21
	U6	.0331	57.18	45.99	45.88
	U7	.03906		54.46	53.51
N_2-benzene -octane	V2	.0073	16.13	12.75	14.77
	V3	.0138	31.20	22.45	23.61
	V4	.0209	48.60	33.30	32.91
	V5	.0280	67.31	44.47	42.65
	V6	.0384	-	51.07	48.37
H_2-benzene	X2	.0059	14.57	13.89	15.11
	X3	.0143	35.40	30.91	29.27
	X4	.02104	52.55	44.79	40.84
	X5	.0292	-	61.67	54.87
	X6	.0323	-	-	60.18
H_2-benzene -octane	Y2	.003	7.38	7.53	9.81
	Y3	.012	29.70	25.79	27.05
	Y4	.01868	46.70	39.57	40.19
	Y5	.0232	58.43	49.02	49.27

TABLE 6-2 (Continued)

System	Run #	x_{gas}	Bubble Pressure atm 298°K	378°K	418°K
H_2-octane	Z2	.0113	16.75	12.53	12.25
	Z3	.02102	31.59	22.74	21.51
	Z4	.04105	45.20	44.25	40.30
	Z5	.06078	63.31	65.62	58.95

TABLE 6-3

VOLUMETRIC PROPERTIES OF CONSTANT COMPOSITION MIXTURES--
COEFFICIENTS FOR EQUATION (6.1)

Run #	T °C	10^2	a	b	10^2c	10^4d
A1	25	.000	89.420	.001	- .87	0.0
	105	.004	99.183	.007	-2.03	0.0
	145	.060	105.780	.153	-3.45	0.0
A2	25	.001	89.204	- .614	- .94	0.0
	105	.070	99.159	-1.356	-2.33	0.0
	145	.002	105.779	- .803	-3.60	0.0
A3	105	.002	98.869	- .311	-2.07	0.0
	145	.006	105.450	4.379	-3.37	0.0
B1	25	.003	125.482	.232	-1.35	0.0
	105	.010	139.216	.517	-3.26	0.0
	145	.050	148.485	.788	-6.02	0.0
B2	25	.005	125.085	.249	-1.35	0.0
	105	.010	138.858	.844	-3.25	0.0
	145	.007	148.147	1.643	-5.96	0.0
B3	25	.002	124.592	.788	-1.29	0.0
	105	.010	138.364	2.841	- .03	0.0
	145	.004	147.778	2.601	- .06	0.0
B4	25	.004	123.981	1.228	-1.30	0.0
	105	.010	137.947	1.174	-3.27	0.0
	145	.000	147.374	2.647	-6.06	0.0
C1	25	.020	162.067	.199	-2.06	0.0
	105	.010	180.132	- .431	-6.25	0.0
	145	.000	192.096	.315	-10.39	0.0
C2	25	.010	160.852	.685	-1.93	0.0
	105	.030	178.697	2.402	-5.05	0.0
	145	.050	190.739	3.798	-9.23	0.0
C3	105	.001	177.679	1.730	-5.21	0.0
	145	.010	189.600	6.748	-9.14	0.0
U1	25	.000	97.070	- .012	-1.07	0.0
	105	.050	107.895	- .039	-2.36	.17
	145	.000	115.174	.017	-2.96	-.01

TABLE 6-3 (Continued)

Run #	T °C	10^2	a	b	10^2c	10^4d
U2	25	.000	96.732	.006	-1.08	0.0
	105	.060	107.661	- .322	-2.26	0.0
	145	.060	115.546	-9.361	-3.59	0.0
U3	105	.005	107.374	1.465	-2.13	0.0
V1	25	.030	93.189	.179	-8.70	0.0
	105	.070	103.406	.393	-1.92	0.0
	145	.000	110.436	.042	-3.08	.18
V2	25	.040	92.780	1.774	- .76	0.0
	105	.001	103.223	.390	-1.97	0.0
	145	.004	110.317	.155	-2.99	0.0
V3	105	.001	103.032	.669	-1.98	0.0
	145	.000	110.098	2.818	-2.87	0.0
X1	25	.000	89.428	- .011	- .89	0.0
	105	.003	99.187	- .055	-2.04	0.0
	145	.003	105.801	- .015	-3.49	0.0
X2	25	.000	89.103	- .007	- .89	0.0
	105	.001	98.913	.142	-2.04	0.0
	145	.002	105.585	.109	-3.51	0.0
Y1	25	.005	125.536	- .116	-1.56	-.22
	105	.004	139.315	- .114	-3.63	-.38
	145	.040	148.591	.765	-6.02	0.0
Y2	25	.100	125.298	- .497	-1.53	0.0
	105	.02	138.964	.469	-3.26	0.0
	145	.03	148.259	.765	-6.04	0.0
Y3	105	.070	138.004	3.184	-3.03	0.0
	145	.010	147.789	1.708	-5.98	0.0
Z1	25	.012	162.057	.304	-2.05	0.0
	105	.007	180.143	- .495	-6.33	-1.36
	145	.000	192.128	.086	-10.51	.14
Z2	25	.001	160.616	.816	-1.97	0.0
	105	.005	178.437	2.003	-5.13	0.0
	145	.030	190.428	3.299	-9.26	0.0
Z3	105	.006	177.033	7.173	-4.93	0.0
	145	.000	189.102	6.612	-9.07	0.0

The pressure range of compression dictates the accuracy with which κ can be determined experimentally. The present experiment was originally designed for compressions up to 200 atmospheres but due to repeated fracture of the glass capillary tubing, the maximum operating pressure was limited to 65 atmospheres.

Volumes and compressibilities calculated from (6.1) and (6.2) are reported in Table 6-4, and compared with corresponding values taken from the literature. At room temperature, the volumes in the benzene and carbon tetrachloride systems agree to $\pm$ .5% with the literature value. The compressibilities agree to within $\pm$ 10%. In the benzene-carbon tetrachloride systems, however, the measured compressibility of the mixture is less than that of either pure component. At the higher temperature, the experimental compressibility of octane is 40% larger than that reported by Connolly, and the volume 1.5% smaller. The literature values will be used in further analysis of the benzene-octane system at this temperature.

Partial molar volumes of the components at constant pressure and temperature were determined from the composition dependence of the volumes. The experimental volumes were fitted to equations of the form

$$v = v^{o} + bx + cx^{2} \qquad (6.4)$$

where x is the solute mole fraction, and v^{o} is the volume of the solute-free solvent. This equation was used only at conditions where the volumes of at least 4 compositions including the pure solvent were known. At low pressures, hence fewer compositions, the coefficient b was estimated from the simplified relation setting c equal to zero.

TABLE 6-4

VOLUMETRIC PROPERTIES OF SOLVENTS

System	T °K	P atm	V cc/mole expt	V cc/mole lit	$\kappa \times 10^4$ $(atm)^{-1}$ expt	$\kappa \times 10^4$ $(atm)^{-1}$ lit	$\frac{1}{\rho\kappa RT}$ expt	$\frac{1}{\rho\kappa RT}$ lit	$\frac{1}{\rho\kappa RT}$ one fluid theory expt	$\frac{1}{\rho\kappa RT}$ one fluid theory lit
Benzene	298	35.0	89.114	88.640[5]	.98	.954[5]	37.16	38.13	37.16	38.13
Benzene + CCl_4	298	35.0	92.893	93.377[5]	.952	1.01[5]	39.88	37.74	36.09	36.15
CCl_4	298	35.0	96.695	97.086[5]	1.106	1.05[5]	35.73	37.84	35.73	37.84
Benzene	298	35.0	89.114	88.640[5]	.98	.954[5]	37.16	38.13	37.16	38.13
Benzene + octane	298	35.0	125.014	-	1.094	-	46.51	-	45.74	51.18*
Octane	298	35.0	160.938	162.444[4]	1.288	1.120[4]	51.18	56.47	51.18	56.47
Benzene	418	41.8	104.318	105.471[6]	3.424	2.82[6]	8.88	10.90	8.88	10.90
Benzene + octane			145.978	-	4.15	-	10.26	-	9.96	13.63*
Octane			186.726	189.618[6]	4.98	3.55[6]	11.00	15.50	11.00	15.50

*Experimental volume used.

[5] G. A. Holder and E. Whalley, Trans. Faraday Soc., 58, 2095 (1962).

[6] J. F. Connolly and G. A. Kandalic, J. Chem. Eng. Data, 7, 137 (1962).

Expression for the partial molar volume at infinite dilution, and the excess volume at composition x are obtained from equation (6.4). Those are

$$\bar{v}_1^o = v^o + b \tag{6.5}$$

$$v^E = cx_1^2 \tag{6.6}$$

The uncertainty in the fitted value of v_1^o is of the same order as that of v, i.e., $\pm$ .4 cc/mole. The corresponding uncertainty in b, however, is much less, $\pm$ .11 cc/mole. b is the unit change in volume of the solvent on addition of the first incremental amount of solute, and the uncertainties in the initial and final volumes are correlated. The experimental partial molar volumes should be accurate to $\pm$ .5 cc/mole. The accuracy of estimating the excess volume parameter, c, is dependent on the highest solute composition of the liquid mixture. A typical composition of 0.2 mole fraction of solute will yield an excess volume parameter accurate to $\pm$ 5%. In the experiments reported here, the maximum composition attained was .06 mole fraction for one system. At best, only an estimate of c can be obtained from this data.

The calculated partial molar volumes are shown in Table 6-5 and compared with values obtained from the literature. At each temperature, the partial molar volumes are shown at the lowest and highest pressures at which they were obtained. In all cases, the experimental $\bar{v}_1^o$ agrees with the literature value to within the reported error.

The last column in this table shows partial molar volumes determined from the generalized correlations (4.3) and (4.6). The

TABLE 6-5

PARTIAL MOLAR VOLUMES OF SOLUTES

System	T °K	P atm	$\bar{v}_1^o$ cc/mole Expt.	Literature	Correlations
N_2-benzene	298	21.4	48.1	52.6[7]	45.3
		55.5	46.7	-	43.2
	378	14.6	73.8	-	68.8
		55.5	69.0	-	65.1
	418	21.4	92.7	-	90.1
		55.5	88.3	-	87.1
N_2-benzene -octane	298	21.4	49.4	-	46.2
		55.5	48.6	-	44.5
	378	14.6	73.2	-	66.2
		55.5	72.7	-	63.7
	418	21.4	92.7	-	86.8
		55.5	89.1	-	82.7
N_2-octane	298	21.4	53.7	-	48.2
		55.5	53.2	-	47.4
	378	21.4	77.2	-	67.1
		55.5	75.7	-	65.7
	418	21.4	95.4	-	87.3
		55.5	91.	-	84.0
H_2-benzene	298	41.8	35.3	35.0 ± 2[8]	33.0
		55.5	35.1	-	31.2
	378	35.0	52.7	52.2 ± 3[9]	45.1
		55.5	51.3	49.3 ± 3[9]	47.7
	418	35.0	65.9	66.6 ± 3[9]	67.9
		55.5	64.3	63.4 ± 3[9]	64.4
H_2-benzene -octane	298	35.0	34.1	-	33.2
		55.5	32.6	-	32.1
	378	35.0	52.7	-	50.6
		55.5	49.3	-	48.2
	418	28.2	67.0	-	64.3
		55.5	65.0	-	61.2
H_2-octane	298	35.0	38.0	35.9 ± 3[9]	35.1
		55.5	37.6	35.9 ± 3[9]	34.2
	378	28.2	57.2	56.0 ± 3[9]	50.3
		55.5	53.6	53.8 ± 3[9]	48.2
	418	28.2	69.3	75.5 ± 3[9]	66.3
		55.5	66.2	69.3 ± 3[9]	62.3

TABLE 6-5 (Continued)

System	T °K	P atm	$\bar{v}_1^o$ cc/mole Expt.	Literature	Correlations
N_2-CCl_4	298	35.0	52.0	53.0 [10]	46.6
		55.5	51.5	-	45.0
	378	35.0	78.0	-	71.1
		55.5	75.1	-	69.0
	418	21.4	99.8	-	98.3
		55.5	97.6	-	95.1
N_2-benzene-CCl_4	298	21.4	49.6	-	46.2
		55.5	48.7	-	44.1
	378	14.6	75.8	-	69.8
		55.5	73.4	-	67.1
	418	21.4	95.6	-	94.7
		55.5	94.3	-	91.5

mixed solvents were represented by a one-fluid model and the experimental volumes used to calculate reduced densities. The resulting $\bar{v}_1^o$ is within 15% of experiment, indicating that the one-fluid model used in conjunction with equations (4.3) and (4.6) yields reliable estimates of the solute partial molar volume.

Activity coefficient parameters and Henry's constants for solute-solvent systems were determined from the experimental bubble pressures. The solute activity coefficient at low concentrations is represented by a one-term Margules expression

$$\ell n\gamma_{1m}^* = f_2^o(x_1^2 - 2x_1) \tag{6.7}$$

A two-term Margules expression represents the excess free energy of the mixed solvent. The activity coefficients for the solvent components in the mixture are

$$\ell n\gamma_{2m} = f_2^o x_1^2 + [(2B - A)X_3^2 + 2(A - B)X_3^3] \tag{6.8}$$

$$\ell n\gamma_{3m} = f_2^o x_1^2 + [(2A - B)X_2^2 + 2(B - A)X_2^3] \tag{6.9}$$

X_2 and X_3 are the solute free mole fractions in the solvent mixture. A and B are the coefficients of the excess free energy expression and are listed in Table 6-6. The temperature variations in the excess free energies were estimated by the Gibbs-Helmholtz equation.

The vapor phase properties are characterized by the Redlich-Kwong equation. The computational method and algorithm for the determination of Henry's constant and activity coefficient parameters from bubble pressures is described in Appendix E. The results of these

TABLE 6-6

EXCESS FREE ENERGIES OF EQUIMOLAR SOLVENT MIXTURES

System	T °K	A	B	g^E cals/mole
Benzene[11] carbon tetrachloride	298	.0331	.0331	82.00
	378	.0233	.0233	73.14
	418	.0196	.0196	68.16
Benzene[12] n-octane	343	.85	.11	70.84
	298	1.1445	.1481	95.38
	378	.6208	.0803	65.62
	418	.3613	.0468	42.23

TABLE 6-7

HENRY'S CONSTANTS AND ACTIVITY COEFFICIENT PARAMETERS
FROM EXPERIMENTAL DATA

System	T °K	f_2	$H_{1,m}$ atm	
			Experiment	Literature
H_2-octane	298	- .36	1438	1464[13]
	378	.054	1045	
	418	.205	929	
N_2-octane	298	- .28	648	673[14]
	378	+ .142	606	
	418	.346	588	
N_2-CCl_4	298	.452	1544	1590[15]
	378	.911	1238	
	418	1.076	1144	
N_2-C_6H_6	298	.502	2290	2280[15]
	378	.874	1541	
	418	1.129	1338	
H_2-C_6H_6	298	.510	2429	3882[16]
	378	.962	1994	2121
	418	1.232	1646	1644
N_2-C_6H_6-CCl_4	298	-1.127	2077	
	378	- .330	1406	
	418	- .075	1254	
N_2-C_6H_6-octane	298	- .761	850	
	378	.381	869	
	418	2.189	959	
H_2-C_6H_6	298	- .684	2408	
	378	.519	2043	
	418	2.270	2072	

calculations are shown in Table 6-7. There is an experimental uncertainty of ± 6% in the Henry's constants. The major contribution to this is from the uncertainty in determining the mole fraction of the solute. For systems of gases dissolved in single solvents, the measured Henry's constant agrees with literature values to within these limits. The sole exception is hydrogen in benzene at 298°K. The disagreement here is 35%; there is no apparent experimental factor to account for a discrepancy of this magnitude. Both values will be used later to analyze the mixed solvents data with the expressions of the distribution function solution theory.

The experimental f_2^o increases with increasing temperature. This is in accordance with the corresponding states correlations discussed in the next chapter. Some negative values of f_2^o are encountered in the mixed solvents systems, indicating a positive slope for the solute activity-coefficient at zero composition. However, this is not inconsistent with the direct correlation function solution theory.

REFERENCES FOR CHAPTER 6

1. W. B. Kay, J. Am. Chem. Soc., 69, 1273 (1947).

2. J. F. Connolly, J. Chem. Phys., 36, 2897 (1962).

3. S. E. Wood and J. P. Brusie, J. Am. Chem. Soc., 65, 1891 (1943).

4. W. A. Felsing and G. M. Watson, J. Am. Chem. Soc., 64, 1822 (1942).

5. G. A. Holder and E. Whalley, Trans. Far. Soc., 58, 2095 (1962).

6. J. F. Connolly and G. A. Kandalic, J. Chem. Engr. Data, 7, 137 (1962).

7. J. Horiuti, Scientific Papers of the Institute of Physical and Chemical Research, 17, 125 (1931).

8. J. E. Jolly and J. H. Hildebrand, J. Am. Chem. Soc., 80, 1050 (1958).

9. J. F. Connolly and G. A. Kandalic, Chem. Engr. Progr. Symposium Series, 59, 8 (1963).

10. J. C. Gjalbaek and J. H. Hildebrand, J. Am. Chem. Soc., 72, 1072 (1950).

11. J. S. Rowlinson, Liquids and Liquid Mixtures, Plenum Press, New York (1969).

12. S. R. M. Ellis, Trans. Inst. Chem. Engrs., 30, 58 (1952).

13. M. W. Cook et al., J. Chem. Phys., 36, 748 (1957).

14. E. S. Thomasen and J. C. Gjalbaek, Acta Chemica Scandinavica, 17, 127 (1963).

15. J. M. Prausnitz et al., Computer Calculations for Multicomponent Vapor-Liquid Equilibrium, Prentice Hall, Englewood Cliffs (1968).

CHAPTER 7

SOLUTION THEORY FOR GAS-LIQUID SYSTEMS

The expressions for thermodynamic properties obtained from the solution theory are most generally applicable to a system of one or more gases in a multicomponent solvent. This system is characterized by the complexities of liquid-liquid and gas-liquid types of interactions. Those methods previously found successful in describing these interactions individually are combined to analyze the complex multicomponent system.

Generalized correlations of the nonideality parameters for gases in single solvents are investigated first. These provide a quantitative description of the gas-solvent interaction. The hydrogen-benzene system, for which complete thermodynamic data is available, is studied to examine the validity of expressions for the composition dependent thermodynamic properties, and the characteristics of triplet correlation functions in gas-liquid systems as opposed to those in liquid-liquid systems. The experimental DCF integrals in ternary systems are next studied for their composition and macroscopic state dependence. In addition to the usual thermodynamic properties, these quantities determine the relations between the Henry's constants of the solute in the mixed and pure solvents, respectively. Finally, the Henry's constants and activity coefficients in the mixed solvent are determined from individual gas-solvent parameters and used to calculate vapor-liquid equilibrium in the ternary mixture.

7.1 Correlations for Activity Coefficient Parameters

A simple representation of the unsymmetric convention activity

coefficients in a binary mixture is

$$\ln\gamma_1^* = f_2^o(x_1^2 - 2x_1) + f_3^o(x_1^3 - \frac{3}{2}x_1^2) \tag{7.1}$$

and

$$\ln\gamma_2 = f_2^o x_1^2 + f_3^o x_1^3 \tag{7.2}$$

In terms of DCF integrals, f_2^o is given by

$$-2f_2^o = (1 - C_{11}^o) - \frac{(1 - C_{12}^o)^2}{(1 - C_{22}^o)} \tag{7.3}$$

Orentlicher[1] has used expressions (7.1) and (7.2), with $f_3^o = 0$, to represent the activity coefficients for hydrogen in croygenic solvents. He finds the coefficient f_2^o to vary inversely with absolute temperature.

Equations (4.3) and (4.6) relate C_{22}^o and C_{12}^o to the density of the pure solvent at system conditions. C_{11}^o, which represents the self-interaction of solute molecules in the solvent medium, is also likely to depend on the solvent density. At this point one would attempt to correlate C_{11}^o as a function of reduced solvent density. However, a close examination of equation (7.3) shows that the accuracy required in correlating C_{11}^o is of the same order as the required accuracy of f_2^o. For the experimental systems studied by Orentlicher, f_2^o varies from 0.0 to 1.0. At low solute compositions, an error of 10% in the activity coefficient corresponds to an equivalent error in f_2^o, i.e., about $\pm$ 0.1 absolute error. This, in turn, requires an accuracy of $\pm$ .2 in the absolute value of C_{11}^o, which has a large negative value.

Isothermal vapor-liquid equilibrium data were used to determine

experimental values of f_2^o and the solute Henry's constant. The activity coefficients for the solute and solvent were represented by equations (7.1) and (7.2), respectively. Vapor phase nonidealities were characterized by the Redlich-Kwong equation. The details of the calculations and the relevant equations are presented in Appendix E. The experimental data for hydrogen systems were those studied by Orentlicher, and the hydrogen-benzene data of Connolly.[2] Data on the methane systems were taken from Sage[3] and from Shim.[4] The fitted parameters for these systems are shown in Table 7-1. The calculated f_2^o shows a significant variation with temperature, or reduced solvent density for all systems. In the methane systems the contribution of f_3^o to the activity coefficients is significant. Under these conditions a proper representation of the activity coefficient requires correlations for f_2^o and f_3^o.

The next step was to search for an effective value of f_2^o which would be an average of the actual f_2^o and f_3^o. This was achieved by plotting $\frac{(\ell n \gamma_1^*)^{exp}}{x_1^2 - 2x_1}$ versus $\frac{x_1^3 - 3/2\ x_1^2}{x_1^2 - 2x_1}$ and selecting the best horizontal line to fit the data over the composition range. A horizontal line implies that $f_3^o = 0$. The zero intercept of the function gave f_2^{eff}. The extracted values of f_2^{eff} for the hydrogen-solvents system and methane-solvents systems are shown in Figs. 7-1 and 7-2, respectively. There is an approximate linear relationship for f_2^{eff} with solvent density. For the methane systems it is

$$f_2^{eff} = 4.355 - 1.570\ \tilde{\rho}_2^o \qquad (7.4)$$

and for hydrogen systems

TABLE 7-1

HENRY'S CONSTANTS AND ACTIVITY COEFFICIENTS FROM EXPERIMENTAL DATA ON BINARY SYSTEMS

System		T °K	$\tilde{\rho}_2$	P_2^s atm	f_2^o	f_3^o	$H_{1,2}^{P_2^s}$ atm	δ	Exp Data
H_2	Ar	87	2.602	.969	1.232	0.0	850.0	.68	5
		94	2.513	1.961	1.400	0.0	748.8	2.40	
		120	2.177	11.970	1.769	0.0	519.4	2.40	
H_2	C_6H_6	433	2.443	7.118	.798	0.0	1505.7	.01	2
		473	2.174	14.84	1.235	0.0	1130.6	1.60	
N_2	$C_{10}H_{22}$	311	2.954	.010	.724	- .583	690.0	100.00	6
CH_4	nC_6H_{14}	298	2.806	.199	.359	- .218	197.3	.10	4
		323	2.705	.533	.383	- .217	220.6	.30	
		348	2.598	1.212	.303	.276	235.2	.12	
		373	2.490	2.430	.310	.405	244.1	.15	
CH_4	$nC_{10}H_{22}$	344	2.844	.026	- .118	.243	214.8	.10	3
		377	2.731	.112	- .073	.304	238.0	1.00	
		410	2.619	.359	- .013	.389	257.2	.10	
		444	2.506	.926	.008	.061	265.9	1.00	

$$\delta = 10^4 \sum \left(\frac{x_{calc} - x_{exp}}{x_{exp}} \right)^2$$; summation extends over experimental compositions.

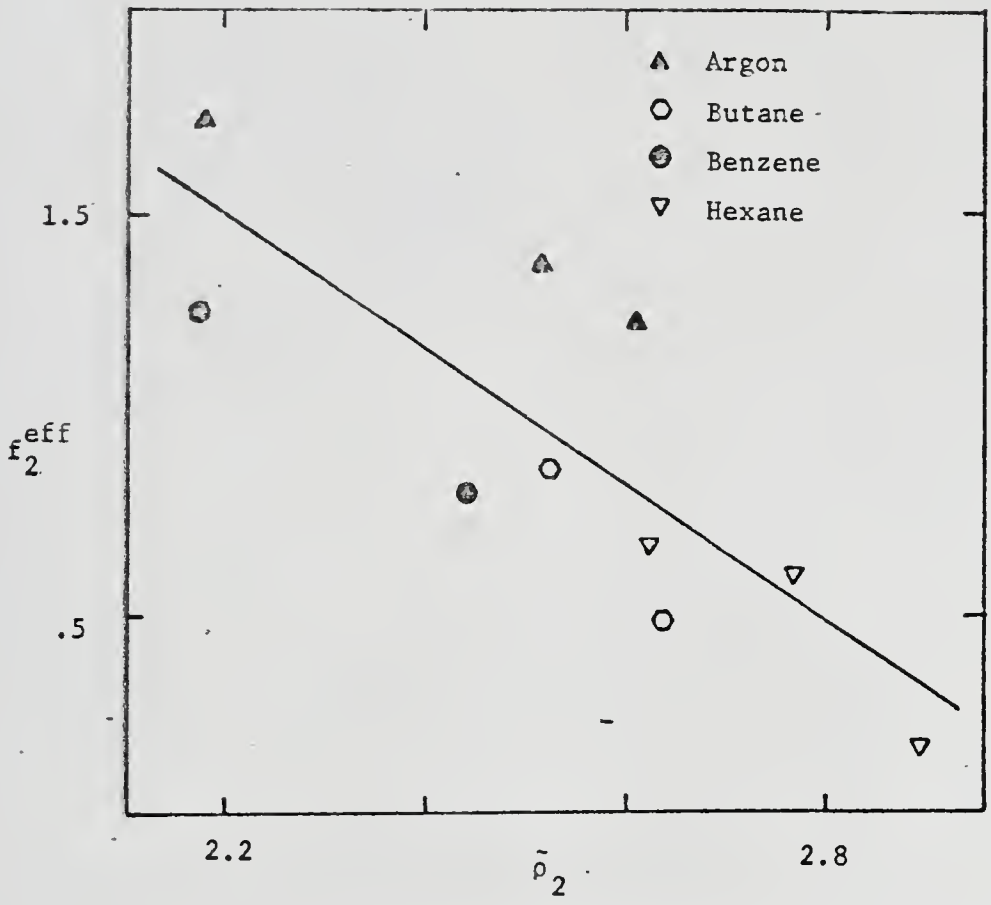

Fig. 7-1. Effective f_2^o for H_2-solvents systems.

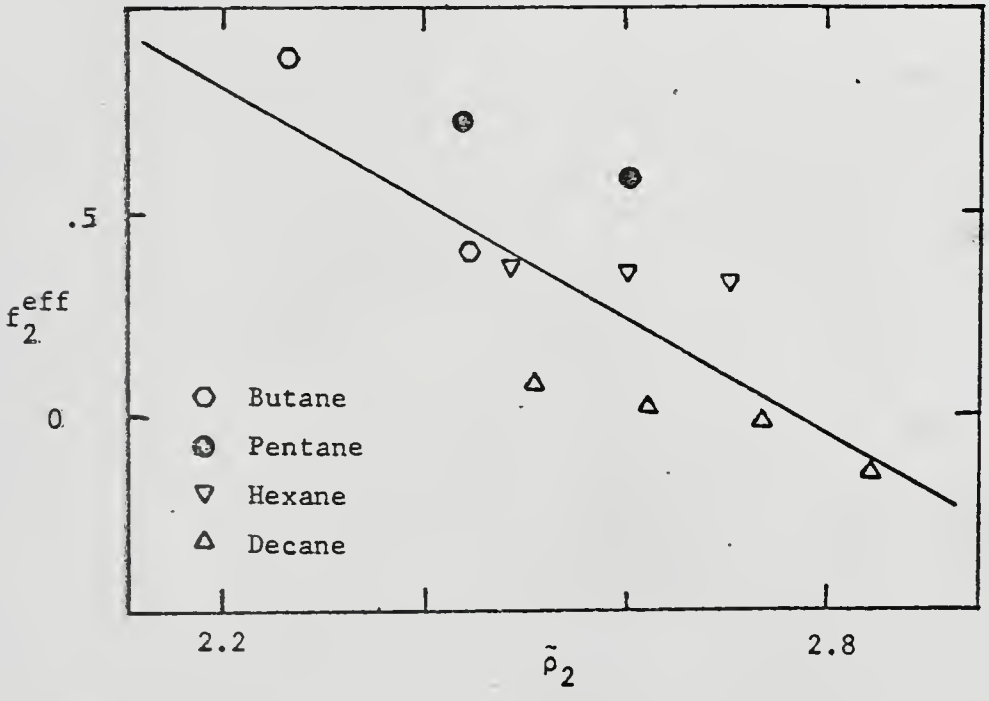

Fig. 7-2. Effective f_2^o for CH_4-solvents systems.

$$f_2^{eff} = 5.182 - 1.679\ \tilde{\rho}_2^o \qquad (7.5)$$

The validity of these approximations was tested by comparing calculated bubble pressures and vapor compositions for some systems with experimental data. The results are shown in Table 7-2 with calculations for some systems not included in the formulation of correlations (7.4) and (7.5). The calculation of bubble pressures is similar to that used in the fitting of parameters. There is good agreement between calculated and experimental vapor compositions. This agreement does not depend on a good calculation of the bubble pressures and may indicate an insensitivity to the equations describing the nonideality. The calculated bubble pressures agree well with experimental data in systems of moderate composition. At larger solute concentrations the pressures may differ by 20% from experiment. The calculations for methane in hexane and hydrogen in butane indicate that for systems in which f_2^{eff} from equation (7.4) differs considerably from the experimental value, the maximum error in the bubble pressure is 15%.

The sensitivity of calculated component mole fractions to the activity coefficient relation is an important consideration in design calculations. (A method of operation of separation equipment is to control the pressure and heat input to a unit and allow the stream compositions to adjust themselves to equilibrium values.) The calculated compositions for some representative systems are reported in Table 7-3. Comparisons are shown with experimental results and the predictions of the activity coefficient relation of Chueh and Prausnitz.[10] This is a widely used representation for liquid phase activity coefficients.

TABLE 7-2

VAPOR-LIQUID EQUILIBRIUM IN BINARY SYSTEMS

System (1)	System (2)	T °K	f_2^o	$H_{1,2}$ atm	x_1	Bubble Pressure atm Calc	Bubble Pressure atm Exp	y_1 Calc	y_1 Exp	Data Ref
CH_4	nC_4H_{10}	344	.421	266	.0307	8.49	6.81	.9960	.9950	3
					.1138	30.41	27.22	.9982	.9980	
					.2079	56.18	54.44	.9981	.9982	
CH_4	nC_6H_{14}	323	.108	221	.086	20.93	20.0	.9636	.9465	4
					.169	43.67	40.0	.9737	.9680	
					.246	68.80	60.0	.9734	.9747	
CH_4	nC_7H_{16}	310	.119	205	.1	21.97	21.65	-	-	7
					.2	47.34	45.54	-	-	
					.3	78.31	72.70	-	-	
H_2	Ar	120	1.527	519	.0418	37.00	36.34	.5561	.5514	5
					.0740	58.16	55.87	.6455	.6406	
					.1299	106.2	94.58	.6654	.6776	
H_2	C_4H_{10}	278	.766	1337	.016	23.09	21.1	.9377	.9326	8
					.111	174.9	162.7	.9819	.9682	
					.182	360.1	282.5	.9807	.9807	
H_2	CH_4	116	.796	962	.0318	34.75	33.36	.9348	.9279	9
					.095	120.5	101.4	.9526	.9466	

TABLE 7-3

BINARY VAPOR LIQUID EQUILIBRIUM

System (1)	System (2)	T °K	f_2^o	$H_{1,2}$ atm	P atm	x_1 Calc[a]	x_1 Calc[b]	x_1 Exp	y_1 Calc[a]	y_1 Calc[b]	y_1 Exp
H_2	C_4H_{10}	278	.766	1337	21.10	.0146	.0145	.0160	.9326	.9326	.9310
					53.98	.0377	.0373	.0360	.9682	.9682	.9670
					162.70	.1045	.1022	.1110	.9830	.9816	.9830
					282.50	.1585	.1555	.1820	.9840	.9819	.9840
CH_4	nC_6H_{14}	323	.108	221	10.0	.0413	.0418	.0422	.9370	.9370	.9371
					20.0	.0823	.0843	.0860	.9625	.9635	.9625
					30.0	.1207	.1254	.1290	.9701	.9702	.9702
					40.0	.1565	.1651	.1690	.9731	.9733	.9734
					50.0	.1898	.2036	.2080	.9742	.9744	.9745
CH_4	C_3H_8	310	.923	154	17.02	.0276	.0269	.0251[c]	.2282	.2279	.2184
					23.83	.0708	.0662	.0652	.4088	.4071	.3949
					34.04	.1416	.1247	.1235	.5471	.5415	.5209
					54.46	.3032	.2429	.2418	.6717	.6512	.6321
					74.88	.4490	.5298	.3731	.7375	.3116	.6738

[a] f_2^o from equations (7.4) or (7.5)

[b] Chueh's equation for activity coefficients

[c] Reference 11

They recommend a modified Van Laar expression. To correct for the size differences between solute and solvent molecules, they use the solute volume fraction rather than the simple mole fraction as the composition variable. For many systems this equation predicts activity coefficients in good agreement with experimental data up to about 0.3 solute mole fraction. However, the model parameters are characteristic for each solute-solvent interaction and must be previously determined from experimental data. A comparison of equation (7.1) with Chueh's equation is meaningful in light of the loss of accuracy, if any, that is incurred in going from a generalized parameter equation such as equations (7.4) and (7.5), to a nongeneralized equation to calculate vapor liquid equilibrium. The calculated vapor compositions, in Table 7-3 are uniformly good and agree consistently with experimental data. Both methods yield an equally accurate liquid composition for the hydrogen system. In the methane systems the liquid mole fractions calculated by equation (7.4) do not agree as well with experimental data as do those from the Chueh equation. The deviations at the highest pressures are up to 20% for equation (7.4) in the methane-propane system and 10% in the methane-hexane system. Therefore, the use of Chueh's equation for systems of known parameters yield uniformly good predictions of equilibrium composition at fixed temperature and pressure. At moderate compositions equations (7.4) and (7.5) which need only one generalized parameter for each component will yield comparable results.

The DCF integral C_{11}^{o} is more significant than the quantity f_2^o in understanding the molecular correlations in the fluid mixture. The qualified success in correlating activity coefficients with f_2^o suggests

that correlations of C_{11}^{o} for individual gas-solvents systems are possible. Experimental values of C_{11}^{o} for hydrogen-solvents and methane-solvents were obtained through equation (7.3). C_{22}^{o} and C_{12}^{o} were calculated from equations (4.3) and (4.6), respectively. The experimental values of f_2^{o} were those obtained from fitting bubble pressures and composition and are reported in Table 7-1.

C_{11}^{o} for the methane systems was correlated by the equation

$$\ln\left[-C_{11}^{o}\left(\frac{v_2^{*}}{v_1^{*}}\right)\right] = .36856 + .9458\,\tilde{\rho}_2 \qquad (7.6)$$

The corresponding equation for hydrogen systems and one nitrogen-decane system is

$$\ln\left[-C_{11}^{o}\left(\frac{v_2^{*}}{v_1^{*}}\right)\right] = -3.049 + 1.92606\,\tilde{\rho}_2 \qquad (7.7)$$

The accuracies with which the equations represent experimental activity coefficients are shown in Table 7-4. f_2^{o}(exp) is the actual representation of experimental data. It is compared with the correlations of f_2^{o}, equations (7.4) and (7.5), and the values of f_2^{o} from the correlation of C_{11}^{o}, equations (7.6) and (7.7). The correlations for C_{11}^{o} generally provide a value of f_2^{o} in closer agreement with the experimental, and the effective f_2^{o}, than the correlation of f_2^{o} itself. Under these circumstances, calculations of binary vapor-liquid equilibrium, using f_2^{o} from a C_{11}^{o} correlation, will agree even more closely with experimental data than from an effective f_2^{o}. In the minority of systems, where the f_2^{o} correlations are better, e.g., methane-butane at 310°K, f_2^{o}(exp), and f_2^{o}(effective), is itself small, and moderate errors in its prediction will have little

TABLE 7-4

ACTIVITY COEFFICIENT PARAMETERS FOR BINARY SYSTEMS

System		T °K	$\tilde{\rho}_2^o$	C_{11}^o	f_2^o			
				Calc[a]	Calc[a]	Exp	Calc[b]	Eff
CH_4	nC_6H_{14}	298	2.806	-5.539	.411	.359	- .05	.30
		323	2.705	-5.035	.363	.383	.108	.32
		348	2.598	-4.549	.351	.303	.276	.34
		373	2.490	-4.108	.378	.310	.446	.36
CH_4	nC_4H_{10}	310	2.446	-5.701	.953	.425	.515	.41
		344	2.253	-4.751	1.067	1.075	.818	.90
CH_4	$nC_{10}H_{22}$	344	2.844	-3.520	- .091	- .118	- .117	- .12
		377	2.731	-3.163	- .101	- .073	- .067	- .02
		410	2.619	-2.844	- .078	- .013	.243	0.00
		444	2.506	-2.557	- .032	- .008	.421	.08
H_2	nC_6H_{14}	278	2.883	-1.707	.496	.193	.341	.20
		311	2.760	-1.347	.498	.632	.548	.62
		344	2.613	-1.015	.522	.665	.795	.70
H_2	C_6H_6	433	2.443	-1.058	1.073	.798	1.080	.81
		473	2.174	- .630	1.204	1.235	1.532	1.25
H_2	nC_4H_{10}	278	2.630	-1.517	1.054	1.061	.766	.77
		298	2.520	-1.228	1.057	1.010	.951	.95
N_2	$nC_{10}H_{22}$	311	2.954	-2.099	.597	.724	-	-

[a] From C_{11}^o correlations

[b] From f_2^o correlations

effect on the calculated activity coefficient. The correlations for C_{11}°, equations (7.6) and (7.7), are preferred over equations (7.4) and (7.5) for representing activity coefficients. Their importance lies in that they provide a state dependence of the DCF, C_{11}°, in binary systems.

7.2 Detailed Analysis of Hydrogen-Benzene System

There is a twofold interest in studying this system. On the one hand, complete experimental data of high accuracy is available to derive the composition dependence of the DCF integrals. Secondly, the predictions of the macroscopic correlations derived earlier can be tested with experimental data.

Connolly and coworkers[2,12,13] have made a systematic investigation of the thermodynamic properties of this system over a wide range of temperature and pressure. They provide analytical representation of the following experimental relations:

(i) Volume of pure benzene with temperature and pressure,

(ii) Volume of hydrogen-benzene mixtures with temperature, pressure and composition,

(iii) Activity coefficient with temperature and composition,

(iv) Henry's constant with temperature.

These expressions are sufficient to extract the composition dependent DCF integrals from the following expressions

$$\left(\frac{1}{\rho \kappa RT} \right)_{mix} = 1 - x_1^2 C_{11} - x_2^2 C_{22} - 2x_1 x_2 C_{12} \qquad (7.8)$$

$$\rho\bar{v}_1 = (1 - x_1C_{11} - x_2C_{12})/(1/\rho\kappa RT)_{mix} \tag{7.9}$$

$$\left(\frac{\partial \ell n\gamma_1^*}{\partial x_1}\right)_{T,P,N_2} = \frac{1}{x_2} - \frac{1 + C_{11} - 2x_1C_{11} - 2x_2C_{12} + x_2^2(C_{12}C_{12} - C_{11}C_{22})}{(1/\rho\kappa RT)_{mix}} \tag{7.10}$$

where hydrogen is component 1. The integrals were determined from the experimental data at selected temperatures and pressures. The set for 513°K are shown plotted in Fig. 7-3. The thermodynamic properties vary rapidly with composition at the higher temperatures, and the DCF integrals also vary considerably with composition. An assumed linear composition dependence will not reproduce the experimental quantities. However, such an assumption would not be useful since the experimental values of C_{22}, C_{12} and C_{11} are not usually available in the mid-composition range.

In systems having only one limiting composition which is physically realizable, series expansions about this composition provide a method for describing thermodynamic properties at other compositions. The solution theory expressions for the thermodynamic properties are

$$\frac{1}{\rho\kappa RT} = 1 - C_{22}^o + x_1[2C_{22}^o - 2C_{12}^o - C_{122}^o - C_{22}^o(1 - \rho\bar{v}_1^o) + C_{222}^o\,\rho\bar{v}_1^o] + \ldots \tag{7.11}$$

$$\rho\bar{v}_1 = \rho_2^o\bar{v}_1^o + x_1\,\frac{[-C_{11}^o - C_{112}^o + \rho_2^o\bar{v}_1^o(3C_{12}^o + 2C_{122}^o) - \rho_2^o\bar{v}_1^oC_{22}^o(1 + \rho_2^o\bar{v}_1^o) - C_{222}^o(\rho_2^o\bar{v}_1^o)^2]}{(1 - C_{22}^o)} + \ldots \tag{7.12}$$

$$\ell n\gamma_1^* = f_2^o(2x_1 - x_1^2) + f_3^o(x_1^3 - \tfrac{3}{2}x_1^2) \tag{7.13}$$

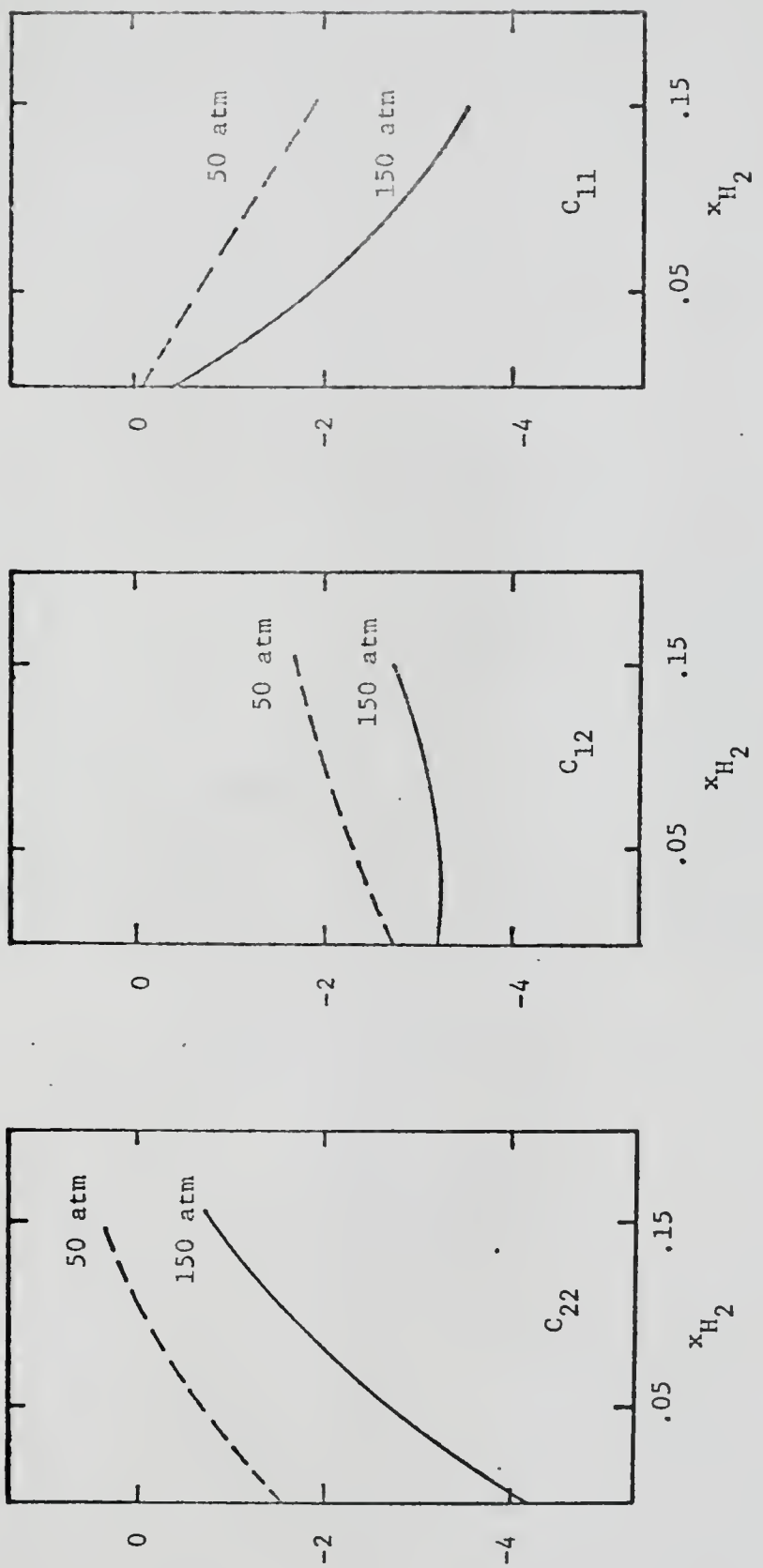

Fig. 7-3. Experimental DCF integrals in H_2–benzene system at 513°K.

The coefficients in these expressions are DCF integrals at zero composition and can be obtained from the correlations derived earlier; the third order functions are obtained from the density derivatives of the pair functions.

The expressions for compressibility and partial molar volume are linear in the hydrogen mole fraction. Consequently, these equations cannot predict any quadratic or higher order composition dependence. However, it is possible to include higher order composition dependence by assuming an expression for the excess volume in the mixture. The simplest such expression in the asymmetric convention is

$$v^E = Ax_1^2 \tag{7.14}$$

This leads to

$$\rho\bar{v}_1 = \frac{\bar{v}_1}{v} = \frac{\bar{v}_1^o + \bar{v}_1^E}{x_1\bar{v}_1^o + x_2\bar{v}_2^o + v^E} \tag{7.15}$$

or

$$\rho\bar{v}_1 = \frac{\rho_2^o\bar{v}_1^{o-o} + \rho_2^oA(2x_1 - x_1^2)}{x_1\rho_2^o\bar{v}_1^{o-o} + x_2 + \rho_2^oAx_1^2} \tag{7.16}$$

which is a complete composition dependent expression for $\rho\bar{v}_1$. The coefficient A is related to the slope of the partial molar volume at zero composition. From (7.16)

$$\left(\frac{\partial\rho\bar{v}_1}{\partial x_1}\right)_{T,P,x_1=0} = 2A\rho_2^o + \rho_2^o\bar{v}_1^{o-o} - (\rho_2^o\bar{v}_1^{o-o})^2 \tag{7.17}$$

A comparison of equations (7.12) and (7.17) now yields A in terms of the DCF integrals. The simplified expression is

$$\rho_2^o A = \frac{[-(C_{11}^o + C_{112}^o) + 2\rho_2^{o-o}\bar{v}_1^o(C_{12}^o + C_{122}^o) - (\rho_2^{o-o}\bar{v}_1^o)^2(C_{222}^o + C_{22}^o)]}{2(1 - C_{22}^o)} \tag{7.18}$$

An expression for the isothermal compressibility is

$$\frac{1}{\rho\kappa RT} = -\frac{(x_1\bar{v}_1^o + x_2\bar{v}_2^o + Ax_1^2)^2}{RT(x_1\bar{v}_1^{o\prime} + x_2\bar{v}_2^{o\prime} + A'x_1^2)} \tag{7.19}$$

where the primes denote partial derivatives w.r.t. pressure at constant temperature. This expression when rearranged and truncated to second order in x_1, yields

$$\frac{1}{\rho\kappa RT} = \frac{(x_2 + x_1\rho_2^{o-o}\bar{v}_1^o + \rho_2^o Ax_1^2)^2}{\rho_2^o\kappa_2^o RT(x_2 + x_1\frac{\bar{v}_1^{o\prime}}{\bar{v}_2^{o\prime}} + \frac{A'}{\bar{v}_2^{o\prime}}x_1^2)} \tag{7.20}$$

where

$$\frac{\bar{v}_1^{o\prime}}{\bar{v}_2^{o\prime}} = \frac{C_{122}^o + 1 - \rho_2^{o-o}\bar{v}_1^o(C_{222}^o + C_{22}^o)}{(1 - C_{22}^o)} \tag{7.21}$$

A' denotes the pressure derivative of the excess volume and is usually small.

Equations (7.20) and (7.16) were used in calculation of the isothermal compressibility and the partial molar volumes. The pair DCF integrals were obtained from the correlations (4.3), (4.6) and (7.7). The triplet functions C_{222}^o, C_{122}^o, and C_{112}^o were obtained from the density recurrence relations

$$C_{ij2}^o = \rho_2^o\left(\frac{\partial C_{ij}^o}{\partial\rho_2^o}\right)_{T,P} - C_{ij}^o \qquad i,j=1,2 \tag{7.22}$$

Lastly, $\rho_2^{\circ}A$ was evaluated from equation (7.18) and A' was set equal to zero. The calculated compressibilities and partial molar volumes are shown in Figs. 7-4 and 7-5. Each figure shows two sets of calculations. The solid lines represent calculations wherein both terms of equation (7.22) were evaluated from the correlations. They reflect the abilities of the correlations to predict these thermodynamic properties from a minimum of experimental data. The only experimental number used in this set of calculations is the molar volume of pure benzene at the system temperature and pressure. There is good qualitative agreement at all state conditions, and the composition dependences show the same trends as the experimental data. But the errors in predicting the infinite dilution values for both properties is a limiting factor in this calculation.

To overcome this restriction, a set of calculations was made using the experimental values of C_{ij}° in equation (7.22), the other term again being obtained from the correlations. These calculations are represented by the broken lines in the figure. As required, they coincide with experimental values at infinite dilution but the slopes at zero composition are too small (in absolute value). This error can arise from erroneous values of C_{222}°, C_{122}° or C_{112}°. To examine the sources of the error, experimental and calculated values of these quantities are shown in Table 7-5. The calculated pair DCF integrals are in good agreement with experimental data, as is C_{222}°, which is the density (or pressure) derivative of the isothermal compressibility. But the calculated C_{122}° and C_{112}° have the opposite sign as the experimental values and differ appreciably in

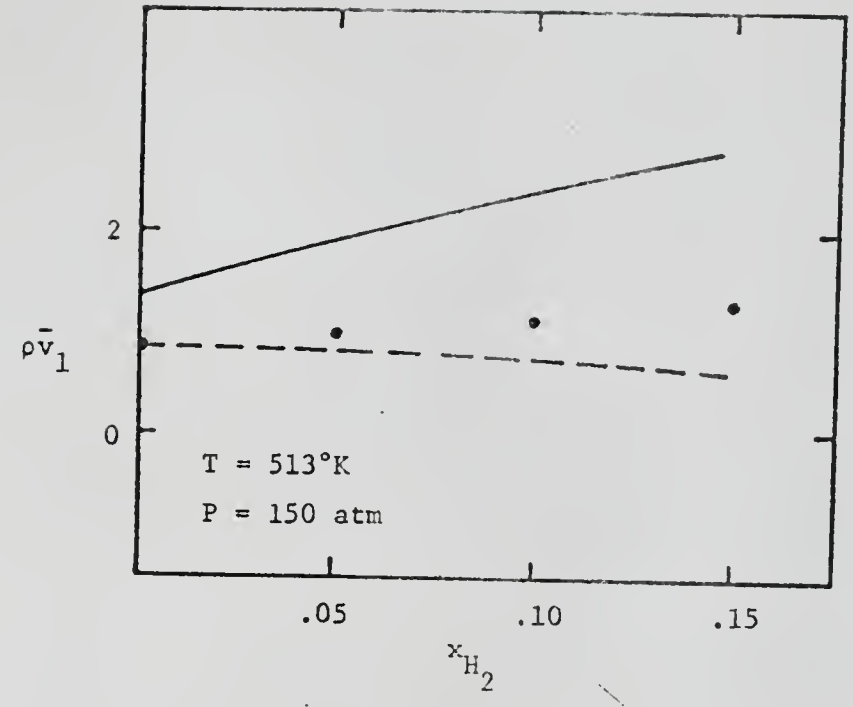

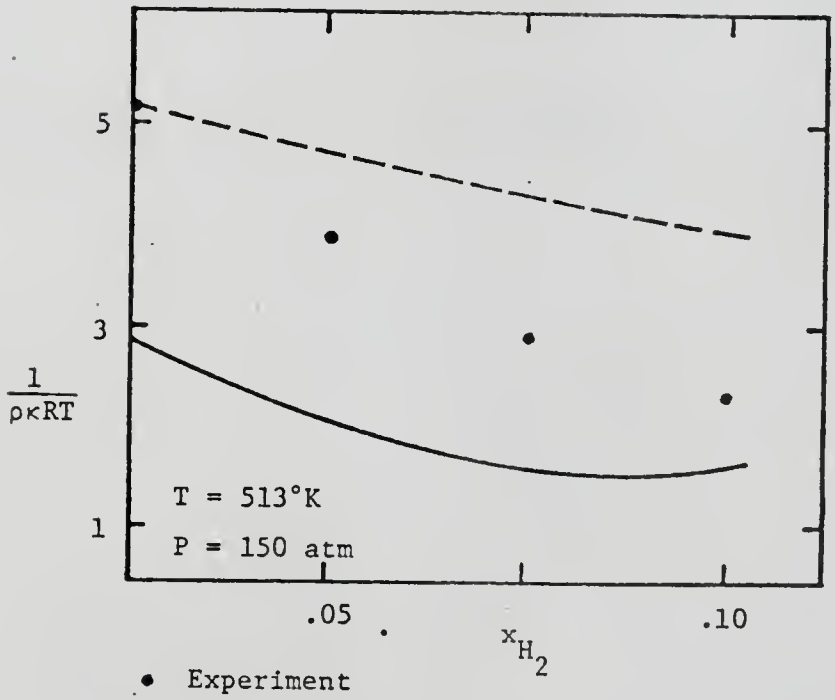

• Experiment

——— Calculated; C^{o}_{ij} and C^{o}_{ijk} from generalized correlations

– – – Calculated; experimental C^{o}_{ij}; C^{o}_{ijk} from correlations

Fig. 7-4. Isothermal compressibility and partial molar volume in H_2-benzene system.

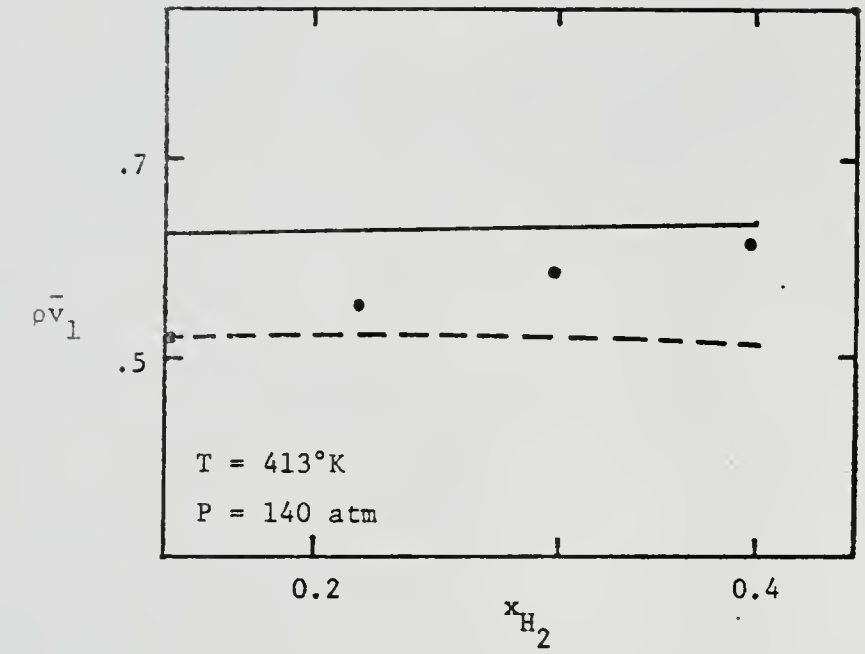

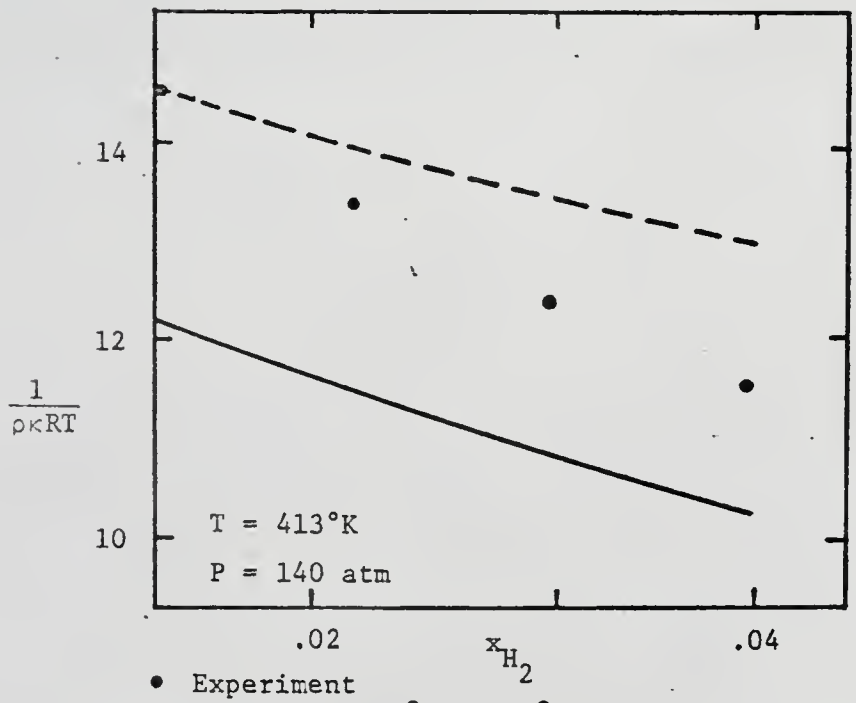

• Experiment

—— Calculated; C^{o}_{ij} and C^{o}_{ijk} from generalized correlations

– – Calculated; C^{o}_{ij} experimental; C^{o}_{ijk} from correlations

Fig. 7-5. Isothermal compressibility and partial molar volumes in H_2-benzene system.

TABLE 7-5

DCF INTEGRALS IN HYDROGEN-BENZENE SYSTEM
AT 413°K, 50 ATM

		Calculated	
	Experiment	b	a
C^{o}_{22}	-10.69	-10.69	- 9.10
C^{o}_{12}	- 6.01	- 6.01	- 5.84
C^{o}_{11}	- .94	- .94	- .48
C^{o}_{222}	-79.14	-77.23	-78.82
C^{o}_{122}	+ 1.59	-24.75	-24.58
C^{o}_{112}	10.00	- 5.00	- 4.62

[a] C^{o}_{ij} from correlations used in equation (7.22).

[b] experimental C^{o}_{ij} used in equation (7.22).

magnitude. The correlations do not yield a satisfactory value of the pressure derivatives of the partial molar volume and the activity coefficients, although the properties themselves are well predicted. Since C^{o}_{122} and C^{o}_{112} appear in the expression for $\rho^{o}_{2}A$, the excess volume in this system cannot be satisfactorily determined from the present correlation alone.

It is interesting to note that neither the Percus-Yevick nor the HNC theories (Appendix F) provides relations for the triplet functions that are consistent with the experimental data. The HNC approximation requires that all C^{o}_{ijk} be zero, which is clearly in contradiction to the data. For the Percus-Yevick approximation, one has

$$C^{o}_{222} = - (C^{o}_{22})^{2} \tag{7.23}$$

$$C^{o}_{122} = - (C^{o}_{12})^{2} \tag{7.24}$$

The first relation is approximately consistent with the data, but the second is not. Further, no relation is available for C^{o}_{112}.

Refinements of the correlations for C^{o}_{12} and C^{o}_{11} should improve the accuracy of the predicted triplet functions. However, this stage of development calls for examining and correlating experimental data which is scarcely available.

7.3 Thermodynamic Properties of Gas-Mixed Solvents Systems

The study of thermodynamic properties of subcritical systems suggests that liquid mixtures are satisfactorily represented by the one-fluid model with a composition dependent characteristic parameter.

When the mixed solvent in the multicomponent gas-solvent system is so represented, the subsequent analysis is that for a gas in a single solvent.

With the assumption of the one-fluid model for the solvent mixture, the expressions for thermodynamic properties of the 1-2-3 ternary become

$$\frac{1}{\rho\kappa RT} = 1 - x_1^2 C_{11} - x_m^2 C_{mm} - 2x_1 x_m C_{1m} \tag{7.25}$$

$$\frac{\bar{v}_1}{\kappa RT} = 1 - x_1 C_{11} - x_m C_{1m} \tag{7.26}$$

$$f_2^m = -\frac{(1 - C_{11}^o)}{2} + \frac{(1 - C_{1m}^o)^2}{2(1 - C_{mm}^o)} \tag{7.27}$$

where the subscripts m denote mixture quantities. It is important to note that C_{mm} and C_{1m} are not mole fraction averages of the respective pure component integrals C_{22}, C_{33}, etc. For example, in general

$$C_{mm} \neq x_2 C_{22} + x_3 C_{33} \tag{7.28}$$

for the one-fluid model, although the equality may hold in certain cases. However, C_{22} and C_{33} <u>are</u> the limiting values of C_{mm} at the extreme compositions. The variation of C_{mm} with composition is determined by the reduced density of the mixture. Similar remarks hold for C_{1m} and C_{11}.

Equations (7.25), (7.26) and (7.27) were used to analyze the experimental data described in Chapter 6. The generalized correlations (4.3) and (4.6) were used to screen the experimental data in the process

of obtaining DCF integrals. The results are presented in Table 7-6. C_{ij}'s as predicted by the generalized correlations are listed as calculated values. For most systems, the quantities C^{o}_{mm} for the solvent mixture lie between those of either pure component. This behavior is anticipated but not required for consistency with the one-fluid model. The trend is not as marked in the integrals C_{1m} and is totally absent for the integrals C_{11}.

More significant is the consistent variation of all these quantities with the reduced density of the solvent. They all increase positively with increasing temperature indicating that on the molecular scale the negative contribution to c(r) from the repulsive part of the intermolecular potential decreases faster than the positive contribution from the attractive part of the potential. Further, regardless of the solvent composition, the integrals involving solute interactions are always less negative than those for solvent interactions. This suggests that the size and energy parameters characterizing the solute-solute interaction are always smaller than those of the solvent-solvent interaction, and the solute-solvent parameters lie in between.

For comparison with experiment the isothermal compressibilities and partial molar volumes for the N_2-C_6H_6-C_8H_{18} system were calculated with equations (7.20) and (7.16). The calculated composition dependence is shown in Figs. 7-6 and 7-7. The solid lines represent calculations for which the experimental DCF integrals (of Table 7-6) were used, with triplet functions from the generalized correlations. The calculations are in good agreement with experimental data over the entire composition range of the solute. The dashed lines represent

TABLE 7-6

DIRECT CORRELATION FUNCTION INTEGRALS IN TERNARY SYSTEMS

System	T °K	$\frac{1}{\rho\kappa RT}$ Expt	$\frac{1}{\rho\kappa RT}$ Lit[a]	C^{o}_{mm} Expt	C^{o}_{mm} Calc[+]	$\rho\bar{v}_1$ Expt	$\rho\bar{v}_1$ Lit	C^{o}_{1m} Expt	C^{o}_{1m} Calc[‡]	f^{o}_{2} Expt	f^{o}_{2} Lit	C^{o}_{11} Expt	C^{o}_{11} Calc[*]	f^{o}_{2} Calc
N_2 Benzene[b]	298	37.02	38.13	-37.13	-38.59	.5252	.591	-19.02	-18.70	.502	-	- .851	-	-
N_2 Mixture		40.12	37.74	-36.74	-38.15	.5252	-	-18.82	78.09	-1.127	-	-11.66	-	-
N_2 CCl_4		35.55	37.84	-37.84	-37.81	.5338	-	-19.73	-17.55	.452	-	-9.16	-	-
	378	15.36	-	-14.36	-15.33	.7287	-	-10.90[d]	-11.11	.874	-	-5.92[e]	-	-
		17.47	-	-16.47	-15.02	.7173	-	-10.49[d]	-10.70	- .330	-	-7.90	-	-
		16.81	-	-15.81	-14.68	.7105	-	-10.14[d]	-10.31	.911	-	-6.91	-	-
	418	9.19	10.90	- 9.90	- 8.55	.8721	-	- 8.51	- 8.00	-1.129	-	-5.04	-	-
		11.99	-	-10.99	- 8.63	.8668	-	- 7.35[d]	- 7.84	.075	-	-6.39	-	-
		12.79	-	-11.79	- 7.88	.8605	-	- 6.64[d]	- 7.30	1.076	-	-3.42	-	-
N_2 Benzene	298	37.02	38.13	-37.13	-38.59	.5250	.591	-19.02	-18.70	.502	-	-8.51	-	-
N_2 Mixture[b]		46.69	-	-45.69	-55.10	.3896	-	-20.86[d]	-19.36	- .761	-	-9.04	-	-
N_2 Octane		55.04	-	-54.04	-65.12	.3324	-	-20.98[d]	-18.76	- .200	-	-6.87	-	-
	378	15.36	-	-14.36	-15.33	.7017	-	-10.46[d]	-11.11	.874	-	-6.23[e]	-	-
		18.63	-	-17.63	-22.15	.5288	-	-11.24[d]	-10.49	.381	-	-6.71	-	-
		19.40	-	-18.40	-26.15	.4260	-	-10.72[d]	-10.38	.142	-	-3.99	-	-
	418	9.19	10.90	- 9.90	- 8.55	.8721	-	- 8.51	- 8.00	1.129	1.130	-5.04	-	-
		10.22	13.63[f]	-12.63	-12.69	.6176	-	- 7.42	- 7.87	2.189	-	- .39[e]	-	-
		10.87	15.50	-14.50	-15.30	.4962	-	- 6.69	- 7.41	.346	-	-2.87[e]	-	-
H_2 Benzene	298	37.02	38.13	-37.13	-38.60	.3947	.393	-15.05	-13.22	.510	-	-3.28	-2.40	.854
H_2 Mixture		48.40	-	-45.69	-55.10	.2613	-	-13.66[d]	-13.69	- .684	-	-4.21	-2.05	.398
H_2 Octane		55.71	-	-54.04	-65.12	.2336	.223	-15.45[d]	-13.27	- .360	-	-2.80	-1.74	.170

TABLE 7-6 (Continued)

System	T °K	$\frac{1}{\rho\kappa RT}$ Expt	$\frac{1}{\rho\kappa RT}$ Lit[a]	C^{o}_{mm} Expt	C^{o}_{mm} Calc[+]	$\rho\bar{v}_1$ Expt	$\rho\bar{v}_1$ Lit	C^{o}_{1m} Expt	C^{o}_{1m} Calc[‡]	f^{o}_{2} Expt	f^{o}_{2} Lit	C^{o}_{11} Expt	C^{o}_{11} Calc[*]	f^{o}_{2} Calc
	378	15.32	-	-14.32	-15.34	.5339	.532	- 7.72	- 7.86	.962	-	-1.73	-1.41	1.197
		18.52	-	-17.52	-22.16	.3569	-	- 7.27	- 7.77	.519	-	- .929	-1.19	.565
		19.40	-	-18.40	-26.51	.3112	.316	- 7.56	- 7.34	.054	-	-1.56	-1.00	.264
	418	9.19	10.90	- 9.90	- 8.55	.6493	.641	- 6.08	- 5.66	1.232	1.130	-1.13	-1.05	1.297
		10.22	13.63[f]	-12.63	-12.69	.3569	-	- 3.86	- 5.57	2.270		+2.37	- .87	.641
		10.93	15.50	-14.50	-15.30	.3674	.365	- 4.69	- 5.24	.205		- .68	- .74	.324
CH_4 Propane	310	-	4.91	- 3.91	- 3.91		1.1380	- 4.59	- 5.96	-	.640	-4.08	-5.69	1.590
CH_4 Mixture[c]		-	14.60[f]	-13.60	-13.60		-	-	-10.21	-	.605	-5.36	-5.62	.718
CH_4 Pentane		-	18.40	-17.40	-17.40		.6306	-11.23	-11.31	-	.560	-5.59	-5.59	.825

[+] Eqn. (4.3)

[‡] Eqn. (4.6)

[*] Eqn. (7.7)

[a] References of Table 6-4, 6-5, 6-7; for CH_4-C_3H_8-C_5H_{12} system, Reference 10.

[b] Equimolar solvent mixture.

[c] 80% pentane.

[d] C^{o}_{1m} from (expt $\rho\bar{v}^{o}_{1}$, calc $(1 - C^{o}_{mm})$

[e] C^{o}_{11} from (expt f^{o}_{2}, calc $(1 - C^{o}_{1m})$, calc $(1 - C^{o}_{mm})$).

[f] one-fluid theory.

Fig. 7-6. Isothermal compressibility of N_2-benzene-octane mixtures at 298°K.

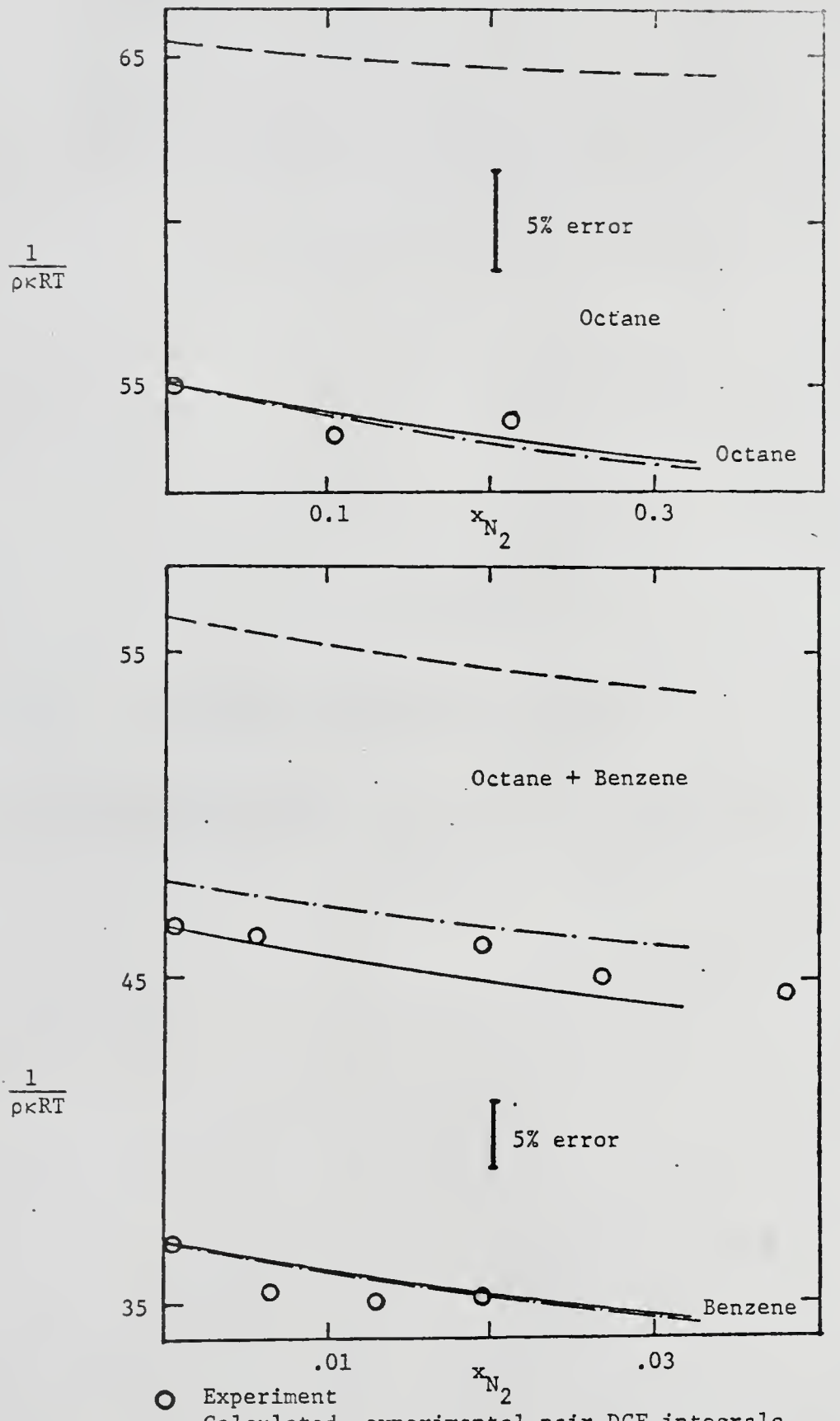
65
55
$\frac{1}{\rho\kappa RT}$
5% error
Octane
Octane
0.1
x_{N_2}
0.3
55
45
35
$\frac{1}{\rho\kappa RT}$
Octane + Benzene
5% error
Benzene
.01
x_{N_2}
.03
Experiment
Calculated, experimental pair DCF integrals
Calculated, correlations for pair DCF integrals
Calculated, adjusted parameters

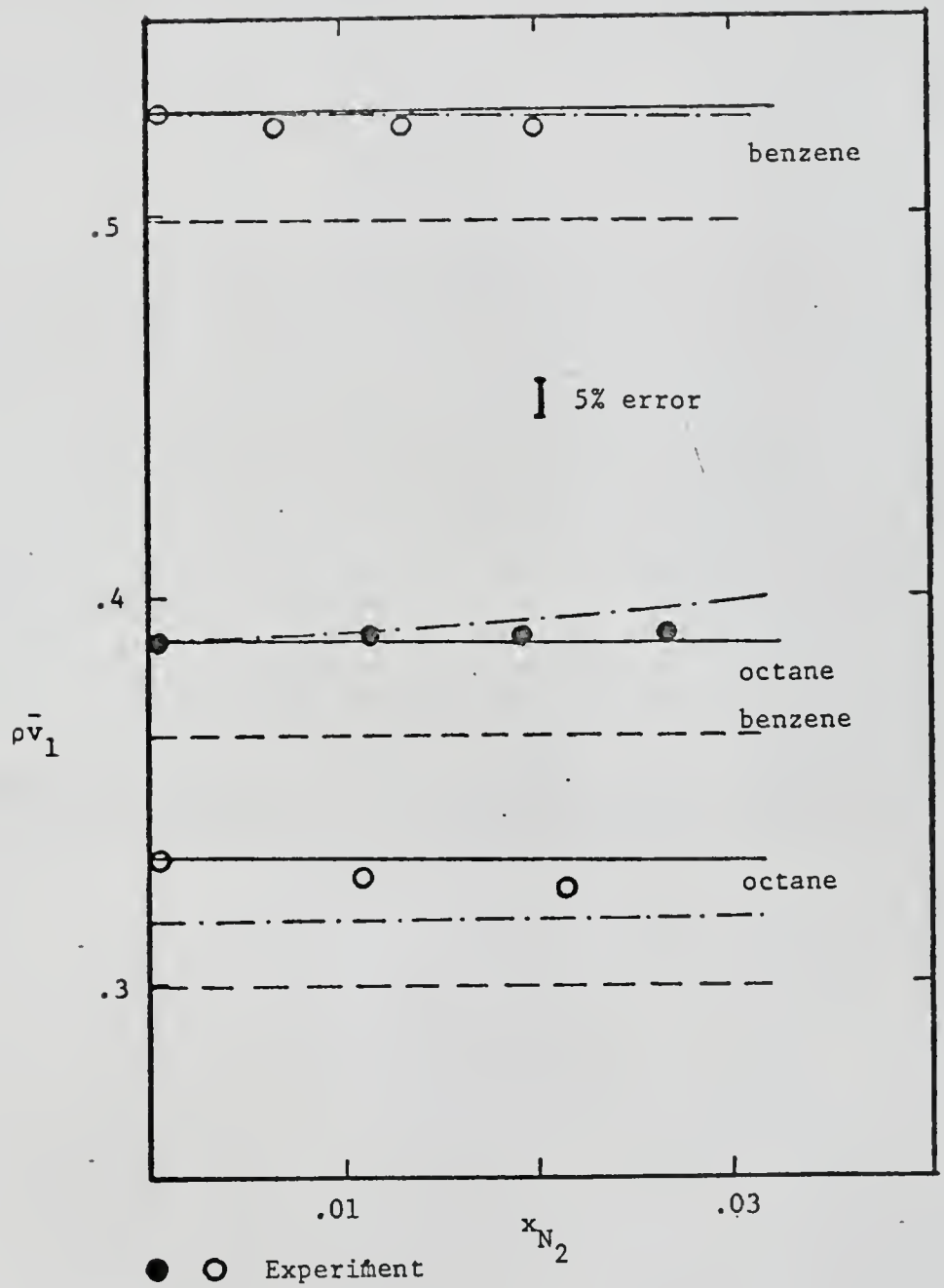

Fig. 7-7. Partial molar volume of N_2 in N_2-benzene-n-octane mixtures.

calculations performed with all DCF integrals (pair and triplet) obtained from the generalized correlations. The only experimental data required for this calculation is the volume of the solvent mixture. The experimental compressibilities of the pure solvents are not satisfactorily represented by equation (4.3), and this causes a considerable error in calculating the compressibility of the solvent mixture, as indicated by the difference between the solid and dashed lines at zero gas composition. Much of the overall error can be eliminated by adjusting the pure component characteristic volumes to obtain agreement between their calculated and experimental compressibilities. The mixture characteristic volume is then revised to be the mole fraction average of the adjusted pure solvent characteristics. The resulting compressibilities and partial molar volumes of the gas-mixed solvent system are represented by the dashed-dotted lines. The improvement in both calculated properties is quite marked, and brings them into satisfactory agreement with the experimental data. Thus the predictive method using the corresponding states correlations with adjusted pure component characteristics gives a good representation of the experimental volumetric properties.

The experimental DCF integrals also provide a relation between Henry's constants of component 1 in the 2-3 mixture and in the individual solvents, respectively. From equation (1.9) we have

$$\ell n H_{1,m} - \sum_{j=1}^{M} X_j \ell n H_{1,j} = f_2^{(m)} - \sum_{j=1}^{M} X_j f_2^{(j)} \qquad (7.29)$$

where $H_{1,m}$ and $H_{1,j}$ are the Henry's constants of the solute in the

mixture and in solvent j, respectively. $f_2^{(m)}$ and $f_2^{(j)}$ are the corresponding activity coefficient parameters. $f_2^{(m)}$ is given by equation (7.27). A simplification of (7.29) results from assuming that C_{11} is a mole fraction average of its limiting value at each of the pure solvent compositions, i.e.,

$$C_{11} = \sum_{j=1}^{M} X_j C_{11}^{(j)} \tag{7.30}$$

Then, equation (7.29) reduces to

$$\ell nH_{1,m} - \sum_{j=1}^{M} X_j \ell nH_{1,j} = \frac{(1 - C_{1m})^2}{2(1 - C_{mm})} - \sum_{j=1}^{M} \frac{X_j(1 - C_{ij})^2}{2(1 - C_{jj})}$$

$$= \frac{(\rho \bar{v}_{1m})^2}{2\rho\kappa_m RT} - \sum_{j=1}^{M} X_j \frac{(\rho \bar{v}_{1j})^2}{\rho\kappa_j RT} \tag{7.31}$$

The above equation relates the Henry's constants deviation to the partial molar volumes of the solute and isothermal compressibilities in the mixture and the pure solvents. These quantities are more readily obtainable than activity coefficient parameters; thus equation (7.31), if valid, is more convenient than (7.29). Two other relations for the Henry's constant deviation are of interest here. The first, used by Chueh and Prausnitz,[10] is

$$\ell nH_{1,m} - \sum_{j=1}^{M} X_j \ell nH_{1,j} = -\frac{g^E}{RT}(\text{solvents}) \tag{7.32}$$

O'Connell[14] presents a relation based on the study of several experimental systems

$$\ell nH_{1,m} - \sum_{j=1}^{M} X_j \ell nH_{1,j} = \frac{X_3}{2} \left(\frac{\partial \ell n \gamma_3}{\partial x_3} \right)^{+}_{T,P,N_2} + A_{23}\Phi_2\Phi_3 \tag{7.33}$$

where

$$A_{23} \equiv \frac{1050|v_2 - v_3|}{T^{1/2}\, v_2 v_3} \tag{7.34}$$

Φ_2 and Φ_3 are component volume fractions in the solute free solvent mixture. An interesting and perhaps restrictive feature of both (7.32) and (7.33) is that no solute properties are involved and the resulting Henry's constant deviation is independent of the nature of the gas. On the other hand, equations (7.29) and (7.31) do account for the solute interactions.

The Henry's constant deviations determined from equations (7.29), (7.31), (7.32) and (7.33) for the experimental systems described previously are shown in Table 7-7 and compared with the experimental results. The results of equations (7.33), (7.32) and (7.31) (with experimental DCF integrals) agree with each other to within the range of uncertainty normally associated with this difference. They are also in reasonable agreement with experiment for the N_2 systems but not for the H_2 system. Equation (7.31) with calculated DCF integrals also gives satisfactory agreement with the N_2-Benzene-carbon tetrachloride system but the trend with temperature is not entirely consistent with experimental values in the N_2-benzene-octane systems. Henry's constant deviations from experimental activity coefficient parameters, (7.29), are much larger than the experimental in all cases but one.

On the basis of the current experimental data, expression (7.29) must be considered unsatisfactory as a representation of the Henry's constant deviation. Equation (7.31) may be as accurate or more so than (7.33) and (7.32) but this cannot be ascertained on the basis of the present limited experimental data.

TABLE 7-7

HENRY'S CONSTANTS IN MIXED SOLVENTS

System	T °K	$\ln H_{1,m} - \sum_j x_j \ln H_{1,j}$ Exptl.	Lit[a]	Eqn.(7.32)	Eqn.(7.33)	Eqn.(7.31) Expt.	Eqn.(7.31) Calc.	Eqn.(7.29) Expt.	Eqn.(7.29) Calc.
N_2-Benzene	298	.099	-	-.0083	.0566	-.189	-.015	-1.604	-
N_2-Carbon Tetrachloride	378	.017	-	-.0058	.0401	-.026	-.015	-1.222	-
	418	.013	-	-.0049	.0367	-.098	+.002	-1.177	-
N_2-Benzene	298	-.360	-	-.1615	-.091	-.099	-.231	- .872	-
N_2-Octane	378	-.106	-	-.0876	-.031	-.040	-.320	- .128	-
	418	.078	-	-.0510	-.005	-.427	-.330	1.452	-
H_2-Benzene	298	.253	.01	-.1615	-.091	-.80	-.127	- .759	-.113
H_2-Octane	378	.347	-	-.0876	-.031	-.353	-.172	.011	-.166
	418	.516	.317	-.0510	-.005	-.805	-.182	1.552	-.170

[a] Literature value of $H^o_{1,j}$ from Table 6-7.

7.4 Vapor-Liquid Equilibrium in Multicomponent Systems

The test of most practical importance for an expression for activity coefficients and the corresponding reference fugacities in a mixture is the calculation of vapor-liquid equilibrium. The calculated bubble pressures and equilibrium compositions can be compared directly with experimental values. The generalized correlations for f_2^o and C_{11}^o, which provide activity coefficient parameters and the Henry's constant deviation, are tested here with the use of the one-fluid model for the solvent mixtures. Bubble pressure calculations were made for two experimental systems, H_2-CH_4-C_2H_6 at 116°K, and CH_4-C_3H_8-C_5H_{12} at 310.9°K.[10] The representation of vapor and liquid phase fugacities followed that described in Chapter 6. The excess free energies of the solvent mixtures CH_4-C_2H_6 and C_3H_8-C_5H_{12} were determined by Chueh's method.[10] However, this quantity could be obtained from an independent source, if possible or desired. Calculated bubble pressures and vapor compositions are shown in Table 7-8. There is generally good agreement between the calculated and experimental vapor compositions, despite some discrepancy in the calculated bubble pressure. This insensitivity of the vapor mole fractions was also observed in the calculations for binary systems.

The CH_4-C_3H_8-nC_5H_{12} (1-2-3) system is discussed first. The solvent volume was assumed to be the mole fraction average of the pure component volumes. The characteristic parameters for the pure components each required less than 1% adjustment to match the experimental compressibility with that predicted by (4.3). $(1 - C_{mm}^o)$ for the mixture

TABLE 7-8

VAPOR LIQUID EQUILIBRIUM IN TERNARY SYSTEMS

System	T °K	x_i	$H_{1,m}$ atm	$f_2^{(m)}$	A_{23}	Pressure atm			K-Factor		
						Expt+	Calc	Chueh+	Expt+	Calc	Chueh+
CH_4-C_3H_8 -nC_5H_{12}	310	.152 .170 .678	186.4	.6046	.0004	34.04	31.47	33.75	5.697 .500 .072	5.710 .523 .064	5.714 .505 .067
	310	.152 .170 .678	185.5	.5470	.0004	34.04	31.84	33.75	5.697 .500 .072	5.710 .519 .063	5.714 .505 .067
	310	.152 .170 .678	110.4	.710	.0004	34.04	18.12	33.75	5.697 .500 .072	5.351 .768 .083	5.714 .505 .067
H_2-CH_4 -C_2H_6	116	.0192 .628 .353	1995.	.701	.0056	34.17	43.15	35.4	49.68 .073 .0002	49.95 .065 .0002	49.53 .078 .0003
	116	.0168 .0788 .9040	3318.	-.242	.0056	66.84	70.34	67.17	59.23 .0685 .0002	59.16 .0761 .0001	59.05 .097 .0001
	116	.0046 .275 .720	2165.	-.123	.0056	13.32	10.96	13.57	208.0 .157 .0002	204.9 .210 .0002	204.9 .207 .0003
H_2-CH_4 -C_2H_6	116	.0192 .628 .353	1711.	.5142	.0056	34.17	36.83	35.40	49.68 .073 .0002	49.78 .071 .0002	49.53 .078 .0003

TABLE 7-8 (Continued)

System	T °K	x_i	$H_{1,m}$ atm	$f_2^{(m)}$	A_{23}	Pressure atm			K-Factor		
						Expt+	Calc	Chueh+	Expt+	Calc	Chueh+
	116	.0046	2685.	.2146	.0056	13.32	13.33	13.57	208.04	206.74	204.95
		.2750							.157	.178	.207
		.7200							.0002	.0002	.0003
	116	.0168	3439.	.0713	.0056	66.84	65.90	67.17	59.23	59.16	59.05
		.0788							.069	.076	.099
		.9040							.0002	.0001	.0001

+Reference 10

was then obtained from the one-fluid theory. Next, the quantities $C^{o}_{1j}(v^{*}_{j}/v^{*}_{1})^{.62}$, j=2,3, were determined from the experimental $\bar{v}^{o}_{1,j}$, and equation (4.3). These were plotted on the graph of the generalized correlation for $C^{o}_{12}(v^{*}_{2}/v^{*}_{1})^{.62}$, equation (4.6), and a straight line drawn between them. The mixture quantity $C^{o}_{1m}(v^{*}_{m}/v^{*}_{1})^{.62}$ was determined from this linear relation at a reduced density $\tilde{\rho}_{m} = v^{*}_{mix}/v_{mix}$. C^{o}_{11} in the mixture was determined similarly from the generalized correlation for methane in solvents, equation (7.6). The derived DCF integrals C^{o}_{mm}, C^{o}_{1m} and C^{o}_{11} are shown in Table 7-6 as experimental values. Corresponding values, obtained from the generalized correlations at the reduced density of the solvent, are shown as calculated values. The mixed solvent Henry's constants and related $f^{(m)}_{2}$ were each determined from both of the relations (7.31) and (7.29). The results with relation (7.31) are the first set in Table 7-8; those of (7.29) are the second set. Both results are comparable, and the K-factors agree well with experiment, although the calculated pressures are somewhat lower than experiment. Chueh's method yields pressures in closer agreement with experiment. The third set of calculations for this system used the calculated DCF integrals (Table 7-6) in relation (7.31) to obtain the Henry's constants and activity coefficient parameters. The resulting bubble pressures and component K-factors compare very poorly with experimental values. This resulted from the large negative value obtained for the Henry's constant deviation.

Three solvent mixture compositions were studied in the H_2-CH_4-C_2H_6, (1-2-3) system. The first set of calculations are similar to those of the CH_4-C_3H_8-C_5H_{12} system. The only differences were the use

of critical volumes for the characteristic parameters of the pure solvents, and $\bar{v}^{o}_{1(3)}$ being taken from the generalized correlation, e.g., (4.6). The Henry's constant deviation and the relation $f_2^{(m)}$ were determined with experimental C^{o}_{mm} and C^{o}_{1m} in (7.31). The calculated pressures differ by more than 10% from the experimental, but the K-factors are in satisfactory agreement. The second set of calculations is quite different from the first, in that an effective $f_2^{(m)}$ is used for the solvent mixture. This is prompted by the fact that the experimental C^{o}_{11} data for H_2 in CH_4 and H_2 in Ar did not correlate well with those for other H_2-solvent systems in equation (7.7). Therefore, an effective value of $f_2^{(m)}$ was determined from equation (7.5). The Henry's constant deviation was obtained from the simplest of the solvent excess free energy expressions, equation (7.32). These were all the data required, no other binary data was necessary. The calculated bubble pressures and K-factors show remarkably good agreement with experimental results, and are somewhat better than those of the Chueh method. This agreement is, indeed, more than a fortunate happenstance, because it is consistently good over all three solvent compositions considered.

The success of the above method indicates its reliability for vapor liquid equilibrium calculations. Its usefulness is important for physical systems in which the detailed data required by Chueh's method are not available. The essential difference in the two methods is the determination of the activity coefficient parameter. In Chueh's method, it is calculated from sets of fitted coefficients for each binary pair, whereas in the present method it is obtained from generalized correlations.

The method can be extended to systems where more than one component is treated as a solute. Smith[15] has shown that when several solutes are present at low concentrations in a liquid mixture, the concentration of each one of these affects only its own chemical potential and that of the solvent components. In simple terms, a solute molecule "sees" only solvent molecules around it. Then the activity coefficient of each solute can be represented by a Margules (or other) type expression, involving only its own mole fraction. Further, its Henry's constant in the liquid mixture will be independent of the other dilute solutes. Bubble pressure calculations can be performed with the solute components independent of each other in the liquid phase. They may be considered interacting in the vapor phase, if necessary.

REFERENCES FOR CHAPTER 7

1. M. Orentlicher and J. M. Prausnitz, Chem. Eng. Sci., 19, 775 (1964).

2. J. F. Connolly, J. Chem. Phys., 36, 2897 (1962).

3. B. H. Sage and W. N. Lacey, Thermodynamic Properties of Lighter Hydrocarbons, New York, API (1950), (1955).

4. J. Shim and J. P. Kohn, J. Chem. Engr. Data, 7, 3 (1962).

5. H. Volk and G. D. Halsey, J. Chem. Phys., 33, 1132 (1960).

6. A. Azarnoosh and J. J. McKetta, J. Chem. Engr. Data, 8, 321 (1963).

7. H. H. Reamer and B. H. Sage, J. Chem. Engr. Data, 4, 98 (1959).

8. H. J. Aroyan and D. L. Katz, I.E.C., 43, 185 (1951).

9. A. L. Benham and D. L. Katz, A.I.Ch.E.J., 3, 33 (1957).

10. J. M. Prausnitz and P. L. Chueh, Computer Calculations of High Pressure Vapor Liquid Equilibria, Prentice-Hall, Englewood Cliffs, N.J. (1968).

11. H. H. Reamer et al., I.E.C., 52, 534 (1950).

12. J. F. Connolly and G. A. Kandalic, J. Chem. Engr. Data, 7, 137 (1962).

13. J. F. Connolly and G. A. Kandalic, CEP Symposium Series, 59, #44 (1963).

14. J. P. O'Connell, A.I.Ch.E.J., 17, 653 (1971).

15. J. E. Smith, Statistical Mechanical Theory of the Henry's Constants, Ph.D. Dissertation, University of Rochester (1965).

CHAPTER 8

CONCLUDING REMARKS

The isothermal compressibility, the partial molar volume and the composition derivative of the chemical potential for fluid mixtures are directly related through a rigorous statistical mechanical formalism to the volume integrals of molecular distribution functions, equations (2.16) through (2.32). Other expressions can be obtained for the internal energy and heat capacity.

The molecular distribution functions and their volume integrals are complex functions of the macroscopic state of the system. At present lack of accurate expressions for the distribution functions prohibit their use in calculating thermodynamic properties directly from molecular parameters. When a complete theory for composition dependent molecular distribution functions does become available, these expressions should be more generally useful. Functional expansions of the expressions for thermodynamic properties are made about limiting compositions to partially circumvent the problem of describing their possibly complex composition dependence, equations (2.33) - (2.48). These expressions describe the limiting slope of the thermodynamic properties quite accurately but hold over restricted composition ranges.

Molecular distribution functions of different orders have been related through density and composition derivatives. These relations can be used to determine the higher order functions from the density dependence of the corresponding lower order distribution functions, thus adding to the present understanding of molecular interactions.

A derived first order perturbation expression, equation (3.3), for the distribution functions uses the hard sphere fluid as a base, with an attractive perturbing potential. The calculated R.D.F.'s for a Lennard-Jones 6-12 fluid in the liquid region agree with molecular dynamics results. The density dependence of the reduced DCF integral, equation (3.8), is similar to the macroscopic density dependence of the isothermal compressibility of pure fluids. This is the basis of a qualitatively accurate, one-parameter microscopic theory for the reduced DCF integrals for pure components and mixtures, with simple mixing rules for mixture parameters. Thermodynamic properties at infinite dilution in subcritical systems as calculated from this microscopic theory agree only qualitatively with experimental data, Table 3-2. Quantitative agreement could possibly be obtained by introducing a temperature related parameter into the microscopic, and per force, the macroscopic theories.

The one-parameter macroscopic generalized correlation for isothermal compressibility as a function of reduced solvent density, equation (4.3), is a good representation of the experimental data. The calculated pressure and temperature derivatives of the compressibility, equations (4.53) and (4.54), also agree well with the limited experimental data available. In the absence of compressibility or volumetric data, the generalized isothermal equation of state, equation (4.10), is useful for compression calculations.

The compressibility correlation breaks down at low reduced densities due to the divergence of the pure liquid isotherms as the critical density is approached. It may be possible to correlate the

divergent behavior in this region by introducing a temperature (or energy) related parameter into the macroscopic model. On the other hand, the present correlation is quite satisfactory in the highly compressed liquid region, and might be used to interpret the molecular significance of the coefficients in the Tait equation.

Experimental partial molar volumes for gases in liquid solutions are represented by equation (4.6). The calculated temperature and pressure derivatives may be useful for preliminary design calculations, but are not accurate enough for an understanding of the molecular interactions in the mixture and their dependence on the macroscopic state. Possible improvements of this correlation could begin with the use of an energy parameter for the solvent obtained from data at lower reduced densities.

The macroscopic one-fluid theory, equation (5.1), with a composition dependent characteristic parameter, equation (5.2), is found satisfactory to represent the isothermal compressibility of binary and ternary liquid mixtures by equation (4.3). Improved agreement is obtained by adjusting the characteristic parameters of the individual components. Little error is introduced by assuming an ideal mixture to determine its volume. In binary liquid mixtures, the assumption that all of the DCF integrals vary linearly between composition extremes yields accurate partial molar volumes and activity coefficients at intermediate compositions, though inaccurate compressibilities. However, activity coefficients determined from experimental pure component compressibilities and partial molar volumes at infinite dilution and a simple mixing rule for the DCF integrals do not represent the experimental data satisfactorily (Table 5-6).

Improved agreement may result with an experimentally determined deviation parameter from activity coefficients at infinite dilution. An alternate approach is the development of correlations for partial molar volumes and activity coefficients of liquids in liquids, i.e., for C_{12}° and C_{11}°, where components 1 and 2 are both subcritical. Such correlations would certainly contribute to the understanding of distribution functions in liquid mixtures.

A detailed analysis of the H_2-benzene system is possible with functional expansions about the pure solvent composition. The slopes of the compressibility and partial molar volume at zero composition involve both pair and triplet correlation functions. The triplet correlation functions are obtained from density derivatives of the generalized correlations for the pair functions. The calculated zero slopes do not agree well with the experimental data, the largest source of error being the density derivative of C_{12}°, i.e., of the partial molar volume. The Percus-Yevick or HNC theories do not yield triplet correlation functions in agreement with experiment.

The infinite dilution activity coefficient parameter f_2° and the related DCF integral C_{11}°, for CH_4 and H_2 in single liquid solvents are represented by generalized functions of the reduced solvent density (7.4), (7.5), (7.6) and (7.7). The results of vapor-liquid equilibrium calculations using equations (7.4) and (7.5) to determine activity coefficients are quite encouraging, Tables 7-2 and 7-3. Calculated vapor compositions agree well with experiment, and bubble pressures generally are predicted satisfactorily. The generalized activity coefficient parameter offers considerable improvement over other

methods wherein activity coefficients are determined from coefficients characteristic of each solute-solvent pair.

In systems of gases in binary solvents, the solvent mixture is represented by the one-fluid model. The volumetric properties of the gas-solvent mixture are described well by the functional expansions with the experimental DCF integrals. The experimental and predicted DCF integrals become more negative as the solvent density increases. The integrals of the solute-solute interaction are always less negative than those of the solvent-solvent interaction, Table 7-6. One concludes that the size and energy parameters characterizing the solute-solute interaction are always smaller than those of the solvent-solvent interaction, and the solute-solvent parameters lie in between.

Several relations between the Henry's constants of a gas in a mixed solvent and in the corresponding pure solvents are analyzed with experimental data, Table 7-7. One of these relations, (7.31), involving the compressibilities of the pure and mixed solvents, and the partial molar volumes of the gases in these, offers advantages in practical applications, but its validity is not clearly established on the basis of the limited experimental data. Further investigation of this and other expressions is clearly warranted due to the increasing use of mixed solvents in industrial applications.

Activity coefficients of CH_4 and H_2 in mixed solvents can be determined from the generalized correlations, equations (7.6) and (7.7), when the mixed solvent is represented by the one-fluid model. The results of vapor-liquid equilibrium calculations are satisfactory,

Table 7-8. Although the predicted bubble pressures often disagree by 20% from the experimental pressure, the calculated K-factors are in close agreement with the experimental data.

This generalized method for the activity coefficient of the solute can be extended to systems of two or more solutes present at dilute concentrations since the activity coefficient of each solute is independent of the concentration of other solutes.

APPENDICES

APPENDIX A

MULTICOMPONENT ORNSTEIN-ZERNIKE EQUATION

For an m-component system[1]

$$g_{ij}(\underline{r},\underline{r}') - 1 = c_{ij}(\underline{r},\underline{r}') + \sum_{\ell=1} \int [g_{ij}(\underline{r},\underline{y}) - 1] c_{\ell j}(\underline{y},\underline{r}') n_{\ell}(y) d\underline{y} \tag{A.1}$$

where $n_{\ell}(y)$ = number density = $\dfrac{N \cdot x_{\ell}}{V}$ (A.2)

Multiplying through by $d\underline{r}'$ and integrating

$$\frac{V}{N} G_{ij} = \frac{V}{N} C_{ij} + \sum_{\ell=1,m} n_{\ell} \int [g_{ij}(\underline{r},\underline{y}) - 1] d\underline{y} \int c_{\ell j}(\underline{y},\underline{r}') d\underline{r}' \tag{A.3}$$

where

$$G_{ij} = \rho \int [g_{ij}(\underline{r},\underline{r}') - 1] d\underline{r}' \tag{A.4}$$

and n_{ℓ} is taken independent of position in a homogeneous system. In the integral of equation (A.3), $\underline{y}$ and $\underline{r}'$ are dummy indices

$$\frac{V}{N} G_{ij} = \frac{V}{N} C_{ij} + \sum_{\ell=1,m} n_{\ell} \frac{V}{N} G_{i\ell} \frac{V}{N} C_{\ell j} \tag{A.5}$$

$$\therefore \quad \underline{\underline{G}} = \underline{\underline{C}} + \underline{\underline{G}}\,\underline{\underline{X}}\,\underline{\underline{C}} \tag{A.6}$$

---

[1] J. L. Lebowitz, Phys. Review, 133, A895 (1964).

APPENDIX B

RECURRENCE RELATIONS FOR DCF INTEGRALS

For the change of variables from constant pressure to constant volume

$$\left(\frac{\partial c_{ij}^{(2)}}{\partial Nk} \right)_{T,P,N_{m\neq k}} = \left(\frac{\partial c_{ij}^{(2)}}{\partial Nk} \right)_{T,V,N_{m=k}} + \left(\frac{\partial c_{ij}^{(2)}}{\partial V} \right)_{T,N} \left(\frac{\partial V}{\partial N_k} \right)_{T,P,N_{m\neq k}} \tag{B.1}$$

$$\therefore \quad N\left(\frac{\partial c_{ij}^{(2)}}{\partial N_k} \right)_{T,P,N_{m\neq k}} = N\left(\frac{\partial c_{ij}^{(2)}}{\partial N_k} \right)_{T,V,N_{m\neq k}} + N\bar{v}_k \left(\frac{\partial c_{ij}^{(2)}}{\partial V} \right)_{T,N} \tag{B.2}$$

$$= N\left(\frac{\partial c_{ij}^{(2)}}{\partial N_k} \right)_{T,\rho_m} - \rho\bar{v}_k \sum_n N_n \left(\frac{\partial c_{ij}^{(2)}}{\partial N_n} \right)_{T,\rho_{m\neq n}} \tag{B.3}$$

We also have

$$v\left(\frac{\partial c_{ij}^{(2)}}{\partial N_k} \right)_{T,V,N_{m\neq k}} = \int c_{ijk}^{(3)} \, d\underline{r}_k \tag{B.4}$$

Equations (B.3) and (B.4) are used to derive the recurrence relation between C_{ij} and C_{ijk}.

$$\left(\frac{\partial C_{ij}}{\partial N_k} \right)_{T,P,N_{m\neq k}} = \frac{\partial}{\partial N_k} \frac{N}{V} \cdot \int c_{ij}^{(2)} \, d\underline{r}_{T,P,N_{m\neq k}} \tag{B.5}$$

and using Liebnitz's rule for the partial derivative of the integral

$$\left(\frac{\partial C_{ij}}{\partial N_k} \right)_{T,P,N_{m\neq k}} = \frac{C_{ij}}{\rho} \left(\frac{V - N\bar{v}_k}{V^2} \right) + \frac{N}{V} \left[c_{ij}^{(2)}(V) \left(\frac{\partial V}{\partial N_k} \right)_{T,P,N_{m\neq k}} \right.$$

$$+ \int \left(\left(\frac{\partial c_{ij}^{(2)}}{\partial N_k} \right)_{T,P,N_{m\neq k}} d\underline{r} \right) \qquad (B.6)$$

But $c_{ij}^{(2)}(V)$ is the microscopic d.c.f. when the separation between molecules is of the order of the macroscopic volume of the system; it is zero.

$$\left(\frac{\partial C_{ij}}{\partial N_k} \right)_{T,P,N_{m\neq k}} = \frac{C_{ij}}{N}(1 - \rho\bar{v}_k) + \frac{N}{V}\left(\int \left(\frac{\partial c_{ij}^{(2)}}{\partial N_k} \right)_{T,V,N_{m\neq k}} d\underline{r} \right.$$

$$\left. - \rho\bar{v}_k \sum_s x_s \int \left(\frac{\partial c_{ij}^{(2)}}{\partial \rho_s} \right)_{T,V,N_{m\neq s}} d\underline{r} \right) \qquad (B.7)$$

where equation (B.3) has been substituted into (B.6). Then

$$\left(\frac{\partial C_{ij}}{\partial N_k} \right)_{T,P,N_{m\neq k}} = \frac{C_{ij}}{N}(1 - \rho\bar{v}_k) + \frac{1}{N}\left[C_{ijk} - \rho\bar{v}_k \sum_s x_s C_{ijs} \right] \qquad (B.8)$$

$$\therefore \quad \left(\frac{\partial C_{ij}}{\partial x_k} \right)_{T,P,N_{m\neq k}} = \left(\frac{N^2}{N - N_k} \right)\left(\frac{\partial C_{ij}}{\partial N_k} \right)_{T,P,N_{m\neq k}}$$

$$= \frac{C_{ij}(1 - \rho\bar{v}_k) + C_{ijk} - \rho\bar{v}_k \sum_s x_s C_{ijs}}{(1 - x_k)} \qquad (B.9)$$

The quantities C_{ij} and C_{ijk} can also be related through density derivatives. We have, from their definitions,

$$C_{ij} = \frac{N}{V^2} \iint c_{ij}^{(2)} \, d\underline{r}_i \, d\underline{r}_j \qquad (B.10)$$

$$C_{ijk} = \frac{N^2}{V^3} \iiint c^{(3)}_{ijk} \, d\underline{r}_i d\underline{r}_j d\underline{r}_k \tag{B.11}$$

Then

$$\left(\frac{\partial C_{ij}}{\partial N_k} \right)_{T,V,N_{m\neq k}} = \frac{\iint c^{(2)}_{ij} \, d\underline{r}_i d\underline{r}_j}{V^2} + \frac{N}{V^2} \iint \left(\frac{\partial c^{(2)}_{ij}}{\partial N_k} \right)_{T,V,N_{m\neq k}} d\underline{r}_i d\underline{r}_j \tag{B.12}$$

Using equation (B.4) above

$$\left(\frac{\partial C_{ij}}{\partial N_k} \right)_{T,V,N_{m\neq k}} = \frac{\iint c^{(2)}_{ij} d\underline{r}_i d\underline{r}_j}{V^2} + \frac{N}{V^2} \frac{1}{V} \iiint c^{(3)}_{ijk} \, d\underline{r}_i d\underline{r}_j d\underline{r}_k \tag{B.13}$$

$$= \frac{1}{V} \left(\frac{\partial C_{ij}}{\partial \rho_k} \right)_{T,\rho_{m\neq k}} = \frac{V^2}{N} \frac{C_{ij}}{V^2} + \frac{N}{V^3} C_{ijk} \frac{V^3}{N^2} \tag{B.14}$$

$$\therefore \left(\frac{\partial C_{ij}}{\partial \rho_k} \right)_{T,\rho_{m\neq k}} = \frac{C_{ij}}{\rho} + \frac{C_{ijk}}{\rho} \tag{B.15}$$

APPENDIX C

FIRST-ORDER PERTURBATION THEORY FOR THE DISTRIBUTION FUNCTIONS OF A DENSE FLUID

Percus showed that molecular distribution functions are functional derivatives of the molecular density at any point in the fluid with respect to a change in potential on the fluid. This provides a precise relation between molecular distribution functions of different orders. The change in potential may be due to the introduction of an external molecule either the same as, or different from, the molecules of the fluid under consideration. The functional derivatives are

$$\frac{\delta n_1(r')}{\delta[-\beta U(0)]} \; n_1(r')\delta(0 - r') + n_2(r',0) - n_1(r')n_1(0) \qquad \text{(C.1)}$$

$$\frac{\delta[-\beta U(r)]}{\delta n_1(r')} \quad [n_1(r')]^{-1}\delta(r - r') - c_2(r,r') \qquad \text{(C.2)}$$

Equation (C.1) relates the change in $n_1(r')$, the single-particle density at r', due to a change in potential at 0, U(0), in terms of one- and two-particle distribution functions $n_1(0)$, $n_1(r')$, and $n_2(0,r')$. The functional inverse shown in equation (C.2) defines $c_2(r,r')$, the second-order direct correlation function. Multiplying equations (C.1) and (C.2) and integrating over r' yields the Ornstein-Zernike relation

$$[n_2(0,r)/n_1(r)] - n_1(0) = n_1(0)c_2(0,r) + \int c_2(r,r')[n_2(0,r') - n_1(r')n_1(0)]dr' \qquad \text{(C.3)}$$

In addition, using the functional relations (C.1) and (C.2), the

quantity $n_1(r)\exp[\beta U(r)]$, which is used in the Percus-Yevick theory, may be expanded in terms of a perturbation in the density to give

$$n_1^*(r)\exp[\beta U^*(r)] = n_1^o(r)\exp[\beta U^o(r)][1 + \int c_2^o(r,r')\{n_1^*(r') - n_1^o(r')\}dr' + \frac{1}{2}\iint \{c_3^o(r,r',r'') + c_2^o(r,r')c_2^o(r,r'')\}\{n_1^*(r') - n_1^o(r')\} \cdot \{n_1^*(r'') - n_1^o(r'')\}dr'dr'' + \ldots] \quad (C.4)$$

In equation (C.4), the superscript ^{o} refers to the unperturbed fluid and the superscript asterisk (*) to the real fluid. If the change in external potential causing the density fluctuation at r' is due to placing a particle or changing the kind of particle at the origin of coordinates, then the first-order distribution functions $n_1^*(r')$ and $n_1^o(r')$ are second-order distribution functions, since they represent the probability of a particle being at r' when it is known that there is a particle at the origin, i.e.,

$$n_1(r'/0) = n_2(0,r')/n_1(0) = n_1(r')g_2(0,r') \quad (C.5)$$

where $n_1(r'/0)$ is the one-particle distribution function at r' in the presence of a particle at 0. Then, to the first order in density, equation (C.5) becomes

$$g_2^*(0,r)\exp[\beta U^*(r)] = g_2^o(0,r)\exp[\beta U^o(r)][1 + \int c_2^o(r,r')n_1(r') \cdot \{g_2^*(0,r') - g_2^o(0,r')\}dr'] \quad (C.6)$$

We shall now explicitly use equation (C.6) in constructing a real molecular interaction from a hard-sphere interaction. Consider the two states shown in Fig. C-1. In state 1, the fluid is composed

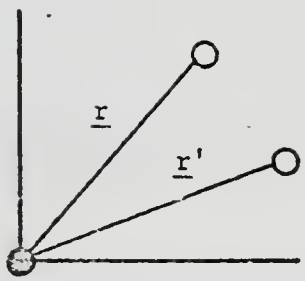

State 1

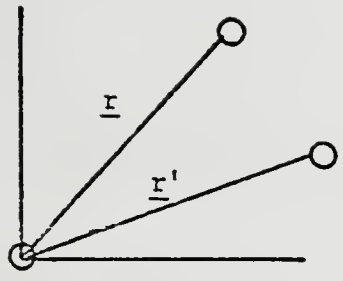

State 2

○ Molecule of real fluid

◎ Molecule of hard sphere fluid

Fig. C-1.

of molecules of the "real" fluid and a molecule whose interaction with the others can be represented by a hard-sphere potential is situated at the origin. [A molecule at r and one at r' are shown; the total potential at r due to all the other molecules in the system is V(r). The interactions between the molecules, e.g., $c_2(r,r')$, are those typical of the "real" fluid.] In state 2, a molecule of the "real" fluid replaces the "hard-sphere" molecule at the origin. Equation (C.6) may be applied to the change in state from 1 → 2:

$$g_2^*(0,r)\exp[\beta[V(r) + \phi^*(0,r)]] = g^o(0,r)\exp[\beta[V(r) + \phi^o(0,r)]]$$

$$\cdot \{1 + \int c^*(r,r')[n_1^*(r')g^*(0,r') - n_1^o(r')g^o(0,r')]dr'\} \qquad (C.7)$$

Writing the Ornstein-Zernike equation for the states 1 and 2

$$g_2^o(0,r) - 1 = c_2^o(0,r) + \int c_2^*(r,r')n_1^o(r')[g_2^o(0,r') - 1]dr' \qquad (C.8)$$

$$g_2^*(0,r) - 1 = c_2^*(0,r) + \int c_2^*(r,r')n_1^*(r')[g_2^*(0,r') - 1]dr' \qquad (C.9)$$

We shall now assume that $g^o = g^{hs}$, the true hard-sphere distribution function; i.e., it is the solution of equation (C.8) when $c_2^*(r,r')n_1^o(r')$ is replaced by $\rho c_2^{hs}(r,r')$ within the integral of equation (C.8), and ρ is the real fluid density. In equation (C.9), all quantities refer to the real fluid (rf) and $n_1^*(r') = \rho$. Subtracting (C.8) from (C.9) and substituting in (C.7), we get

$$g^{rf}(r)\exp[\beta\phi^{rf}(r)] = g^{hs}(r)\exp[\beta^{hs}(r)]\{1 + g^{rf}(r) - g^{hs}(r)$$

$$- c^{rf}(r) + c^{hs}(r)\} \qquad (C.10)$$

Equation (C.10) is valid at all values of r, so the intermolecular

potential and distribution functions of the real fluid are different from those of the hard-sphere fluid over the entire range. In the range $r < a$, where a corresponds to the hard-core distance of the hard-sphere fluid, we have

$$g^{rf}(r) = g^{hs}(r)\exp[\beta\phi^{hs}(r)][1 - c^{rf}(r) + c^{hs}(r)]/\{\exp[\beta\phi^{rf}(r)] - g^{hs}(r)\exp[\beta\phi^{hs}(r)]\} \tag{C.11}$$

The quantities $c^{rf}(r)$ and $c^{hs}(r)$ and the $g^{hs}(r)\exp\{\beta\phi^{hs}(r)\}$ are all finite. Thus, $g^{rf}(r)$ varies inversely as the exponential of the real fluid potential and quickly becomes very small as r decreases. The distribution functions in the real fluid are now completely defined in terms of the hard-sphere distribution functions and the differences in the intermolecular potentials.

The reference hard-sphere fluid may be chosen to be an ideal gas, where

$$g^{hs}(r) = 1, \tag{C.12}$$

$$c^{hs}(r) = \phi^{hs}(r) = 0 \qquad \text{for all } r$$

Then, $$g^{rf}(r)\exp[\beta\phi^{rf}(r)] = g^{rf}(r) - c^{rf}(r) \tag{C.13}$$

which is the relation of the usual first-order Percus-Yevick theory. Thus, equation (C.10) is a general form of the Percus-Yevick equation with a hard-sphere reference.

Equation (C.10) can be used for any intermolecular potential and reference distribution function with the procedure described above. When it is substituted into the Ornstein-Zernike equation, an integral equation for either $g^{rf}(r)$ or $c^{rf}(r)$ results.

APPENDIX D

TEMPERATURE DERIVATIVE OF LIQUID DENSITY AT CONSTANT PRESSURE

From equation (4.8)

$$\frac{P - P^s}{RT\rho_2^*} = \int_{\tilde{\rho}_2}^{\tilde{\rho}_2} [F(\tilde{\rho}_2) - 1] d\tilde{\rho}_2 \tag{D.1}$$

Taking a partial derivative w.r.t. T at constant P, and using Liebnitz's rule

$$\frac{d}{dx} \int_{A(x)}^{B(x)} F(x,t)dt = \int_{A}^{B} \frac{\partial F(x,t)}{\partial x} dt + F(x,B(x)) \frac{dB}{dx} - F[x,A(x)] \frac{dA}{dx} \tag{D.2}$$

$$\frac{1}{RT\rho_2^*} \left[0 - \left(\frac{\partial P^s}{\partial T} \right)_P \right] - \frac{P - P^s}{RT^2\rho_2^*} = \frac{(F_1(\tilde{\rho}) - 1)}{\rho_2^*} \left(\frac{\partial \tilde{\rho}_2}{\partial T} \right)_P$$

$$- \frac{(F_1(\hat{\rho}_s) - 1)}{\rho_2^*} \left(\frac{\partial \rho_2^s}{\partial T} \right)_P \tag{D.3}$$

Now

$$\left(\frac{\partial \rho_2}{\partial T} \right)_P \left(\frac{\partial T}{\partial P} \right)_{\rho_2} \left(\frac{\partial P}{\partial T} \right)_P = -1 \tag{D.4}$$

$$\left(\frac{\partial \rho_2}{\partial T} \right)_P = - \left(\frac{\partial P}{\partial T} \right)_{\rho_2} \left(\frac{\partial \rho_2}{\partial T} \right)_P = - \left(\frac{\partial P}{\partial T} \right)_{\rho_2} \frac{1}{RT[F_1(\tilde{\rho}_2) - 1]} \tag{D.5}$$

From (D.3)

$$\left(\frac{\partial \rho_2}{\partial T} \right)_P [F_1(\tilde{\rho}_2) - 1] = [F_1(\tilde{\rho}_2^s) - 1] \frac{d\rho_2^s}{dT} - \frac{1}{RT} \frac{dP^s}{dT} - \frac{P - P^s}{RT^2} \tag{D.6}$$

which gives the temperature dependence of the density a compressed liquid.

The pressure variation with temperature at constant density can be determined from (D.5) and (D.6).

APPENDIX E

EXTRACTION OF HENRY'S CONSTANTS AND ACTIVITY COEFFICIENTS FROM VAPOR-LIQUID EQUILIBRIUM DATA

For binary vapor-liquid equilibrium

$$y_1\phi_1^v P = x_1\gamma_1^*(T,P_2^s,x_1)H_{1,2}(T,P_2^s,x)\exp\int_{P_2^s}^{P}\frac{\bar{v}_1(T,x)}{RT}\,dP \qquad (E.1)$$

where P_2^s, the saturation pressure of the solvent, is the reference pressure for the fugacity of componentl; $\bar{v}_1(T,x,P)$ is the partial molar volume of the solute at composition x. At low concentration x_1, $\bar{v}_1(T,x,P)$ can be approximated by the partial molar volume at infinite dilution, i.e.,

$$\bar{v}_1^o(T,P,x) = \bar{v}_1^o(T,P) \qquad (E.2)$$

Then
$$y_1\phi_1^v P = x_1\gamma_1^*(T,x_1)H_{1,2}(T)\exp\int_{P^s}^{P}\frac{\bar{v}_1^o(T,P)}{RT}\,dP \qquad (E.3)$$

The solvent fugacity is

$$y_2\phi_2^v P = x_2\gamma_2(T,x_1)f_2^{P^s}(T)\exp\int_{P^s}^{P}\frac{v_2^o}{RT}\,dP \qquad (E.4)$$

and
$$f_2^{P^s} = P_2^s\phi_2^s \qquad (E.5)$$

where P_2^s, the solvent saturation pressure, and ϕ_2^s, its fugacity coefficient in the pure liquid state are calculated from generalized correlations.[1] The two (or three) term Margules equation is chosen to

[1] J. M. Prausnitz et al., Computer Calculations for Multicomponent Vapor Liquid Equilibrium, Prentice-Hall, Englewood Cliffs, N.J. (1968).

describe the composition dependence of the liquid phase activity coefficients

$$\ell n\gamma_1^*(x_1,T) = A(x_1^2 - 2x_1) + B(x_1^3 - \frac{3}{2}x_1^2) \tag{E.6}$$

$$\ell n\gamma_2 = Ax_1^2 + Bx_1^3 \tag{E.7}$$

Vapor phase properties are represented by the Redlich-Kwong equation, as modified by Chueh and Prausnitz.[2] They use the general Redlich-Kwong equation

$$P = \frac{RT}{v - b} - \frac{a}{T^{0.5}v(v + b)} \tag{E.8}$$

but determine the parameters empirically. Mixing rules are empirically derived for the critical properties of mixtures. The relation for the fugacity coefficient is

$$\ell n\Phi_k = \ell n \frac{v}{v - b} + \frac{b_k}{v-b} - \ell n \frac{v + b}{v} \cdot 2 \sum_{i=1}^{N} y_i a_{ik}/RT^{3/2}b$$

$$+ \frac{ab_k}{RT^{3/2}b^2} \ell n \frac{v + b}{v} - \frac{b}{v + b} - \ell n \frac{Pv}{RT} \tag{E.9}$$

The fugacities of the two components in both phases are now completely defined in terms of experimental quantities and the parameters to be evaluated.

At each state point, the temperature, bubble pressure, liquid compositions, and partial molar volumes for each component are supplied

---

[2] P. L. Chueh and J. M. Prausnitz, Computer Calculations for High Pressure Vapor-Liquid Equilibria, Prentice-Hall, Englewood Cliffs, N.J. (1970).

to the computer program. The calculational algorithm is schematically presented in Fig. E-1. At the given temperature and pressure, and guessed values of the parameters, the liquid composition is adjusted until the vapor mole fraction sum to unity. The sum square error in liquid composition is calculated at this point. The program searches over different parameter sets until a minimum in the sum square error of the liquid composition is obtained. (The searching algorithm (RMINSQ) is based on the Fletcher Powell method)

For a binary solvent system, the two suffix Margules equation represents the excess free energy of the solvent mixture, e.g.,

$$RT\ell n\gamma_2 = (2D - C)x_3^2 + 2(C - D)x_3^3 \qquad (E.10)$$

The excess free energy in the 1-2-3 mixture relative to the 2-3 mixture is again represented by a Margules equation which gives

$$RT\ell n\gamma_{1m}^{*} = A_{123}(x_1^2 - 2x_1) \qquad (E.11)$$

$$RT\ell n\gamma_{2m} = A_{123}x_1^2 + (2D - C)X_3^2 + 2(C - D)X_3^3 \qquad (E.12)$$

$$RT\ell n\gamma_{2m} = A_{123}x_1^2 + (2C - D)X_2^2 + 2(D - C)X_2^3 \qquad (E.13)$$

X_2 and X_3 are mole fractions in the solute-free mixture.

The fugacity reference states for the two solvent components are their respective saturation pressures. For the solute component, it is the infinitely dilute solution at its equilibrium pressure, i.e., the saturation pressure of the liquid mixture. The Henry's constant and solute activity coefficients are referred to this pressure and not to zero pressure as in Prausnitz and Chueh.

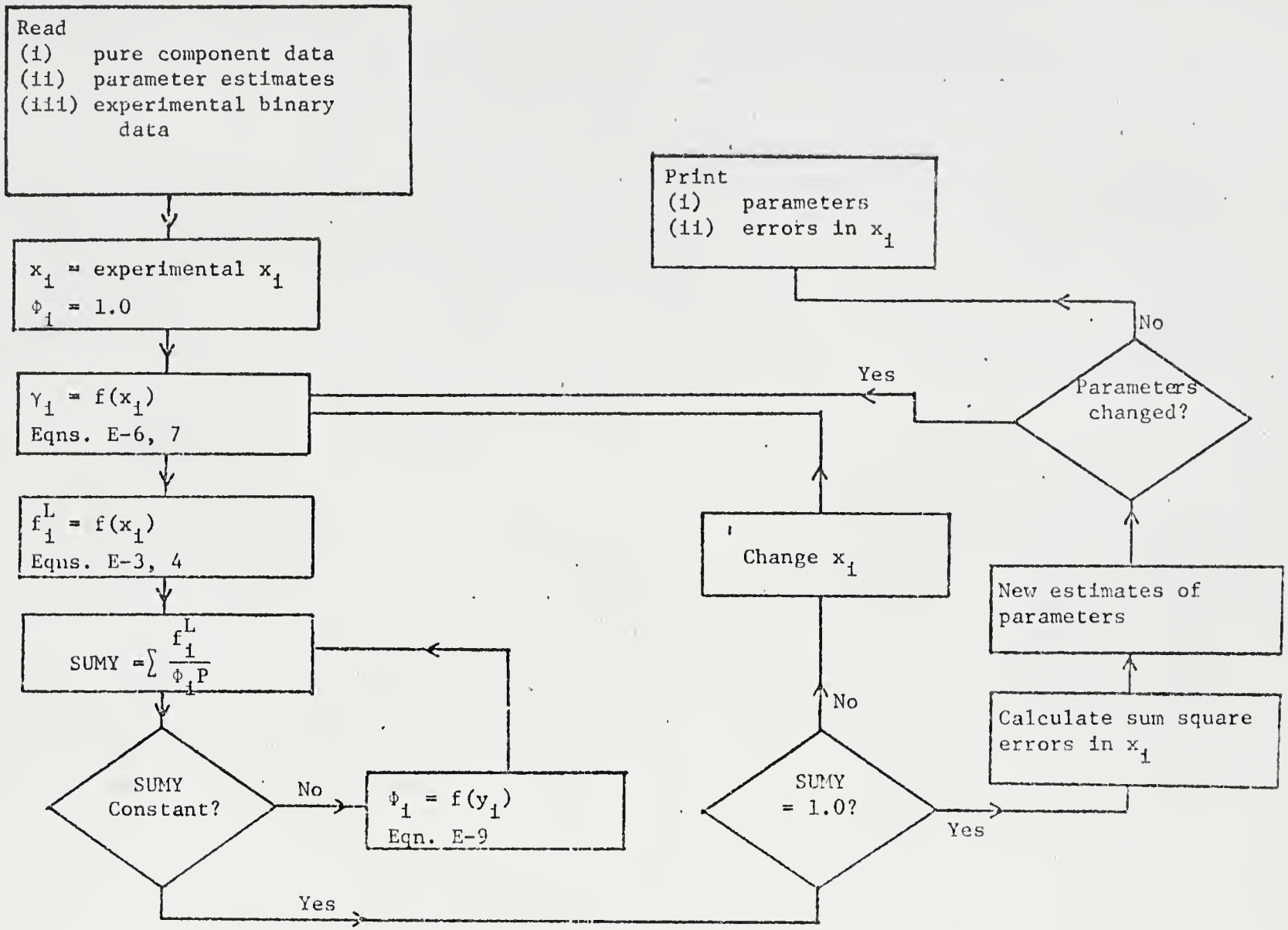
Read
(i) pure component data
(ii) parameter estimates
(iii) experimental binary data
x_i = experimental x_i
Φ_i = 1.0
$\gamma_i = f(x_i)$
Eqns. E-6, 7
$f_i^L = f(x_i)$
Eqns. E-3, 4
SUMY = $\sum \frac{f_i^L}{\Phi_i P}$
SUMY Constant?
No
$\Phi_i = f(y_i)$
Eqn. E-9
Yes
SUMY = 1.0?
No
Change x_i
Yes
Calculate sum square errors in x_i
New estimates of parameters
Parameters changed?
No
Yes
Print
(i) parameters
(ii) errors in x_i

Fig. E-1.

APPENDIX F

PERCUS-YEVICK AND HYPERNETTED CHAIN APPROXIMATIONS FOR TRIPLET CORRELATION FUNCTIONS

The first-order PY and HNC expression for the pair distribution functions are obtained from general density expansion by setting terms of second and higher order to zero.[1,2] These conditions, in turn, provide relations for the triplet and higher distribution functions. For an M-component mixture, under the Percus-Yevick approximation, we have

$$\sum_{j=1}^{M}\sum_{k=1}^{M}\rho_j\rho_k\iint[c^{(3)}_{ijk}(\underline{r}_i,\underline{r}_j,\underline{r}_k)+c^{(2)}_{ij}(\underline{r}_i,\underline{r}_j)c^{(2)}_{ik}(\underline{r}_i,\underline{r}_k)]$$

$$\cdot[g_{ij}(\underline{r}_i,\underline{r}_j)-1][g_{ik}(\underline{r}_i,\underline{r}_k)-1]d\underline{r}_j d\underline{r}_k = 0 \qquad \text{(F.1)}$$

for all i

Then, setting the integrands to zero, and assuming that $[g_{ij}(\underline{r}_i,\underline{r}_j)-1]$ and $[g_{ij}(\underline{r}_i,\underline{r}_k)-1]$ are not zero, there results

$$x_1^2(C_{111}+C_{11}^2)+2x_1x_2(C_{112}+C_{11}C_{22})+x_2^2(C_{122}+C_{12}^2)=0 \qquad \text{(F.2)}$$

and

$$x_1^2(C_{112}+C_{12}^2)+2x_1x_2(C_{122}+C_{12}C_{22})+x_2^2(C_{222}+C_{22}^2) \qquad \text{(F.3)}$$

---

[1] J. K. Percus in Classical Fluids, edited by H. L. Frisch and J. L. Lebowitz, Benjamin, New York, 1964.

[2] J. L. Lebowitz, Physical Review, 133, A895 (1964).

in a binary. For infinite dilution of component 1 in 2

$$C^{o}_{122} = - C^{o2}_{12} \tag{F.4}$$

and

$$C^{o}_{222} = - C^{o2}_{22} \tag{F.5}$$

Similarly, for the HNC approximation

$$\sum_{j=1}^{M} \sum_{k=1}^{M} \rho_j \rho_k \iint c^{(3)}_{ijk}(r_i,r_j,r_k)[g_{ij}(r_i,r_j) - 1][g_{ik}(r_i,r_k) - 1]dr_j dr_k = 0$$

for all i (F.6)

leading to

$$x_1^2 C_{111} + 2x_1 x_2 C_{112} + x_2^2 C_{122} = 0 \tag{F.7}$$

and

$$x_1^2 C_{112} + 2x_1 x_2 C_{122} + x_2^2 C_{222} = 0 \tag{F.8}$$

Again, for infinitely dilute 1 in 2

$$C^{o}_{122} = 0 \tag{F.9}$$

and

$$C^{o}_{222} = 0 \tag{F.10}$$

BIBLIOGRAPHY

E. H. Amagat, Ann. de Chim et Phys., 29, 68-136, 505-574 (1893).

H. J. Aroyan and D. L. Katz, I.E.C., 43, 185 (1951).

A. Z. Azarnoosh and J. J. McKetta, J. Chem. Engr. Data, 8, 321 (1965).

K. E. Bachman and E. L. Simons, I.E.C., 44, 202 (1952).

J. A. Barker and D. Henderson, J. Chem. Phys., 47, 2856 (1967).

_____, Ibid., 4714.

A. L. Benham and D. L. Katz, Z.I.Ch.E.J., 3, 33 (1957).

V. Berry and B. H. Sage, J. Chem. Engr. Data, 4, 204 (1959).

P. W. Bridgman, Proc. Am. Acad. Arts & Sci., 69, 389 (1934).

I. Brown and F. Smith, Austr. J. of Chem., 15, 9 (1962).

S. D. Chang and B. C. Lu, Can. J. Chem. Engr., 48, 261 (1970).

J. F. Connolly, J. Chem. Phys., 36, 2897 (1962).

J. F. Connolly and G. A. Kandalic, Chem. Engr. Progr. Symposium Series, 59, 8 (1963).

_____, J. Chem. Engr. Data, 7, 137 (1962).

M. W. Cook et al., J. Chem. Phys., 36, 748 (1957).

W. G. Cutleret al., J. Chem. Phys., 29, 727 (1959).

Norman Davidson, Statistical Mechanics, McGraw-Hill, New York (1962).

K. G. Denbigh, Chemical Equilibrium, Cambridge University Press, Cambridge (1956).

A. K. Doolittle and B. Doolittle, A.I.Ch.E.J., 6, 157 (1960).

H. E. Eduljee et al., J. Chem. Soc., London, 3086 (1951).

S. R. M. Ellis, Trans. Inst. Chem. Engrs., 30, 58 (1952).

W. A. Felsing and G. M. Watson, J. Am. Chem. Soc., 64, 1822 (1942).

R. E. Gibson and O. H. Loeffler, J. Am. Chem. Soc., 61, 2515 (1939).

_____, Ibid., 2877.

J. C. Gjalbaek and J. H. Hildebrand, J. Am. Chem. Soc., 72, 1072 (1950).

E. Hala et al., Vapor-Liquid Equilibrium Data at Normal Pressures, Pergamon Press, London (1968).

T. L. Hill, Statistical Mechanics, McGraw-Hill, New York (1956), p. 113.

G. A. Holder and E. Whalley, Trans. Far. Soc., 58, 2095 (1962).

G. W. Holtzlander and J. W. Riggle, A.I.Ch.E.J., 1, 312 (1955).

J. Horiuti, Scientific Papers of Institute of Physical and Chemical Research, 17, 125 (1931).

A. V. Itterbeek et al., Physica, 29, 742 (1963).

J. E. Jolly and J. H. Hildebrand, J. Am. Chem. Soc., 72, 1072 (1950).

_____, Ibid., 80, 1050 (1958).

W. B. Kay, I.E.C., 32, 358 (1940).

W. B. Kay, J. Am. Chem. Soc., 69, 1273 (1947).

J. G. Kirkwood and F. P. Buff, J. Chem. Phys., 19, 774 (1951).

J. P. Kohn, "Volumetric and Phase Equilibria of Methane-Hydrocarbon Binary Systems at Low Temperatures and High Pressures," A.I.Ch.E. Meeting, Houston (1967).

I. Kritchevsky and A. Illinskaya, Acta Physicochemica U.R.S.S., 20, 327 (1945).

P. Kumagai and T. Toriumi, J. Chem. Engr. Data, 16, 293 (1971).

T. W. Leland and P. S. Chappelear, in Applied Thermodynamics, American Chemical Society, New York (1968).

G. N. Lewis and M. Randall, Thermodynamics, 2nd Edition, McGraw-Hill, New York (1961).

D. A. Lowitz et al., J. Chem. Phys., 74, 3014 (1970).

E. C. Lyckman et al., Chem. Engr. Sci., 20, 685, 703 (1965).

F. Mandel et al., J. Chem. Phys., 52, 3315 (1970).

F. I. Mopsik, J. Chem. Phys., 50, 2559 (1969).

D. W. Newitt and K. E. Weale, J. Chem. Soc., London, 3092 (1951).

Y. Ng and J. Walkley, J. Phys. Chem., 73, 2274 (1969).

J. P. O'Connell, A.I.Ch.E.J., 17, 653 (1971).

J. P. O'Connell, Mol. Phys., 20, 27 (1971).

M. Orentlicher and J. M. Prausnitz, Can. J. of Chem., 45, 373 (1967).

_____, Ibid., 595.

_____, Chem. Engr. Sci., 19, 775 (1964).

J. K. Percus, in Classical Fluids, edited by H. L. Frisch and J. L. Lebowitz, Benjamin, New York (1964).

J. M. Prausnitz, Molecular Thermodynamics of Fluid Phase Equilibria, Prentice-Hall, Englewood Cliffs, N.J. (1969).

J. M. Prausnitz et al., Computer Calculation for Multicomponent Vapor-Liquid Equilibria, Prentice-Hall, Englewood Cliffs, N.J. (1968).

J. M. Prausnitz and P. L. Chueh, Computer Calculations for High Pressure Vapor-Liquid Equilibria, Prentice-Hall, Englewood Cliffs, N.J. (1969).

H. H. Reamer et al., I.E.C., 52, 534 (1950).

H. H. Reamer and B. F. Sage, J. Chem. Engr. Data, 4, 98 (1959).

R. C. Reid and T. K. Sherwood, Properties of Gases and Liquids, McGraw-Hill, New York (1966).

S. E. Richards and J. Chadwell, J. Am. Chem. Soc., 47, 2283 (1925).

J. S. Rowlinson, Liquids and Liquid Mixtures, Butterworths, London (1958).

_____, Liquids and Liquid Mixtures, Plenum Press, New York (1969).

_____, Mol. Phys., 10, 533 (1966).

_____, Rept. Progr. Phys., 28, 169 (1965).

B. H. Sage et al., I.E.C., 26, 1218 (1934).

B. H. Sage and W. N. Lacey, Thermodynamic Properties of Lighter Hydrocarbons, American Petroleum Institute, New York (1950).

L. G. Schornack and C. A. Eckert, J. Phys. Chem., 74, 3014 (1970).

R. H. Schum and O. L. I. Brown, J. Am. Chem. Soc., 75, 2520 (1953).

J. Shim and J. P. Kohn, J. Chem. Engr. Data, 7, 3 (1962).

J. E. Smith, Statistical Mechanical Theory of the Henry's Constant, Ph.D. Dissertation, University of Rochester (1965).

W. R. Smith and D. Henderson, Mol. Phys., 19, 411 (1970).

P. S. Snyder and J. Winnick, "P-V-T Properties of Liquid n-Alkanes at Elevated Pressures," 5th Symposium on Thermophysical Properties, ASME (1970).

C. F. Spencer and R. P. Danner, J. Chem. Engr. Data, 17, 236 (1972).

E. S. Thomasen and J. Gjalbaek, Acta Chemica Scandinavica, 17, 127 (1963).

L. Verlet, Physical Review, 165, 201 (1968).

L. Volk and G. D. Halsey, J. Chem. Phys., 33, 1132 (1960).

R. O. Watts and D. Henderson, Mol. Phys., 16, 217 (1969).

J. D. Weeks et al., J. Chem. Phys., 54, 5237 (1971).

S. E. Wood and A. E. Austin, J. Am. Chem. Soc., 67, 480 (1945).

S. E. Wood and J. P. Brusie, J. Am. Chem. Soc., 65, 1891 (1943).

BIOGRAPHICAL SKETCH

Waseem Brelvi graduated from I.I.T. Bombay in December, 1963. In 1966 he received an M.S. in Chemical Engineering from the University of California. He joined the Ph.D. program at Florida in 1968.

I certify that I have read this study and that in my opinion it conforms to acceptable standards of scholarly presentation and is fully adequate, in scope and quality, as a dissertation for the degree of Doctor of Philosophy.

J. P. O'Connell, Chairman
Associate Professor of Chemical Engineering

I certify that I have read this study and that in my opinion it conforms to acceptable standards of scholarly presentation and is fully adequate, in scope and quality, as a dissertation for the degree of Doctor of Philosophy.

T. M. Reed, III
Professor of Chemical Engineering

I certify that I have read this study and that in my opinion it conforms to acceptable standards of scholarly presentation and is fully adequate, in scope and quality, as a dissertation for the degree of Doctor of Philosophy.

K. E. Gubbins
Professor of Chemical Engineering

I certify that I have read this study and that in my opinion it conforms to acceptable standards of scholarly presentation and is fully adequate, in scope and quality, as a dissertation for the degree of Doctor of Philosophy.

C. F. Hooper, Jr.
Associate Professor of Physics

This dissertation was submitted to the Dean of the College of Engineering and to the Graduate Council, and was accepted as partial fulfillment of the requirements for the degree of Doctor of Philosophy.

March, 1973

Dean, College of Engineering

Dean, Graduate School